STUDIES ON THE CONFORMATIONAL STABILITY, DYNAMICS AND VISCOSITY OF IMMUNOGLOBULINS

By

Santoshanand Vijay Thakkar

Submitted to the graduate degree program in Pharmaceutical Chemistry and the Graduate Faculty of the University of Kansas in partial fulfillment of the requirements for the degree of Doctor of Philosophy.

_____

Chairperson – C. Russell Middaugh, Ph.D.

_____

Teruna J. Siahaan, Ph.D.

_____

Jennifer S. Laurence, Ph.D.

_____

David B. Volkin, Ph.D.

_____

David D. Weis, Ph.D.

Date Defended: September 13, 2012

The Dissertation Committee for Santoshanand Vijay Thakkar

certifies that this is the approved version of the following dissertation:

STUDIES ON THE CONFORMATIONAL STABILITY, DYNAMICS AND VISCOSITY OF IMMUNOGLOBULINS

_____

Chairperson - C. Russell Middaugh, Ph.D.

Date approved: September 13, 2012

ABSTRACT

Proteins, such as immunoglobulins, are inherently dynamic molecules with unique biological functions. The intra- and intermolecular interactions that govern the dynamic nature and function of immunoglobulins may also influence their stability. A molecular understanding of interrelationship between dynamics, function and conformational stability of immunoglobulins, both in solution and in presence of co-solutes, can be important for their pharmaceutical development. In addition, it is important to understand the differences in any such correlations between closely related immunoglobulins. Furthermore, molecular interactions in immunoglobulins can be unique at low and high concentrations, which necessitate newer complementary approaches to investigate such complex systems. Therefore, a better understanding of interactions that govern protein structure, dynamics and conformational stability at low and high concentrations and in presence of excipients should aid in designing, optimizing and developing rational formulation conditions for protein based therapeutics.

A variety of experimental methods sensitive to structure, dynamics and conformational stability of proteins in solution were employed in these studies. External perturbations such a change in pH, ionic strength and temperature were used to probe the response of proteins, both at low and high concentrations. Different monoclonal antibodies within IgG1 isotype were used to investigate interrelationships between protein dynamics and conformational stability in absence and presence of co-solutes. In addition, an ultraviolet spectroscopy based approach was developed to understand interactions modulating solution viscosity in high concentration immunoglobulin solutions.

These studies provide evidence that immunoglobulins belonging to the same IgG1 subtype can have notable differences in their conformational stability, dynamics, aggregation propensity, hydration properties and their response to co-solutes. In addition, alterations in protein dynamics (at a global protein level and in local regions with differences in solvent exposures) by stabilizing or destabilizing excipients were found to modulate the conformational stability of a monoclonal antibody. Furthermore, it was determined that potential interactions and factors modulating solution viscosity at high protein concentrations may also result in changes in their extinction coefficients. The work presented in this dissertation provides evidence that factors modulating protein dynamics and those governing intra- and intermolecular interactions can influence the conformational stability, aggregation and viscosity of proteins in solution.

Dedicated to:

My

Dad

(Vijay Jayram Thakkar),

Mom

(Kaumudi Vijay Thakkar),

Wife

(Urvashi Thakkar)

and

Sister

(Dimple Thakkar)

ACKNOWLEDGEMENTS

First of all, I take this opportunity to thank my research advisor, Dr. C. Russell Middaugh, for his mentoring and encouragement throughout my time in Pharmaceutical Chemistry graduate program at the University of Kansas (KU). Dr. Middaugh has challenged my imagination beyond what I thought was ever possible. I sincerely appreciate his time and efforts in my scientific upbringing.

I am ever so grateful to Dr. Sangeeta Joshi for her constant support, patience and friendship. Thank you for being around in all the good and tough times throughout my doctoral work. I also want to thank my thesis committee, Dr. Teruna Siahaan, Dr. Jennifer Laurence, Dr. David Volkin and Dr. David Weis, for their constant guidance and help during my doctoral research. I am also grateful to our industrial collaborators, Drs. Sathish Hasige, Steve Bishop and Hardeep Samra from MedImmune, for providing an opportunity to pursue research projects relevant to industry.

I was fortunate to have worked with wonderful colleagues in Middaugh laboratory and I thank each one of them for their contribution and support. Special mention of thanks to Drs. Chris Olsen, Yuhong Zeng, Tim Kamerzell and Olivier Mozziconacci for their help in providing me the necessary training in biophysical research. I acknowledge all the faculty members in KU Pharmaceutical Chemistry department, with special thanks to Drs. Stella, Schoneich and Berkland, for offering an excellent course work in the department. The rigorous course work in Pharmaceutical Chemistry program helped build the required foundation in chemistry, biophysics and pharmaceutical sciences necessary for my doctoral research.

Finally, I want to dedicate this section to my family and in-laws. Dad, Mom, Urvashi (my wife), Dimple (my sister) and my in-laws, you have been a source of inspiration and courage for all my ventures, including pursuing doctoral research. I cannot express in words how much I admire, respect and love you. Dad, getting a Ph.D. was a dream that you have treasured for yourself for over 30 years. It is a moment of satisfaction to have lived through your dream and accomplishing it today. Mom, your unconditional love and care has been a source of strength for the whole family. We all sincerely value your presence around us. Urvashi, you have been an unwavering support through long working days and nights during graduate school. Your dedication to the family is the reason why we accomplished things that we had only imagined at some point. Dimple, your love and support is always treasured and needless to say I now hope to spend more time with you all. We all have been through trying times together and I believe completing my doctoral work would not have been possible without your support and sacrifices. Thank you for believing in me. I owe and dedicate this accomplishment to YOU, My FAMILY!!

TABLE OF CONTENTS

Chapter 1

Introduction

1.1 Overview

1.1.1 Understanding protein structure, folding, dynamics and stability

Most biologically active proteins adopt a characteristic three-dimensional native structure from an ensemble of unstructured or partially structured polypeptide chains[1]. Recently, a class of proteins known as "natively unfolded" has been identified[2] and is being investigated. Folded polypeptides chains have large accessible conformational space; yet, these structural elements have a natural propensity to lower their free energy and fold into highly ordered native structures. The rationale for protein folding has evolved on the basis of a number of different fundamental concepts; i.e., non-random interactions within the unfolded state of proteins are thought to limit the conformational space available for the initiation of a folding reaction[3]. Secondly, folding intermediates are considered as ubiquitous stepping stones, in which even the smallest proteins are stabilized by native and non-native interactions involving such intermediates en route to the native state[4]. Thirdly, a rugged, funneled energy landscape model describes protein folding as a consequence for unstructured polypeptide chains which lowers their free energy to form ensembles of native three-dimensional structures that increase their stability[5]. Protein folding energy landscapes are rugged due to the fact that numerous weak stabilizing interactions necessary for protein folding cannot simultaneously exist at any given time during a folding process. This leads to 'frustration' in the energy landscape[6,7]. In addition, such ruggedness can be considered as mechanisms which counteract evolutionary pressures, thus enabling protein sequences to fold reliably into biologically active proteins, thus preventing their aggregation[6,7]. An arsenal of highly sensitive methods such as fluorescence spectroscopy[8-10], circular dichroism[11], vibrational spectroscopy[12,13], small-angle X-ray scattering[14], real-time

NMR[15], native-state hydrogen exchange[16], pulsed H/D exchange by NMR/mass spectrometry[16,17] and protein engineering[18] have been employed to study the non-native unfolded or partially folded intermediate species that are involved in the process of protein folding into their stable functional forms. These techniques provide highly sensitive tools for monitoring of structural transitions on the timescales of picosecond to seconds (or even longer) and spatial order of 0.01 to > 5 Å. Newer advances in single-molecule techniques[10,19] can potentially map the folding events of individual molecules, thus enabling characterization of intermediate species that are less populated and those that are difficult to detect by the inherent averaging of ensemble-based experimental approaches[20].

The stability of the native structure of proteins results from contributions from covalent bonds within the peptide backbone and also between cysteine residues as well as non-covalent interactions comprised of apolar interactions, intra-peptide and/or peptide-water hydrogen bonds and entropic contribution from configurational degrees of freedom[21,22]. Attractive or repulsive electrostatic interactions involving charges and both static and transient dipoles within a protein molecule and with the surrounding solvent further contribute to the overall structural stability of proteins[21,23]. The surface characteristics of proteins determine the structure and organization of hydration water, which in turn also modulates the stability and molecular (intra- and inter-) interactions of individual protein molecules[24,25]. In addition, the packing of the apolar protein core is primarily governed by short-ranged van der Waals repulsions and attractive dispersion forces[21]. The complex interplay of these contributions plays an important role not only in determining the conformational stability of proteins[22] but also in modulating their functional characteristics. Despite the propensity of proteins to fold by lowering their free energy (and thus increase stability), they are generally only marginally stable with ~ 20 – 40 kJ mol^{-1} of unfolding

free energy[26]. It is postulated that the limited stability of proteins help retain their inherent flexibility which is necessary for biological roles such as transport across membranes, binding of substrates and ligands, natural turnover within cells and for processes such as allostery and signal transduction[27]. The roles of protein flexibility have been extensively debated with evidence, for example, to support inter-relationships between flexibility and conformational stability of enzymes in the ground state and the highly dynamic nature of their transition states necessary for enzyme catalysis[28-30]. The dynamic nature of proteins arises from statistical fluctuations in thermodynamic parameters such as enthalpy and volume changes of different conformational ensembles. These fluctuations can be studied by evaluating thermal expansivity, compressibility and changes in heat capacity[31,32] of proteins. The challenge, however, in studying such thermodynamic parameters is that similar fluctuations between individual molecules may not be coordinated and the experimental observable will result in averaging and non-fluctuating thermodynamic parameters. Modern biophysical tools including time-resolved and single-molecule analysis have addressed these challenges[10,12] with limited success. Techniques involving amide hydrogen/deuterium exchange coupled with infrared spectroscopy[33], NMR[34] and mass spectrometry[35] are promising alternative approaches to investigate changes in local and regional flexibility in proteins. Thus, the connection between flexibility/dynamics, function and stability continue to evolve in the literature[29,36-41].

1.1.2 Biological water and hydration: Influence on the folding, dynamics and stability of proteins

Biological water, defined as water associated with tissues and cells, is a critical substance which plays a key role in the control of different processes within biological systems. Both excesses and deficiencies in hydration may result in loss of protein activity and may trigger cell

malfunctioning and eventually cell death[42]. Water, despite its simple chemical structure has unusual thermodynamic behavior. For example, the melting/boiling points or heat of fusion and vaporization are higher than other liquids that are composed of hydrogen and oxygen. Biological water that forms a hydration shell around proteins exists in highly confined environments and usually only a few molecular layers thick. The characteristics of this hydration water are strikingly different than that of bulk water. The high dielectric constant of water is believed to play a critical role in protein folding, in which water serves as an excellent solvent which screens electrical charges preventing non-functional interactions. The conflicting properties of apolar sidechains in amino acids and the polar nature of water are believed to result in the hydrophobic collapse of polypeptide chains into natively folded structures in which the tightly packed core of a typical protein primarily contains nonpolar sidechains. Such "hydrophobic effects" are considered to be central to protein folding mechanisms[43,44].

It is now well accepted that water is not an inert environment for biomolecules; its role is well recognized in defining the structural and dynamic characteristics of various other biomolecular[44,45] and pharmaceutical systems[46,47]. The dynamics of protein-solvent interactions, especially water in hydration layers, are therefore important to characterize. Techniques such as dielectric relaxation, X-ray diffraction, neutron scattering, ultrafast laser spectroscopy and NMR can be employed to study them[48]. A few of the findings from these studies are summarized here. It was determined that the dielectric properties of hydrating and bulk water properties are different. For instance, relaxation times of 8.3 ps, 40 ps, 10 ns and 80 ns were measured for the hydration water of myoglobin in contrast to 8.2 ps for bulk water at 298 K[49]. These results suggest that the residence time of water at a protein's surface is different than the characteristics of the bulk water. These distinct properties reflect differences in the behavior of hydration water

potentially due to its interaction with the surface of a protein. X-ray diffraction studies illustrate both static view of buried bound water and have also elucidated the solvation layer of proteins containing both ordered and partially disordered water in solvent shells[50]. It was determined using high-resolution protein NMR that a small number of water molecules with residence times on the order of 10^{-2} to 10^{-8} seconds are located in identical positions in the interior of proteins, both in crystals and in solution[51]. In contrast, the water molecules hydrating the surface of a protein were found to have residence times in the range of sub-nanoseconds (~ 300 – 500 ps)[52]. The above examples all illustrate that biological water, hydration water in particular, has a profound effect on the physics and functional properties of biological molecules. A comprehensive knowledge of the design of proteins and macromolecules and their interaction with water is therefore necessary to understand the folding, dynamics and stability of biologically and pharmaceutically relevant proteins. A protein's conformational stability, dynamics and function are often coupled to the properties of its surrounding environment[53-55]. The stability of proteins is determined by a marginal preference of a plethora of counteracting enthalpic and entropic contributions for the folded over unfolded states of proteins. In addition, native states of proteins contain a large number of energetically nearly equivalent microstates that can rapidly interconvert, giving rise to a protein's dynamic behavior. Interconversions of microstates originate from any number of different sources, including the movement of secondary structure elements relative to each other, alterations in loop conformations and/or reorientations of amino acids side chains[56]. The variability of such dynamically interconvertible conformers has been extensively studied to better understand their role in biological functions such as ligand recognition and enzyme catalysis[57-61]. In solution, conformational flexibility and dynamics are often accompanied by a wide range of hydration states unlike the situation in

crystals[44]. These fast conformational fluctuations in proteins are a consequence of constantly changing patterns of hydrogen-bonding networks due at least partially to the dynamic nature of associated hydration states[62,63]. It has therefore been suggested that the intimate coupling of solvent and protein dynamics can result in "slaving" of protein dynamics to solvent fluctuations[53,55], which eventually affect the function of proteins[64-67]. Solvent fluctuations are thought to originate from changes in the dielectric relaxations rate coefficients of solvent molecules resulting in alterations in their average tumbling time[53]. Temperature, among other factors, is known to modulate solvent fluctuations and any coupled motions in proteins[53].

1.2 Cosolvents and osmolytes: Effect on protein stability and dynamics

Since proteins are marginally stable in solution and the surrounding aqueous solvent plays a dominant role in determining folding, dynamics and stability, it is important to understand the effects of changes in solvent properties induced by the presence of cosolvents and osmolytes (naturally occurring or those used as pharmaceutical excipients) on the behavior of proteins. For instance, changes in the chemical potential of the solvent due to the presence of different cosolvents may have a profound effect on protein dynamics, stability and protein-solvent interactions[68]. In addition, changes in solution pH may influence the stability and dynamics of proteins by influencing the ionization state of various amino acid side chains in different conformational states (folded, dynamic microstates and/or unfolded). Such changes in the nature of the solvent may eventually lead to alterations in intramolecular interactions in proteins, restructuring of the solvent around the surface and its solvation energy.

At a molecular level, potential mechanisms for solvent effect on proteins can be broadly categorized as following: (a) a direct interaction between the protein's surface and cosolvents,

(b) an indirect effect due to alterations in the water of hydration, both on the protein's surface and its interior and, (c) changes in the structuring and/or ordering of water molecules in the hydration shell such that it enables interaction of cosolvent with the protein surface. Based on these potential mechanisms, cosolvents can be categorized into 'compatible' and 'non-compatible' cosolvents. Compatible cosolvents, such as osmolytes and kosmotropes (water structure-making), are those that help retain the structure and functional properties of proteins, potentially by influencing the surrounding water. Non-compatible cosolvents (e.g., urea, guanidinium hydrochloride) are those which disrupt protein structure and hence their functionality. The latter includes chaotropes (water structure-breaking) that disrupts the structure of hydration water as well as bind directly to the proteins. The chemical properties of the solvent, in both the absence and presence of cosolvents, are therefore critical determinants of a protein's structure, stability, function and dynamics. Nevertheless, these effects at a molecular level should influence the forces that are involved in maintaining folding, stability and dynamics of proteins in both solution and in the dried state. Some of these dominant forces[22] in the context of protein stability and dynamics are reviewed in the following section.

1.2.1 Molecular factors governing stability and dynamics of proteins in the presence of solvent[21,22,38,43,69,70]

1.2.1.1 Intra- and inter- molecular interactions

A majority of the intramolecular interactions that modulate the stability and dynamics of proteins are comprised of, but not limited to, long-ranged electrostatics, hydrogen bonding and van der Waals interactions, apolar interactions and entropic contributions. All of the forces (with some weaker and others more dominant) mentioned above have positive contributions to protein

folding except for conformational entropy, which opposes protein folding and negatively contributes to stability. These forces are responsible not only for overall protein folding but also are critical in determining the internal organization of irregular and regular structures such as helices, sheets and turns within globular proteins. The dependence of protein structure and stability on pH and ionic strength highlights the importance of electrostatic contributions to the proper folding of unstructured polypeptides. Electrostatic contributions to protein stability and dynamics can be influenced by specific charge interactions such as ion pairing (salt bridges) or non-specific repulsive interactions that are prominent at extreme solution pHs and away from the isoelectric point of the protein.

Hydrogen bonding is a pseudo-linear arrangement of a shared hydrogen atom between a donor – acceptor pair. The electronegativity, distance and orientation of these atoms along with their electrostatic, charge-transfer, steric-repulsive and dispersive interactions eventually determine the number and strength of hydrogen bonds. On other hand, Van der Waals interactions arise between fluctuating induced dipoles. Hydrogen bonding and van der Waals forces are arguably considered weak forces in protein folding and stability. These forces can, however, be critically involved in the conformational changes of proteins because some amino acid side chains comprised in proteins are dipolar in nature and can readily be involved in hydrogen bonding. Secondly, the stability of secondary structure elements such as helices and sheets in a protein's architecture, as well as their transitions, may largely be governed by fluctuations in local hydrogen bonding networks within these elements. In contrast, some unfolded proteins are known to possess residual secondary structure. Solvent unfolding studies indicate that both hydrogen bonding and van der Waals forces may be weak forces contributing to protein folding and may not be critical determinants of overall protein stability. A significant

role for these forces, however, has been well recognized as being involved in determining the internal architecture of proteins including the formation and spatial distribution of turns, which do not generally depend on the packing forces alone as described later in the text for overall globular stability. The dynamics of hydrogen bond formation and/or breaking is believed to be a critical determinant in the inherent dynamic nature of proteins, in which several interconvertible conformational microstates with small differences in energy are in equilibrium with each other. The intermolecular bond angle between water molecules, the dynamics of H-bond formation (generally are < 1 ps timescale) and the interactions of water molecules with a protein's surface and other neighboring water molecules potentially govern the stability and interconversion of the microstates and thus play a key role in governing the dynamics and function of proteins[56,71].

Apolar interactions, often called hydrophobic interactions, are considered to be one of the dominant forces contributing to protein folding and stability. Their role in protein folding stems from the fact that apolar amino acid sidechains in unstructured polypeptides coalesce away from polar water molecules which results in 'hydrophobic collapse' into natively folded structures. The impact of these interactions to protein stability is unique due to their complex dependences on temperature. The transfer of non-polar solutes into water is accompanied by large and positive change in heat capacity[72,73]. At low temperatures (~ 25 ^{o}C), the structure of water around apolar residues is more ordered and water prefers to form hydrogen bonds with other water molecules. These low temperature interactions are driven mainly by entropic contributions. At higher temperatures, the aversion of nonpolar residues for water is accompanied by a maximum free energy of transfer and in these conditions, the entropy is close to zero. Therefore in such a system, enthalpic contributions become more prominent in governing the overall interactions of nonpolar solutes in solution. Similar phenomena are also

present for apolar amino acid side chains in proteins. Both temperature and changes in solution conditions therefore become critically important in determining apolar contributions to the stability and dynamics of proteins, with potentially distinct effects at low and high temperatures.

Finally, a dominant force that opposes protein folding and stability is *entropy*. Local entropy that opposes formation of helices is an important contributor to the overall entropic contributions to the system. In addition, non-local or configurational entropy originates from steric constraints or excluded volume effects. These are temperature dependent effects associated with changes in thermodynamic parameters due to solute concentration, their colligative properties, compressibility and expansibility and various non-ideality effects. Proteins undergoing unfolding are known to gain considerable entropy. Conversely, during hydrophobic collapse and protein folding, there is a considerable loss of non-local entropy in converting from the large volume of unfolded states of polypeptide chains to the smaller collapsed volumes of native states. These resulting native structures are known to have lower compressibilities and their configurational freedom is severely restricted, similar to those found in crystals or glasses. Since these contributions are intimately linked to temperature and solution properties, it is possible that conditions which destabilize proteins in solution may have a profound influence on such interactions and thus modulate the overall stability and dynamics of proteins.

Protein solutions containing additives such as osmolytes or pharmaceutical excipients or at high protein concentrations, such as in cells or high concentration biopharmaceuticals, also experience intermolecular interactions between proteins or between proteins and solute molecules. Osmolytes are natural compounds which stabilize cells against dehydrating stress in vivo and maintain their osmotic equilibrium. These compounds are also employed exogenously

to stabilize proteins and macromolecules in both the solution and dried state against various external stress conditions. These include changes in temperature and pH of solutions, alterations in the moisture content of dried solids and the presence of salts and other additives. At a molecular level, osmolytes and/or other additives are believed to influence proteins by either being attracted or repelled from the surface of the protein[74-77]. This is in turn related to their differential interactions with the surrounding water[78].

Overall, the mechanisms of such intermolecular interactions, primarily involving the protein surface and surrounding solvent, were categorized by Ohtake S et al.[78] into four different categories: the cohesive force of water, unfavorable interactions with peptide backbones, steric or excluded volume effects and preferential interactions (both exclusion and binding). Stabilizing cosolvents are known to increase the surface tension of water and thus exert a cohesive force or attraction pressure[79,80] on water. Even though protein surface – additive interactions continues to be a field of active research, the seminal work by Traube provided the mechanistic knowledge necessary to understand the correlations between attraction pressure and protein stability. Solutes that are larger than water are generally excluded from a protein's surface. Such a repulsive process is thermodynamically unfavorable. It is therefore assumed that due to such effects, stabilizing excipients that are excluded from a protein's surface commonly result in a lowering of the protein's surface area, eventually making the native structure more compact. An unfavorable interaction of solutes with the peptide backbone is also proposed as a potential stabilizing mechanism. Such interactions are related to excluded volume effects in which the stabilizing excipient remains in the bulk solvent more than the hydration layer near the protein's surface. Finally, probably the most widely accepted mechanism involves 'preferential interaction' or 'preferential exclusion' of cosolvent from the protein surface. In this

situation, the cosolvent/solute concentration in the local region near a protein's surface varies. Such an effect is known to influence the thermodynamic properties of proteins which in turn influence their solubility and conformational stability.

These interactions are routinely quantified using a parameter known as the preferential interaction coefficient (Γ_{23}), the magnitude and sign of which are related to the propensity of a solute to either preferentially bind to or be excluded by a protein's surface. A positive Γ_{23} value indicates that the additive concentration in the protein's hydration shell is higher than bulk water due to the preferential binding to a protein's surface. A negative Γ_{23} value is indicative of preferential exclusion (also called preferential hydration) of additive from the protein surface. In this case, the hydration shell around the protein is usually more structured and ordered in the presence of such excluded solutes. These interactions not only influence the chemical potential of a protein but also result in volume exclusion (repulsive) interactions and alteration of surface free energy. Specific interactions such as hydrogen bonding[81], electrostatic interactions[82], apolar interactions[81] and cation-π interactions[83] have also been reported between proteins and solutes. Kosmotropes (structure-making) and chaotropes (structure-breaking) are known to alter the structure and ordering of bulk water. Such an effect also, arguably, causes an indirect effect on protein-water interactions and thus influences their stability[84,85]. Finally, intra-solvent interactions have recently garnered significant attention in which additive-additive interactions in solution influence protein stability. The Hofmeister Series of ions have been extensively studied to better understand whether such intra-solvent interactions can explain the unique serial behavior and ranking of these ions in solution.

It is evident that the effects of cosolvent or solute interactions on protein stability have been and continue to be exhaustively studied. Studies evaluating the effect of solutes on protein

dynamics, however, are rather limited[38,86-97]. Attempts to address this void are therefore presented in the current studies and an effort is made to obtain molecular insights into excipient effects on global and local protein dynamics, conformational stability, intra- and inter-molecular interactions, and potential correlations that may exist among them.

1.2.1.2 Fluctuations in thermodynamics parameters

Protein dynamics is associated with fluctuations in thermodynamic parameters such as the volume and enthalpy of different conformational microstates of native proteins. The fluctuations in volume can be related to changes in the compressibility of a protein. Alterations in specific heat can explain enthalpy fluctuations. The coefficient of thermal expansion correlates with both volume and enthalpy fluctuations. Compressibility, the coefficient of thermal expansion and specific heats can all be obtained experimentally in the presence of various solvents and solutes enabling an investigation of cosolvent effects on the dynamics of proteins. Isothermal compressibility represents the relative change in volume of proteins with infinitesimal changes in pressure and can be experimentally obtained using ultrasonic spectroscopy[38,98-101]. The relationship between isothermal compressibility and volume fluctuations can be given as,

$$< \delta V^2 > = k_B T V \beta_T \qquad \text{and,} \qquad \beta_T = -V^{-1} (\frac{\delta V}{\delta p})_T$$

Where k_B is the Boltzmann constant, V is the intrinsic volume of a protein, T is absolute temperature and β_T is the isothermal compressibility. The compressibility of a protein has contributions from packing density (i.e., cavities), non-covalent and covalent (disulfide bonds)

interactions that stabilize proteins and contributions from hydration. In general, protein compressibility is thought to inversely correlate with stability. The coefficient of thermal expansion, obtained from pressure perturbation calorimetric experiments[100,102-104], represents relative changes in volume upon changes in temperature and this parameter is used to correlate volume and energy fluctuations of a protein. These terms can be mathematically represented as,

$$< \delta H \delta V > = k_B T^2 V \alpha_p \qquad \text{and,} \qquad \alpha_p = V^{-1} (\frac{\delta V}{\delta T})_p$$

Where α_p is coefficient of thermal expansion, which also has contributions from both intrinsic and hydration components. The enthalpy fluctuations of a protein system can be evaluated using the isobaric heat capacity at constant T and P. Since the absolute value of the partial molar enthalpy cannot be experimentally determined, the heat capacity is not a relative parameter (unlike compressibility and coefficient of thermal expansion). The relationship between heat capacity and enthalpy fluctuation can therefore be given as,

$$< \delta H^2 > = k_B T^2 C_p \qquad \text{and,} \qquad C_p = (\frac{\delta H}{\delta T})$$

Where C_p is the partial molar hear capacity with this parameter also representing both intrinsic (minor) and significant hydration contributions. Even if these parameters can be studied in the presence of solutes, it is important to note that the dynamic information obtained from these measurements represent global dynamic phenomena in proteins. Solute effects on local protein dynamics can be evaluated using fluorescence spectroscopy and other methods. The findings of such studies are presented in Chapter 3.

1.2.1.3 Candidate solutes/excipients: Sucrose and arginine.

Sugars and amino acids are frequently used as additives/excipients to increase conformational stability and/or inhibit aggregation of proteins and biopharmaceuticals, both in the solution and dried states[78]. Disaccharides such as sucrose (the major stabilizer used in these studies) are known to act as osmolytes and are found naturally to stabilize micro-organisms under severe environmental conditions. These disaccharides stabilize proteins in solution by the preferential hydration mechanism[105]. Since osmolytes-protein surface interactions are thermodynamically unfavorable, compounds such as sucrose are believed to increase the free energy of both the native and unfolded states of proteins. The magnitude of increase in free energy, however, is greater for unfolded forms of the protein due to their increased surface area. The resulting increased free energy of unfolding in the presence of stabilizing solutes such as sucrose is therefore hypothesized to be responsible for their stabilizing effect. In addition, the prevention of aggregation by osmolytes is thought to be due to a smaller free energy of association, which results in shifting the monomer-aggregate equilibrium towards the monomeric form of the protein. Amino acids are generally known to stabilize proteins by various mechanisms such as preferential hydration, direct binding, buffering properties and antioxidant behavior[106,107].

The mechanism of arginine and its salts (the major destabilizer of this study) is unique among amino acids and is a topic of active research[106,108-110]. The structure of arginine results in the potential to form a variety of intra- and inter-molecular interactions due to its following characteristics[70]; the size of the molecule is larger than water and therefore can be excluded from a protein's surface while increasing the surface tension of the solution. Its zwitterionic nature and the salt form (usually HCl salt) create a polyanion with a delocalized positive charge, which

can significantly influence a protein and water structure via electrostatic interactions[70,78]. The H-bond accepting carboxylate group and H-bond donating amino group provide H-bond forming capability of the compound with water, the protein surface and other charged and aromatic amino acid side chains in proteins. Additionally, the three carbon alkyl side chain imparts hydrophobic character to a part of the molecule. Historically, arginine effects were commonly attributed to the presence of the guanidium group. Quite a few alternative explanations, however, have been proposed to explain the complex effects of arginine on protein stability and aggregation. For instance, arginine, unlike other amino acids, does not affect the folding equilibrium of a majority of proteins[106]. Arginine is also believed to have a kinetic effect on protein association, which was explained by the 'Gap Effect' theory[111]. A recent study in regards to preferential interaction of arginine showed that the arginine is neutral at low concentrations, whereas it becomes highly excluded at higher concentrations[112,113]. This plethora of explanations makes arginine interactions extremely specific for individual proteins, and therefore, it appears that these effects need to be investigated on a case-by-case basis.

The highly dynamic and flexible nature inherent to most folded, globular proteins may significantly influence the intrinsic stability of proteins. Any approach including the use of additives/excipients that affects the conformational stability of proteins or biopharmaceutical products may potentially exert its effect through perturbations of the dynamic behavior of proteins. Sucrose and arginine were found to stabilize and destabilize candidate immunoglobulins, respectively, in the studies presented in Chapter 2 and Chapter 3 of this dissertation. Since both of these excipients have effect on the properties of water around proteins, it was hypothesized that the stabilizing and destabilizing effects of these excipients may

influence both the hydration dynamics and the coupled global and/or local dynamics in immunoglobulins.

1.3 Monoclonal antibodies as candidate systems: Structure and dynamics

1.3.1 Structure, function and dynamics

Natural immunoglobulins[114] (Ig) or recombinant monoclonal antibodies (mAb) are an important class of dynamic glycoproteins with a wide variety of biological and biopharmaceutical roles, respectively. These are characteristic Y-shaped structures (Figure 1) containing four polypeptide chains; two heavy (each ~ 50 kDa) and two light (each ~ 25 kDa) chains. These light and heavy chains can be sub-categorized into variable and constant regions. The light chain and heavy chains are held together by disulfide bonds to form an antigen binding region (F_{ab}) that binds to foreign antigens such as bacteria or virus to initiate an immune response. The constant region is held together by covalent disulfide bonds and apolar interactions to form a crystallizable fragments (F_c) that is responsible for complement activation and effector functions. The two F_{ab} domains are connected to the F_c domain by a highly flexible hinge region, which is believed to be responsible for the major dynamic motions of immunoglobulins[115].

Antibodies are categorized into five major classes i.e., IgG, IgM, IgA, IgE and IgD, depending upon the number of Y-shaped units and the type (size and sequence) of heavy-chain polypeptides. The type of heavy-chains present in IgG, IgM, IgA, IgE and IgD are γ-, μ-, α-, ε- and δ-chains, respectively. The differences in heavy-chains determine the distinct biological role of these antibody classes which are known to be functional at different stages of the immune response to an external stimulus. In addition, these different classes of antibodies vary in the number of Y-shaped units that combine to form a functional protein.

For instance, IgM has five Y-shaped units combined together to eventually have 10 similar antigen binding sites. The heavy chains in different classes of antibodies have minor variations in their sequence such that μ- and ε-chains in IgM and IgE, respectively, have four constant domains in their heavy chain (C_H) while the γ-, α- and δ-chains in IgG, IgA and IgD antibodies are relatively shorter with only three C_H domains. It is known that the sequences of C_H1, C_H3 and C_H4 in IgM and IgE correspond to C_H1, C_H2 and C_H3 domains in IgG, IgA and IgD. Furthermore, a classical hinge regions is absent in IgM and IgE with the flexibility of the F_{ab} arms in these classes of antibodies conferred by their C_H2 (unrelated to the C_H2 domains of IgG, IgA, IgD) domains.

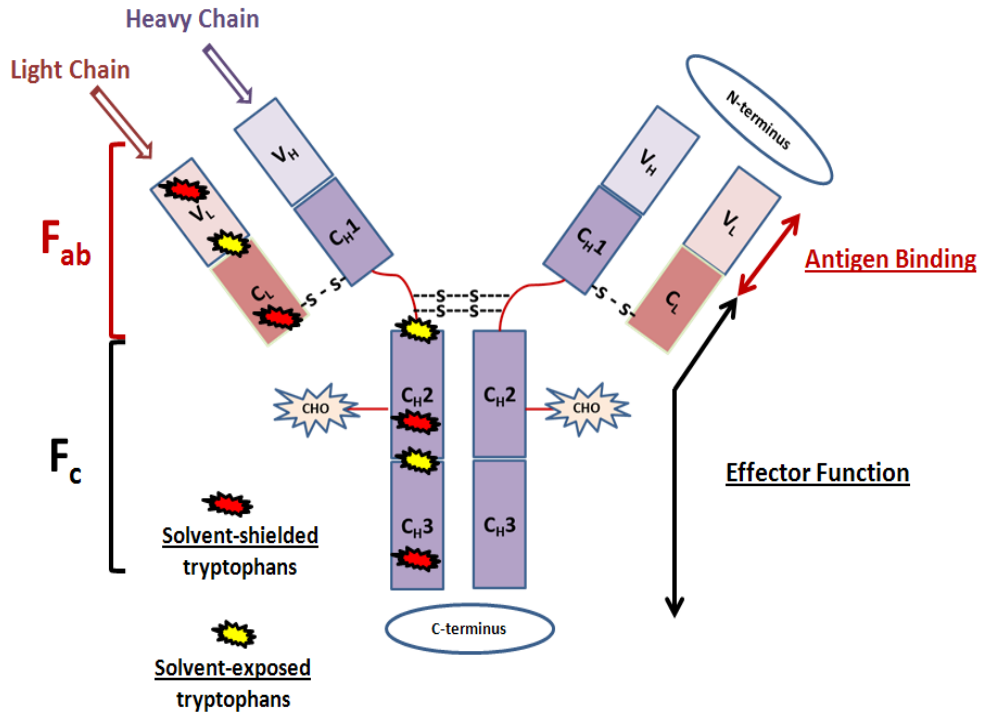

Figure 1: Representative structure of an IgG antibody. A similar organization of conserved solvent-exposed and solvent-shielded tryptophan residues are also located on the other half of the molecule.

In contrast, IgG and IgD have extended hinge regions that impart distinct dynamic properties to these molecules. The variations in the structure of the hinge region in different classes of antibodies may therefore be responsible for the differences in the structural arrangement and dynamics of the F_{ab} and F_c regions[116]. Typically, the hinge region is known to contain many proline residues which are thought to impart rigidity to the top of the stem in the antibodies. The glycine residues in the hinge region, however, create a flexible secondary structure in which the F_{ab} regions can move semi-independently around the proline-stabilized focal point. The disulfide bonds in the hinge region are also believed to have an effect on stability, dynamics and functional characteristics of the different antibody classes. The variations in the amino acid sequences of γ- and α-heavy chains in IgG and IgA, along with the number/location of disulfide bonds and the length of the hinge regions give rise to Ig subclasses such as IgG1, IgG2, IgG3 and IgG4, and IgA1 and IgA2. In addition to differences in heavy-chains, immunoglobulins have two distinct light chains, κ and λ, bound in any number of different combinations with heavy chains helping to determine the variability in functional properties of the antigen binding (F_{ab}) regions.

Immunoglobulins are categorized as glycoproteins by virtue of their carbohydrate content, which varies with Ig isotype. The carbohydrate content is relatively higher (~ 12 – 14%) for IgD, IgE and IgM, while a lower content (~2 – 3%) is found in IgA and IgG. The number and location of oligosaccharide units differ between different molecules secreted from the same clone of a B-cell and also depend upon physiological variables at the time of protein's post-translational modification. The carbohydrate moieties are usually located on the C_H2 domain (C_H3 domain for IgM and IgE) of IgG, IgA and IgD. The carbohydrate containing domain, in contrast to other constant domains in heavy chains (C_H), generally does not interact with the

corresponding domain on the complementary heavy chain due to the presence of these oligosaccharide units. The lack of strong interactions and relatively easy accessibility of this domain usually has a significant impact on stability and reversibility, function and dynamics of this region of the antibody. The C_H3 (or C_H4 if present) domain is believed to be involved in noncovalent interactions with its counterpart on the other heavy chain.

The biological function of a variety of proteins including immunoglobulins is closely related to their dynamics and flexibility[57,97,117]. The primary function of immunoglobulins is to bind and clear foreign antigens and thus protect the host. Antigen binding is carried out by variable regions of the antibody, the specificity of which depends upon hypervariable sequences in the V_H and V_L regions in the antibody. The effector functions of the antibody are mediated by the crystallizable fragment of the molecule which signals the innate immune response via F_c receptors on leukocytes. Since different classes of antibodies differ in their F_c region, the clearance mechanism varies depending upon the binding of foreign antigen to each specific Ig class. The effector functions are commonly categorized into four major roles; neutralization, opsonization, complement activation and antibody-dependent cell-mediated cytotoxicity. Since these molecules are evolved to perform highly specific roles, significant effort has been directed towards developing tools to characterize their structural, functional and dynamics properties.

Various analytical techniques such as fluorescence anisotropy[115,118-120], resonance energy transfer[121], two dimensional correlation FTIR spectroscopy[33], X-ray and neutron scattering[116], ultrasonic spectroscopy[38,120], pressure perturbation calorimetry[38,120], red edge excitation spectroscopy[120] and nuclear magnetic resonance spectroscopy[117,122] have been used to study the flexibility, dynamics and conformational stability of antibodies. Different molecules within an Ig subclass are broadly similar in their structure and sequence homology but still may strongly

differ in their dynamics, function and conformational stability. To evaluate such differences and understand their effects on protein dynamics and conformational stability is a major goal of the investigation presented in these studies. Furthermore, the conformational stability, and potentially dynamics, of antibody drugs formulated at both low and high concentrations is significantly influenced by environmental and formulation factors during their manufacturing, storage stability and delivery [123-125]. The highly dynamic nature and unique multi-domain structure of antibodies makes them ideal candidates for studying the inter-relationship between conformational stability and dynamics in a variety of different solution and formulation conditions.

1.3.2 Instability and stabilization approaches for antibodies at low and high concentrations

Immunoglobulins, more specifically monoclonal antibodies, are been increasingly developed as protein therapeutics. Many advantages to antibodies such as functional specificity, fewer side effects, potential application in conjugating and targeting chemical drugs and targeted drug delivery, diagnostic applications upon conjugation of radioisotopes and potential to make less immunogenic humanized antibodies makes them attractive drug candidates. Like any other protein based drug, development of monoclonal antibodies as biopharmaceuticals has significant challenges involving physical and chemical instability in both solution and solid forms. As discussed earlier, the highly dynamic nature of immunoglobulins adds an additional dimension of complexity, which is currently perhaps not highly appreciated during protein drug or product development. Understanding immunoglobulin dynamics and their influence on conformational stability may not only help produce drugs but will also help in understanding their intra- and inter-molecular interactions with cosolvents, excipients and delivery devices among others.

Excellent reviews[46,125-128] are available to describe instability considerations and stabilization approaches for proteins. Some aspects are briefly summarized in the following section.

1.3.2.1 Physical and chemical instabilities of immunoglobulins

The major physical pathways to render immunoglobulins unstable are conformational changes and aggregation. *Conformational changes* (including unfolding and ultimately denaturation) can be caused by a variety of factors including pH, temperature, shear, freeze/thaw and the presence of chaotropes. Manufacturing and other processes such as lyophilization can also result in unfolding or other structural changes in the native structure of antibodies. *Protein aggregation* is usually considered a major challenge in protein drug development and can have deleterious immunological consequences. Aggregation can result in particles which can significantly vary in their size, shape and morphology. Such heterogeneity makes studying this phenomenon[129] and their consequences[130-132] extremely complex but important. A primary mechanism for protein aggregation is protein-protein interaction, in which various factors such as protein concentration, pH, temperature, salts, and physical phenomenon such as diffusion rates and steric constraints play a dominant role in determining the rate and extent of self-association. Various additional factors such as freeze-thaw, shaking, and long-term storage among others are responsible for differences in the extent of aggregation, morphology and number/size distribution of aggregated particles. These factors eventually influence chemical characteristics and reversibility of protein aggregates. *Surface adsorption* is another aspect of protein behavior which has gained significant attention recently. Such a phenomenon can lower the protein concentration in solution and adversely perturb the conformational stability of proteins.

Chemical instability in proteins has serious consequences that not only affect the physical stability of proteins but may also have undesirable biological effects. Major chemical

degradation pathways include deamidation[133,134], isomerization[135], oxidation[133], cross-linking and disulfide bond scrambling[136-138], C-terminal clipping[139], peptide bond hydrolysis and fragmentation[140] and in some cases formation of glycated products[141] in presence of reducing sugars. If such changes occur in the hypervariable regions of antibodies, their binding properties can be negatively affected.

1.3.2.2 Stabilization approaches

Immunoglobulins can be stabilized either by changing the structural characteristics of the protein and/or changing its interaction with the surrounding solvent by the addition of cosolvents or solutes. It is often observed that changing the intrinsic structural features of protein (i.e. altering its sequence) often affects its thermodynamic characteristics, which can influence its functional stability or dynamic properties. A more simplistic and commonly employed approach is to modulate the chemical properties of the surrounding solvent using excipients such that the intra-molecular interactions in proteins are enhanced and the protein retains its native conformational properties. Various potential mechanisms by which excipient can alter a protein's stability and dynamics are discussed earlier in Section 1.2.1. A few promising yet challenging approaches towards increasing a protein's stability are modification of specific amino acids by mutagenesis[142], glycosylation[143], pegylation[144] and formation of disulfide bonds[145]. These modifications can significantly improve the stability of proteins although they often adversely affect the biological activity of the protein.

1.3.2.3 Challenges in high concentration protein formulations[126-128]

Protein drugs sometimes require multiple dosing atleast partially due to the inherent stability challenges discussed earlier. In addition, parenteral administration of protein drugs via

subcutaneous or intramuscular routes (using <1.5 mL) may necessitate that protein drugs be formulated and manufactured at high concentrations up to hundreds of milligrams per milliliter. Many of the characteristics of protein solutions at low and high concentrations are strikingly different due to the fact that proteins will experience increased interactions with themselves as well as other solutes at high protein concentrations. These intermolecular interactions dramatically increase at high protein concentrations and can result in a variety of protein specific and process related challenges. The solubility, stability, viscosity and colloidal properties of proteins significantly change in high concentration proteins. The contributions of various intra- and inter-molecular forces (i.e., hydrogen bonding, electrostatic, van der Waals forces, apolar interactions and excluded volume effects), which commonly stabilize proteins, can be very different in dilute and concentrated protein solutions. For instance, electrostatics and apolar interactions have greater contributions to protein-protein interactions in dilute solutions compared to hydrogen bonding, van der Waals effects and excluded volume phenomenon. Activity coefficients of proteins at high concentrations can also become quite large (>1000), causing atypical behavior[146,147]. Excluded volume effects and proximity energies[23] become more critical in concentrated protein solutions.

One major challenge in such solutions is concentration dependent protein aggregation, which not only involves formation of non-native aggregates and particles but may also involve reversible self-association. Self-association in high concentration proteins primarily involves formation of dimers or other defined oligomers via non-covalent interactions. Such processes can occur on a temporal scale of few seconds to months. Self-associating proteins in crowded environments such as in a cell or high concentration biopharmaceutical products is accompanied by increased short-range interactions, with consequences such as increased solution viscosity as

well as prolonged biological half-life and possibly increased immune responses upon parenteral administration. Additional aspects such as increased opalescence may also compromise quality and acceptability of a protein based products. Since the consequences of self-association are unique, there continues to be a quest for developing newer analytical approaches to better understand such interactions in high concentration proteins. Chapter 4 in this dissertation presents one such unique approach. It has been reported that reversible self-association makes proteins amenable to formation of covalent linkages that may affect the reversibility of associated structures and can also lead to the formation of irreversible aggregates[148]. Such a 'switch' can have deleterious effects on the stability of native proteins and consequently their biological activity.

Reversible self-association in IgG molecules has been proposed to occur by two distinct mechanisms[149]: (1) $F_{ab} - F_{ab}$ interaction involving idiotypic and anti-idiotypic interacting sites on two IgG molecules and, (2) $F_c - F_c$ contacts involving apolar interaction between the C_H domains of two antibody molecules. Such interactions can be more pronounced in crowded environments in which excluded volume effects and proximity energies[23] (high thermodynamic activity) can lead to the complex attractive and repulsive contributions governing intermolecular interactions. In addition to well accepted steric constraints and repulsive interactions that explain high concentration behavior, the dependence of these interactions on the sign and magnitude of surface charges and the dipolar characteristics of adjacent molecules have recently come to the fore[23]. Furthermore, such processes not only govern intermolecular interactions but can have effects on protein (un)folding and the formation of structured (amyloid-like) and unstructured aggregates. Since protein dynamics may have a significant effect on both attractive and repulsive interactions on a wide range of timescales, it still remains unclear how dynamic aspects

of protein structural behavior govern these phenomena and their subsequent consequences. The findings presented in this dissertation and current research in progress are aimed at addressing some of these unanswered questions.

1.4 Empirical phase diagrams: Analytical tool in evaluating stability and dynamics of proteins (immunoglobulins)

The effect of varying solution conditions on the inter-relationship between structure, dynamics and stability is of profound biological and pharmaceutical importance. Various high resolution analytical techniques such as X-ray crystallography (which does yield temperature factors) and nuclear magnetic resonance (NMR) have inherent experimental challenges such as the relevance of the crystalline state or the need for isotope labeling which limit their application to routine high throughput analysis of biopharmaceutical systems. A variety of lower resolution techniques such as UV-absorption, fluorescence, circular dichroism, light scattering, calorimetric and chromatographic techniques can therefore be employed to characterize higher order protein structure and hydrodynamic properties[38,150-158] in a rapid and high throughput manner. It has becomes clear that internal molecular motions in macromolecules have a significant effect on their conformational stability and therefore measurements which can sample a wide range of motions with different timescales should ultimately become a routine set of measurements to characterize conformational stability. Various techniques sensitive to dynamic properties of proteins which can be employed in a high throughput manner such as high-resolution ultrasonic spectroscopy (HR-US), pressure perturbation calorimetry (PPC), red-edge fluorescence excitation shifts (REES), time-resolved (lifetime and anisotropy) fluorescence spectroscopy

(TCSPC) and temperature-dependent 2nd derivative peak position shifts of UV-absorption spectra over a variety of different solution conditions[38,100,120,152,153].

To establish the identity and integrity of macromolecules, and to better understand the complex inter-relationships between structure, stability and dynamics of large populations of conformational microstates, it is imperative to generate and analyze large sets of experimental data using multiple techniques that can probe both the static (time-averaged) and/or dynamic (time-resolved) properties of proteins and macromolecules[33,38,100,120,153]. The complexity of these data sets and their multi- dimensional nature make data difficult to analyze and interpret with simple approaches such as visual inspection of the data in two dimensional spaces and/or mathematical fitting of unfolding plots to functions such as sigmoidal or polynomial functions. Such local data inspection may not always reveal the details of behavior of high-dimensional data spaces, which may be required to understand the global features of complex macromolecular systems and further relate them to dynamics and/or stability. A mathematical analysis approach based on singular value decomposition, the empirical phase diagram (EPD) was therefore developed which globally analyzes complex multi-dimensional data sets generated from static (time-averaged) and dynamic techniques that are used to study biopharmaceuticals and vaccines. The multi-dimensional data sets are projected down to three dimensions as described earlier[159,160] and these three dimensional data sets are converted to different ratios of red, green and blue color to provide a simple visual representation, which manifests distinct segmented regions representing changes in the apparent conformational (or dynamic) properties of proteins or macromolecules over a range of solution conditions. Numerous such applications of EPDs have been reported which have evaluated the stability of a wide variety of macromolecular candidate systems such as proteins, plasmid DNA, viruses, virus-like particles

and antigens in the presence of adjuvants[120,159,161-181]. These EPDs have traditionally been used to aid in preformulation and formulation of biopharmaceutical drugs and vaccines.

In recent studies[86,120], however, EPDs generated using techniques (HR-US, PPC, REES, TCSPC) sensitive to the dynamic properties of IgG1 monoclonal antibodies (designated a "dynamic empirical phase diagram") were compared with a static phase diagram (which primarily represent the time-averaged structures) of the same antibody as a function of pH and temperature under similar solution conditions. The key finding in these studies was that the dynamic empirical phase diagram showed a more complex pattern of apparent phase transitions at lower temperatures in pre-transition regions before any detectable unfolding event compared to a corresponding empirical phase diagram using time-averaged measurements. The pre-transition region can be defined as the range of temperature and pH in which the protein retains its native structure and no major conformational change is observed. Therefore, EPDs can be successfully employed as a data analysis and/or a representation tool in evaluating the dynamic characteristics of proteins, such as immunoglobulins, in a variety of solution conditions as well be shown in depth below.

1.5 Chapter reviews

1.5.1 Effect of excipients on the conformational stability and 'global' dynamics of immunoglobulins (Chapter 2)

Chapter 2 is focused on (1) characterization and comparison of the conformational stability and global dynamic properties of two humanized IgG1 monoclonal antibodies, (2) identification of stabilizers and destabilizers from a library of Generally-Regarded-As-Safe (GRAS) excipients and, (3) evaluating the effect of candidate stabilizing and destabilizing

excipients on the conformational stability and global dynamics of the two IgG1 monoclonal antibodies, primarily in the pre-unfolding transition temperature range. The working hypothesis of this work was that formulation excipient(s) may affect conformational motions and/or solvent fluctuations in immunoglobulins. A combination of static (time-averaged) and dynamic-based techniques were employed to characterize the effect of pH and temperature on conformational changes and global dynamics of an IgG1 monoclonal antibody (mAb-A). Two separate empirical phase diagrams, one containing data from static (time-averaged) techniques and other containing additional data from HR-US measurements, were constructed to better understand the influence of global dynamic measurements on the pH/temperature behavior that can be detected in mAb-A by the EPD approach. The thermal stability of two IgG1s (mAb-A and mAb-B) were compared by measuring the transition midpoint of thermal unfolding (T_M) as a function of pH using differential scanning calorimetry (DSC). A high-throughput steady-state intrinsic fluorescence spectroscopic assay was used to screen a GRAS library of excipients to identify potential stabilizers and destabilizes. The effect of different concentrations of excipients on the conformational stability of mAb-A and mAb-B were studied by differential scanning calorimetry. Finally, the effect of candidate excipients on global dynamics was evaluated using ultrasonic spectroscopy and red edge excitation spectroscopy.

Even though the two mAbs are of the same IgG1 subtype, the unfolding patterns, aggregation behavior, and pre-transition dynamics of these two antibodies were strikingly different in response to external perturbations such as pH, temperature, and the presence of excipients. The potential reasons for such differences in solute effects between two IgG1mAbs are discussed in this chapter.

1.5.2 Effect of excipients on 'local' dynamics of a monoclonal antibody and correlations with its global conformational stability (Chapter 3)

Proteins such as immunoglobulins can exhibit motions with different magnitudes of spatial and temporal scales which may arise from distinct local regions within the protein. These regions may have different degrees of exposure to the solvent in their immediate vicinity which should involve water of hydration. Many compounds such as osmolytes are known to influence the hydration potential of proteins by modulating protein-solvent interactions in solution. Chapter 3 is thus aimed at (1) evaluating the conformational stability, dynamics and excipient effects on regions with distinct solvent-exposure in an IgG1 monoclonal antibody (mAb-B) as a function of temperature, as measured by fluorescence spectroscopy using red-edge excitation (REE) and, (2) better understanding correlations between local dynamics and global conformational stability of mAb-B, both in the absence and presence of stabilizing or destabilizing excipients.

The principles of site-selective photoselection upon red-edge excitation, accompanied by acrylamide quenching of tryptophan fluorescence were employed in this study. The initiation of mAb-B thermal unfolding occurs by structural alterations in the more solvent-exposed regions of the antibody, which subsequently leads to a cascade of structural alterations in its relatively more solvent-shielded regions. In addition, an increase in internal dynamics of solvent-shielded regions made mAb-B more susceptible to thermally induced structural perturbations resulting in its global destabilization. Sucrose and arginine were found to exert their stabilizing and destabilizing effects by predominantly influencing the conformational stability of solvent-exposed regions in mAb-B. The complex molecular effects of sucrose and arginine on local dynamics of different regions in mAb-B and their correlation with the protein's conformational

stability are described within the pre-transition range, at the onset temperature (T_{onset}) and at the thermal melting temperature (T_M).

1.5.3 Understanding interactions in high concentration protein solutions (Chapter 4)

As discussed in section 1.3.2.3, proteins at high concentration present unique challenges and limited experimental data are currently available that measure non-ideality effects in highly concentrated (>50 mg/mL or volume fraction >0.1) protein solutions or that employ non-hydrodynamic approaches.. Current analytical methods used to study protein interactions, however, rely primarily on the detection of non-ideality in relatively dilute (<50 mg/mL) solutions. Chapter 4 presents an application of variable path-length UV-Visible absorption spectroscopy to examine and better understand interactions over a wide concentration range (5 to 240 mg/mL) using several representative proteins. In this study, the change in ultraviolet absorption (or extinction coefficient) was monitored by determining delta absorbance (ΔAbs), the difference between the measured absorbance and the corresponding theoretical absorbance (calculated from gravimetric dilution), over a wide range of protein concentrations. The ΔAbs, corrected for light scattering, was found to increase with protein concentration for three model proteins (BSA, lysozyme and a monoclonal antibody). Since PPIs influence solution viscosity, we studied the correlation between ΔAbs measurements and viscosity as a function of protein concentration. The magnitude of ΔAbs and solution viscosity followed similar trends with increasing protein concentration, albeit to different extents for different proteins. These data support the use of such ΔAbs measurements as an alternative approach to monitor and evaluate interactions in protein solutions at high concentration.

1.5.4 Summary, conclusions and future directions (Chapter 5)

Chapter 5 summarizes our findings and conclusions concerning how excipients affect the conformational stability and dynamics at a global level and in distinct local regions within immunoglobulins. The potential applications of ultraviolet spectroscopy to studying interactions and excipients effects that modulate solution viscosity for high concentration proteins are presented. Finally, current and future goals to evaluate inter-relationships between protein dynamics, solute effects and molecular interactions on the conformational stability and aggregation of proteins are proposed.

Chapter 2

Effect of excipients on the conformational stability and global dynamics of immunoglobulins

2.1 Introduction

Proteins in solution are inherently conformationally dynamic molecules composed of atoms that are in a state of constant motion at ambient temperatures[182]. At equilibrium, the native form of a protein is believed to sample a statistical ensemble of interconverting microstates which undergo continuous fluctuations, resulting in protein motions on the spatial scale of sub-nanometer to tens of nanometers and a temporal scale of femtoseconds to hours[183]. Protein dynamics are known to influence a wide variety of biological processes including folding[182], enzymatic activity[184,185], signaling[186], allostery[187], ligand binding[57,59,188] and stability[38]. Several studies suggest that examining the dynamics of proteins could play a role in elucidating more complex correlations that may exist between protein stability and function[29,30,36,37,39].

Changes in solution properties (e.g., pH, temperature, ionic strength and the presence of cosolvents) as well as the structure of water itself (predominantly in the hydration layer) may significantly influence the structure, stability, dynamics and function of biologically and pharmaceutically important proteins[53,54,68,100,189,190]. A variety of biophysical techniques such as X-ray crystallography[191,192], nuclear magnetic resonance[184,193-195], neutron scattering[192], isotope exchange[33], ultrasonic spectroscopy[38,98-101,196] and pressure perturbation calorimetry[100,102-104,197] have been employed to probe fluctuations in the internal motions of proteins and/or their surrounding solvent. Numerous lower resolution techniques such as UV-absorption, fluorescence, circular dichroism and light scattering among others have commonly been employed to characterize higher order structures, hydrodynamic properties and conformational stability of proteins[38,150-158]. Data from these multiple biophysical techniques can be combined in a vector-based stress/response method known as an empirical phase diagram (EPD)[120,159,160]. An

EPD displays distinct colored regions which represent different conformational states of proteins and other macromolecular systems as a function of solution conditions such as pH and temperature. In a recent study[120], an EPD was generated for an IgG1 monoclonal antibody (mAb-B) based on techniques sensitive to the dynamic properties of proteins such as high-resolution ultrasonic spectroscopy, pressure perturbation calorimetry, red-edge excitation shifts and time-resolved fluorescence spectroscopy. The results showed a more complex pattern of apparent structural transitions at lower temperatures in the pre-transition region (below any detectable unfolding event) compared to an EPD generated from biophysical data using static (time-averaged) measurements such as circular dichroism, steady-state fluorescence spectroscopy and light scattering. The pre-transition region is defined as a temperature range over which the change in parameters traditionally used to evaluate a protein's secondary structure, tertiary structure and conformation stability does not deviate from a continuous change with temperature, as studied by methods such as circular dichroism, fluorescence spectroscopy and differential scanning calorimetry. A better understanding of any relationship between conformational stability and dynamics, especially in the pre-transition region, may be important to our understanding of the development and formulation of biopharmaceutical drugs such as monoclonal antibodies.

Monoclonal antibodies (mAbs) are an important class of dynamic, Y-shaped proteins that are good models for studying the inter-relationships between conformational stability and dynamics. The two F_{ab} domains of immunoglobulins are connected to the F_c domain by a highly flexible proline-rich hinge region which is believed to affect the structure and dynamics of immunoglobulins[115,116]. Various analytical techniques have been used to study the flexibility and dynamics of antibodies[33,100,115-122]. Different molecules within an immunoglobulin subclass,

despite their overall similarly in structure and sequence homology, may display significant differences in their conformational stability, flexibility and dynamics. The conformational stability of antibody drugs, formulated at both low and high concentrations, is significantly influenced by environmental and formulation factors during manufacturing, long-term storage and administration[123-125]. The effect of these factors on protein dynamics, however, has not been examined to any great extent. It is therefore important not only to understand better any relationship between conformational stability and dynamics for different monoclonal antibodies, but also to examine the effect of various environmental factors (e.g., pH, temperature, excipients, etc.) on their conformational stability and dynamics.

In this study, the effect of stabilizing and destabilizing excipients on conformational stability and intra-molecular protein dynamics of two different IgG1 mAbs (mAb-A and mAb-B) is compared to further understand the relationships between stability and dynamics.

2.2 Experimental methods

2.2.1 Materials

The IgG1 monoclonal antibodies (mAb-A and mAb-B) were provided by MedImmune (Gaithersburg, MD). The stock protein solutions were stored as received at 2-8°C. The dialysis of stock protein solutions was carried out overnight (at 4 ^{o}C) using a 10 kDa MWCO dialysis cassette (Pierce, Rockford, IL) into 20 mM citrate-phosphate buffer at pH values ranging from 3 to 8 at one unit intervals, unless otherwise noted. The final ionic strength of the buffer was adjusted to 0.1 using NaCl. All of the buffer components and other chemicals were purchased from Sigma (St. Louis, MO) and Fisher Scientific (Pittsburgh, PA). The protein concentration was measured at room temperature by absorbance measurement at 280 nm using an extinction

coefficient 1.45 mL $mg^{-1}cm^{-1}$ in an Agilent 8453 UV-Visible spectrophotometer (Palo Alto, CA), and diluted to the final concentration as indicated in each experiment.

2.2.2 Methods

2.2.2.1 Steady-state intrinsic (Trp) and extrinsic (ANS) fluorescence spectroscopy

Intrinsic tryptophan fluorescence spectra and static light scattering intensities were acquired using a two-channel, peltier-controlled, four-position PTI Quanta Master Spectrophotometer (Lawrenceville, NJ). The sample temperature was precisely controlled at 10.0 to 90.0 ^{o}C with 2.5 ^{o}C intervals and an equilibration time of 4 min at each temperature point. The IgG concentration used was 0.1 mg/mL (~ 6.7 x 10^{-4} mM) in a quartz cuvette with pathlength of 1 cm. The excitation and emission slit widths were initially set to 3 nm. Intrinsic tryptophan fluorescence spectra were collected using excitation wavelength of 295 nm, which excites tryptophan residues predominantly, and the emission range of 300 to 400 nm. The intrinsic Trp fluorescence peak position and peak intensity was determined after respective buffer subtraction by polynomial fitting and first derivative analysis of the processed spectra. Static light scattering intensity was acquired in the same experiment by monitoring scattered light at 90^{o} relative to the excitation source. The emission detector slit width was set to 0.5 nm. ANS fluorescence experiments were performed with similar experimental set up using excitation wavelength of 375 nm and emission range of 400–550 nm. The molar ratio of ANS: protein was maintained at 20:1. To obtain protein specific spectra corrected for background fluorescence, the spectra of ANS in buffer alone was subtracted from the sample spectra.

The excipient screening study using intrinsic tryptophan fluorescence assay was performed with similar instrumental settings in presence and absence of GRAS excipients. The

transition midpoint of thermal unfolding (T_M) was determined by fitting the temperature dependent change in intrinsic tryptophan fluorescence intensity using a Sigmoidal-Boltzmann function, in which temperature corresponding to the half transition point of peak fluorescence intensity was considered as a T_M value.

2.2.2.2 Far-UV circular dichroism

Far-UV circular dichroism signals were used to monitor changes in secondary (β-sheet) structure of IgG1 using a Jasco J-810 spectrometer (Tokyo, Japan) equipped with a six-cell sample holder and a peltier to precisely control the temperature. The effect of pH and temperature was studied by monitoring molar ellipticity of 0.2 mg/mL of IgG at 217 nm over the pH range of 3 to 8 (at one unit intervals) and temperatures of 10 – 90 ^{o}C at 0.5 ^{o}C intervals. Each measurement was acquired as an average of four accumulations with the temperature ramp rate of 15 ^{o}C/h, a response time of 1 s and the bandwidth of 1 nm. The sample specific spectra were obtained by subtracting the buffer spectrum from the sample spectrum.

2.2.2.3 OD_{350nm} turbidity measurements

The aggregation propensity of mAbA was studied using an orthogonal method by monitoring the optical density of 0.5 mg/mL of antibody at 350 nm using an Agilent 8453 UV-Visible spectrophotometer (Palo Alto, CA) as a function of pH and temperature. The temperature range studied was 10 to 90 ^{o}C at 2.5 ^{o}C intervals, pH ranging from 3 to 8 at unit intervals and an equilibration time of 4 min. The experiments were performed in triplicate.

2.2.2.4 High resolution ultrasonic spectroscopy (HR-US)

Ultrasonic measurements[97,100,120,198,199] were performed using an HR-US 102 Spectrometer (Ultrasonic Scientific, Dublin, Ireland) with a frequency range of 2 – 18 MHz and a resolution of 0.2 mm/s for velocity and 0.2% for attenuation measurements. The sample and reference cells contained 1 mL of protein and corresponding buffer solution, respectively. The differential velocity and attenuation were monitored at 12 MHz from 10 to 85 ^{o}C and pH 3 to 8 using 5 mg/mL of mAb-A. The temperature of the cells was controlled by a Phoenix P2 water circulator (Thermo Haake, Newington, NH). The sample and reference solutions were thoroughly degassed before each measurement. Appropriate amounts of sucrose or arginine were added to both protein and buffer solutions while evaluating excipient effects. Data were analyzed using HRUS v4.50.27.25 software. The coefficient of adiabatic compressibility (β_s) was determined using the following equations [100]:

$$\beta s = -\frac{1}{V}\left(\frac{\partial V}{\partial P}\right)s = -\left(\frac{1}{\nu o}\right)\left(\frac{\partial \nu o}{\partial P}\right)s = \left(\frac{\beta o}{\nu o}\right)\lim_{c\to 0}\frac{\left(\frac{\beta}{\beta o}\right)-Vo}{c}$$

$$where \quad Vo = \frac{\rho - c}{\rho o} \quad and \quad \nu o = \lim_{c\to 0}\frac{1-Vo}{c}$$

β and β_0 are the adiabatic compressibility of the solution and buffer respectively, ρ and ρ_0 are the density of the solution and the corresponding buffer, ν_0 is the partial specific volume of the IgG, V_0 is apparent volume fraction of the buffer and c is the protein concentration. The adiabatic compressibility of the sample and buffer are related to the density (ρ) and ultrasonic velocity (u)

by the Laplace equation[200], $\beta=1/\rho u^2$. The effect of excipients on the compressibility of mAb-A and mAb-B was studied similarly using solution conditions described later in the text.

2.2.2.5 Density

The density of protein samples (5 mg/mL) and corresponding buffer solutions was measured using a DMA-5000 high precision densitometer (Anton Paar, Graz, Austria) at a precision of 1 $x10^{-6}$ g/cm^3 and 0.001 ^oC. The densities of degassed solutions were measured from 5 – 55 ^oC at 2.5 ^oC intervals. The instrument was calibrated daily with dry air and degassed water before analysis. For the excipient studies, both the protein sample and corresponding buffer solution contained equal predetermined quantities of each excipient.

2.2.2.6 Differential scanning calorimetry (DSC)

The differential scanning calorimetric studies were performed using a MicroCal VP-Capillary DSC with an autosampler (MicroCal, Northampton, MA). The pH (pH 3 to 8 at 1-pH unit intervals) experiments for mAb-A and mAb-B were performed using 1 mg/mL of protein in 20 mM citrate-phosphate buffer (I = 0.1 adjusted by the appropriate addition of NaCl). The temperature ramp was programmed from 10 to 90 ^oC at a scanning rate of 60 $^oC/h$ and a filtering period of 16 s. Protein thermograms were obtained by subtracting the corresponding buffer blank from the sample thermogram. The transition midpoints were obtained by determining the baseline using linear or cubic functions, normalizing it to protein concentration, and fitting the processed thermogram to a non-two-state unfolding model. The endothermic peak maximum of the heat capacity was considered to be the apparent transition midpoint (T_M) for the individual peaks that could be deconvoluted from the thermogram. The effect of varying concentrations of excipients was studied similarly at pH 4 and pH 4.5 for mAb-A and mAb-B, respectively.

2.2.2.7 Empirical phase diagrams

EPDs are constructed to visually represent changes in the structural[120,159] and dynamic[120] properties of proteins in the form of colored diagrams as a function of solution variables such as pH and temperature. The rationale and methodology of EPD construction are described elsewhere[159,160]. Two separate EPDs were constructed using mAb-A. For the first EPD, experimental data as a function of pH and temperature from the following static biophysical techniques were used: intrinsic tryptophan fluorescence intensity, tryptophan peak position shifts, static light scattering intensity, ANS fluorescence intensity, circular dichroism at 217 nm and OD_{350nm} values. The second EPD was constructed to include measurements of dynamic properties on mAb-A by adding compressibility data from HR-US. The latter reflects changes in global dynamics as a function of pH and temperature. These two EPDs for mAb-A are compared with previously published results for mAb-B[120]. Different protein concentrations were used for different techniques (e.g., 0.1 mg/mL for fluorescence measurements and 5 mg/mL for ultrasonic measurements) and the concentration was chosen to obtain higher signal-to-noise in individual measurements. Because the concentrations used fall within the dilute solution regime as determined in control (concentration-dependent) experiments, the differences in protein concentration do not alter the pre-transition region significantly and hence should not influence the conformational stability and dynamics of the proteins as measured by these techniques.

2.2.2.8 Excipient screening

Intrinsic tryptophan fluorescence and static light scattering were used to screen a Generally-Regarded-As-Safe (GRAS) library of excipients to identify compounds which either increased or decreased the stability of mAb-B, as determined by changes in the transition

midpoint (T_M) of mAb-B unfolding. The concentrations of excipients used were higher than those commonly used in protein formulations to facilitate screening of excipients. The transition midpoint (T_M) was determined from a sigmoidal fit of the first transition in intrinsic fluorescence intensity versus temperature plots. The data were acquired between 10 and 90ºC in increments of 2.5ºC. Static light scattering was used to assess the propensity of the IgG1 antibody to aggregate. Prior to experimentation, mAb-B was dialyzed into 20 mM citrate-phosphate buffer (containing NaCl to adjust I= 0.1) at pH 4.5. These stress conditions were selected based on the reduced stability of mAb-B at this pH[120] which should facilitate the identification of stabilizing compounds. The protein concentration employed was 0.1 mg/mL. A few selected candidate stabilizers and destabilizers from this primary screen were used to further evaluate their effect on the second IgG1 molecule (mAb-A), either by the fluorescence method and/or differential scanning calorimetry.

2.2.2.9 Red-edge excitation spectroscopy (REES)

Red edge excitation is a characteristic property of polar fluorophores which exhibit excitation wavelength dependent emission spectra[201,202]. This phenomenon depends upon motional restriction of the environment of fluorophores. The steady-state fluorescence measurements of red-edge excitation shifts were performed using a PTI Quanta Master Spectrophotometer (Lawrenceville, NJ). The excitation and emission slit widths were set to 2.5 and 3 nm, respectively. The emission spectra (300 to 400 nm) were collected using different excitation wavelengths from 292 to 308 nm at 4 nm intervals. Both mAb-A and mAb-B at 0.1 mg/mL were studied in the absence and presence of selected excipients using a 1-cm pathlength quartz cuvette. A temperature ramp from 10 ^{o}C to 70 ^{o}C at 2.5 ^{o}C increments was used with an equilibration time of 3 min. An appropriate blank spectrum was subtracted from the sample

spectrum. The emission peak position (and intensity) was determined by a mean spectral center of mass (MSM) method, which increased reproducibility and signal-to-noise ratio and thus improved our ability to measure the relative shifts in peak position in the presence of excipients. The peak position maxima obtained by the MSM method is ~8 – 10 nm higher than the actual peak position obtained by derivative analysis.

2.3 Results

2.3.1 Characterization of higher-order structure, conformational stability and dynamics of mAb-A as a function of pH and temperature.

2.3.1.1 Static (time-averaged) measurements

The results from a variety of biophysical characterization measurements of mAb-A as a function of pH and temperature are shown in Figure 1 (a – f) and supplementary Figure S1 (a – f). A well-defined structural transition occurs in mAb-A at 65 to 75 ^{o}C over the pH range of 5 – 8 as detected by increases in Trp fluorescence intensity (Figure 1a) and a red-shift of emission peak maximum (Figure 1b). The onset temperature (T_{onset}) of unfolding at pH 5 starts ~60 ^{o}C with a broad unfolding curve (Figure 1b). The early T_{onset} at pH 5 is accompanied by an increase in ANS fluorescence intensity (Figure 1c) suggesting the exposure of apolar sites. The presence of intermolecular β-structure rich structures at pH 5 – 8 is also detected ~63 to 78 ^{o}C as suggested by a decrease in the CD signal (Figure 1f). The unfolding event at pH 5 – 8 leads to further aggregation which is apparent from the increase in light scattering intensity (Figure 1d) and $OD_{350\ nm}$ (Figure 1e) measurements. The T_{onset} for the unfolding transition (Figure 1c) in the range of pH 5 – 8, however, follows an inverse trend compared to the T_{onset} of aggregate formation (Figure 1d, e). For example, the T_{onset} of unfolding is lowest (~60 ^{o}C) at pH 5

(followed by pH 6 < pH 7 < pH 8) while its T_{onset} of aggregation is the highest (~ 85 ^{o}C) at pH 5 (followed by pH 6 > pH 7 > pH 8). In addition, at pH 4, the overall structural changes observed for mAb-A as a function of temperature were similar (Figure 1b, c, f) to that at pH 5 up to ~70 ^{o}C, albeit the transitions were observed at lower temperatures. The CD signal at pH 4, however, continues to decrease above 75 ^{o}C, suggesting that the intermolecular interactions continue to increase with increases in temperature. The behavior of mAb-A at pH 3 is significantly different than at other pH values below 65 ^{o}C, where the protein manifests multiple distinct structural transitions apparent from ANS fluorescence intensity change (Figure 1c), Trp peak position shifts (Figure 1b) and circular dichroism (Figure 1f). No increase in light scattering intensity (Figure 1d) or optical density (Figure 1e) was observed at pH 3 and 4 up to 90 ^{o}C. Fluorescence emission spectra (intrinsic and ANS) for mAb-A at 15, 35 and 60 ^{o}C are shown as a function of pH in supplementary Figure S1 (a – f). These data suggest that mAb-A retains its native-like structure (supplementary Figure S1 a, b, d, e) at temperatures in the pre-transition region (15 and 35 ^{o}C) compared to results at higher temperatures (e.g., 60 ^{o}C), resulting in structural disruptions (supplementary Figure S1 c, f). Upon excitation at 295 nm, the intrinsic Trp fluorescence emission represents the average emission signal from all the Trp residues (~ 22) present in the IgG1 molecules used in this study.

2.3.1.2 High resolution ultrasonic spectroscopy

The global dynamics of mAb-A were studied by determining compressibility (volume fluctuations with changes in pressure) as a function of pH and temperature using high-resolution ultrasonic spectroscopy (HR-US) (Figure 2). The adiabatic compressibility of mAb-A was calculated as a function of pH and temperature by determining the relative changes in the ultrasonic velocity between the sample and reference. As expected, the adiabatic compressibility

of mAb-A was found to increase as a function of temperature at all pH values. Plots of adiabatic compressibility versus temperature, however, show a unique non-linear increase in the pre-transition regions (<45 ^{o}C) starting at pH 4 and above. These HR-US deviations occur at lower temperatures than the respective T_{onset} and T_M1 values as measured by DSC (see next section). This non-linear dependence of adiabatic compressibility therefore may reflect some form of change in the global dynamics of mAb-A in the pre-transition region.

2.3.1.3 Empirical phase diagrams for mAb-A

The EPD constructed for mAb-A using the time-averaged measurements is presented in Figure 3a. A broad structural transition is apparent between 60 and 75 ^{o}C for pH 5 – 8. At pH 4, two distinct structural transitions occur at ~50 and ~70 ^{o}C. The contributions from ANS fluorescence intensity changes (Figure 1c) and CD signals (Figure 1f) may contribute the most to these apparent transitions at pH 4. The transitions in mAb-A at pH 3 start at ~20 ^{o}C with multiple subsequent minor transitions observed every 10 – 15 ^{o}C. The EPD in Figure 3a has been divided into three distinct phases, i.e., Phase I, II and III, representing regions of stable, unstable and aggregated form of mAb-A, respectively. It has previously been reported[120] that a 'dynamic' EPD constructed using another IgG1 (mAb-B) was able to detect an additional transition region in the low temperature (< 45 ^{o}C) region arising from contributions of the adiabatic compressibility measurements. An EPD using mAb-A was constructed combining static and compressibility measurements as a function of pH and temperature (Figure 3b). Red-edge excitation shift data were not included in the EPD because of lower resolution of these data at higher temperatures. This 'dynamic' EPD for mAb-A shows an additional transition region (Phase 1') at pH ≥ 4 and at temperatures < 45 ^{o}C compared to the static EPD (Figure 3a). This EPD with mAb-A, together with the previously published[120] results with mAb-B, suggest that

ultrasonic measurements provide additional information about conformational fluctuations and flexibility in IgG1 that are not apparent with the use of conventional biophysical techniques alone, especially in the pre-transition regions. The presence of additional structural effects in the pre-transition regions of the two IgG1 antibodies at ~pH 5 – 8 emphasizes the need for developing a better understanding of the effect of formulation components not only on equilibrium conformational stability but also on the dynamic properties of protein therapeutic drugs in solution.

2.3.1.4 Thermal stability of mAb-A and mAb-B

Differential scanning calorimetry (DSC) is routinely used to study the thermal stability of antibodies[100,203] by measuring the differential heat capacity to determine the midpoint of a thermal unfolding event (T_M). DSC was used to compare directly the conformational stability of mAb-A and mAb-B as function of solution pH (Figure 4; Supplementary Table 1). Three distinct conformational transitions (T_M1, T_M2, T_M3) were apparent for mAb-A at pH 3 – 7, albeit at variable temperatures. Only two major structural transitions, however, were observable at pH 8 (Figure 4b). In contrast, mAb-B showed only two distinct transitions in the pH range of 5 – 8 by DSC (T_M2 and T_M3 in Figure 4c and 4d). In the case of mAb-B at pH 3 and 4, an additional lower temperature transition (T_M1) was detected.

2.3.1.5 Screening of a GRAS library of excipients

To better understand the effect of formulation excipients on conformational stability and global dynamics of these two IgG1 monoclonal antibodies, a first set of experiments screened a GRAS library of excipients to identify potential stabilizing and destabilizing excipients using mAb-B. The EPDs for mAb-A (Figure 3) and mAb-B (Ramsey JD et al.[120] Figure 3) indicate

conformational instability in the range of 55 – 65 ^{o}C at pH ~4 – 4.5. The intrinsic Trp fluorescence intensity method was utilized to identify stabilizing excipients. The change in stability of mAb-B's tertiary structure by excipients was determined by computing the difference in T_M (ΔT_M) of mAb-B in absence and presence of excipients under these accelerated pH conditions (Table 1). This methodology allowed for determination of the protein unfolding temperature (T_M) as well as an assessment of aggregation behavior (Table 1). Sugars and polyols in general increased the T_M of mAb-B, whereas amino acids, such as arginine and histidine, lowered the transition temperature. A few selected candidate stabilizers (sucrose, dextrose and mannitol) and destabilizers (arginine) were then tested with mAb-A (using DSC) at pH 4 to identify common excipients that either stabilize or destabilize both of the IgG1 antibodies (data not shown). Based on their effects on the T_M values, as measured by fluorescence spectroscopy with mAb-B and DSC with mAb-A, sucrose was selected as a representative candidate stabilizer, and arginine was used as a destabilizing excipient for both proteins. All subsequent studies evaluating the effect of excipients on conformational stability and pre-transition dynamics were performed at pH 4 and pH 4.5 for mAb-A and mAb-B, respectively. These solution conditions were selected because the magnitude of stabilizing and destabilizing effects of these two excipients under neutral pH conditions was smaller than the chosen more acidic pH solutions conditions. The selection of lower pH, however, does not preclude our ability to study the effect of excipients on the pre-transition conformational dynamics of the mAbs since the T_{onset} of unfolding for both the proteins under these conditions is still $\geq$ 45 ^{o}C.

2.3.2 Effect of arginine and sucrose on conformational stability and dynamics of IgG1 mAb-A and mAb-B.

2.3.2.1 Effect on conformational stability

The effect of sucrose and arginine on the conformational stability of mAb-A and mAb-B was studied using DSC and intrinsic Trp fluorescence spectroscopy (Figure 5, 6 and Supplementary Table 2). DSC and fluorescence measurements were used to determine the effect of excipients on the overall thermal stability and tertiary structure stability, respectively. Figure 5a shows a representative DSC thermogram for mAb-B at pH 4.5. Three distinct transitions were detected for mAb-B at pH 4.5 with T_M1 being the first low temperature transition, T_M2 the second transition, and T_M3 the third transition seen at the highest temperature. Similarly, three distinct transitions were observed for mAb-A at pH 4 (data not shown). Arginine (up to ~300 mM) was found to destabilize both mAb-A (Figure 5c; Supplementary Table 2a) and mAb-B (Figure 5e; Supplementary Table 2c) in a concentration dependent manner. Sucrose (up to ~500 mM) showed a concentration dependent stabilization effect on mAb-A (Figure 5d; Supplementary Table 2b) and mAb-B (Figure 5f; Supplementary Table 2d).

One goal of a protein formulation strategy would be to identify excipients that stabilize the first conformational transition (which is typically the unfolding of CH2 domain for IgG1)[204] and inhibit subsequent protein unfolding. Figure 5b shows the effect of arginine and sucrose concentration on the T_M1 values for both mAb-A and mAb-B. Arginine was more potent at destabilizing mAb-A than mAb-B. For example, to achieve ~2.5 ^oC destabilization, a lesser amount of arginine (highlighted with a rectangle) was required for mAb-A compared to mAb-B. Sucrose, however, was a more potent stabilizer for mAb-B compared to mAb-A. As shown in

Figure 5b, to achieve ~2.5 ^{o}C stabilization, a lesser amount of sucrose (highlighted with a rectangle) was required for mAb-B compared to mAb-A.

Figure 6 shows the effect of the two excipients on the tertiary structure stability of mAb-A (Figure 6a) and mAb-B (Figure 6b) as monitored by Trp peak position shifts as a function of temperature. Arginine does not influence the tertiary structure stability of mAb-A throughout the temperature range examined. For mAb-A in presence of sucrose, however, the protein showed blue-shifted Trp peak positions above 25 ^{o}C suggesting that aromatic residues are shielded from the solvent. In the case of mAb-B, in the absence of excipients, the protein shows a red shift in Trp peak position (T_{onset} ~45 ^{o}C) upon thermal unfolding indicating exposure of aromatic residues to the solvent (Figure 6b) with increasing temperature. Sucrose was found to stabilize while arginine destabilized the tertiary structure of mAb-B in terms of both T_{onset} and T_M.

2.3.2.2 Effect on protein dynamics

The effect of sucrose and arginine on the global dynamics of mAb-A and mAb-B was first examined by determination of compressibility values using HR-US as shown in Figure 7. The measurements of protein compressibility are directly related to the fluctuations in volume of the protein, thereby reflecting a form of the dynamics and flexibility of proteins. Figure 7a shows that the adiabatic compressibility increases with temperature for both mAb-A (pH 4) and mAb-B (pH 4.5). An increase in compressibility suggests that the relative difference in the ultrasonic velocity between the sample and the reference is decreased, while the absolute value of the velocity increases as a function of temperature. Mobile or less structured molecules possess a lower elastic modulus compared to rigid, more structured species. This results in a decrease in sound velocity through the unstructured or mobile material. A higher compressibility value is therefore indicative of a less structured and/or a more dynamic protein. As seen in

Figure 7a, the compressibility of mAb-A is relatively greater than mAb-B in the temperature range 10-50 ^{o}C, i.e., before any major detectable conformational transitions.

The effect of sucrose and arginine on mAb-A compressibility as a function of temperature is shown in Figure 7b. Sucrose does not significantly influence the compressibility of mAb-A in the pre-transition region while arginine marginally decreases the compressibility of mAb-A, especially in the pre-transition region. Figure 7c represents the effect of sucrose and arginine on the compressibility of mAb-B. The compressibility of mAb-B in the presence of arginine was found to be marginally increased in the pre-transition region. The significant increase in the compressibility of mAb-B in the presence of arginine above 55 ^{o}C most likely can be explained by the formation of highly compressible, irreversible aggregates. The compressibility of mAb-B in the presence of sucrose was significantly reduced throughout the range of temperatures used in this study, but predominantly in the pre-transition region. The lowering of compressibility suggests that the global dynamics of mAb-B are dampened in presence of stabilizing concentrations of sucrose.

Figure 8 shows the red edge excitation shift results for mAb-A and mAb-B in the presence of sucrose and arginine. The red edge excitation effect (REES) is a phenomenon in which there is a shift in emission spectra maxima upon red edge excitation[201,202]. Such an effect is primarily observed when the lifetime of solvent relaxation is equal to or larger than the lifetime of the fluorophore of interest. The solvent reorientation or relaxation around an excited state fluorophore is influenced by dynamic motions within proteins and solvent fluctuations around the fluorophore's environment. At 10 ^{o}C, both mAb-A and mAb-B show red edge shifts in the absence of excipients suggesting that the fluorophore(s) examined (Trp in this case) are in an environment where the lifetime of solvent relaxation is either equal to or longer than the

lifetime of the fluorophore. Such a system is suitable for studying the effects of excipients on the conformational flexibility and dynamics of proteins by monitoring their effect on the magnitude of any observed red edge shifts. The REES effect occurs because the longer wavelength excitation results in photo-selection of fluorophores that are strongly interacting with polar solvent molecules in their vicinity, and as such, a less dynamic (or more rigid) fluorophore environment will lead to a decrease in solvent relaxation of the fluorophore and thus the magnitude of red edge shifts will increase. As shown in Figure 8a and Figure 8b, neither sucrose nor arginine altered the red edge shifts observed in mAb-A in the temperature range spanning the pre-transition region of the antibody. This result suggests that these two excipients do not significantly affect the internal dynamics of mAb-A in which the local environment around Trp residues was sampled. In contrast, concentrations of sucrose which stabilized the tertiary structure of mAb-B were found to increase the magnitude of red edge shifts in the pre-transition region (Figure 8d). Arginine did not alter the magnitude of the red edge shifts in the pre-transition region (< 55 ^{o}C) of mAb-B (Figure 8c).

2.4 Discussion

2.4.1 Comparison of higher order structure, thermal stability behavior and EPDs between mAb-A and mAb-B[120]

The biophysical data suggest that mAb-A undergoes multi-step unfolding upon thermal unfolding with formation of intermolecular β-structure rich oligomeric structures at pH 4 – 8 at temperatures prior to major unfolding/aggregation events. These intermolecular interactions appear to be accompanied by shielding of aromatic residues from the solvent, as suggested by the blue shift in Trp peak position observed at pH 5 – 8 between ~ 45 – 65 ^{o}C (Figure 1b). The T_{onset}

of unfolding for mAb-A was inversely related to the T_{onset} of aggregation between pH 5 – 8. For example, mAb-A at pH 5 had the lowest T_{onset} of unfolding but the highest T_{onset} of aggregation as measured by ANS fluorescence intensity and static light scattering (or optical density) respectively (Figure 1 c, d, e). An initial increase in ANS intensity (Figure 1c) at pH 5 reaches a plateau above 65 ^{o}C. This result along with a continuous decrease in the CD signal (Figure 1f) at pH 5 above 65 ^{o}C suggests that no additional apolar residues are exposed in this temperature range. There is, however, an increase in β-structure rich intermolecular oligomeric structures. These results suggest that mAb-A at pH 5 forms partially altered structures that are either stable in solution and/or form oligomeric species that are resistant to the formation of larger aggregates that can be detected by static light scattering and optical density measurements. Furthermore, a steep increase in ANS fluorescence intensity and increase in CD signal (Figure 1c, f) at pH 6 – 8 above 78 ^{o}C suggests that additional aromatic residues are being exposed and that the intermolecular β-structures begin to dissociate. The T_{onset} for such a dissociation event above 78 ^{o}C is found to be in the following order: pH 8 < pH 7 < pH 6 (Figure 1f). Once these structures dissociate and additional aromatic residues are exposed, the antibody may become more prone to formation of irreversible aggregates. The detection of larger aggregated species (Figure 1d, e) follows a similar trend as above (i.e., T_{onset} for aggregation pH 8 < pH 7 < pH 6), arguing that a dissociation of relatively stable oligomeric species may precede the formation of larger aggregates in solution at higher pH. The sudden drop in light scattering intensity and optical density (after an initial increase at temperatures above 83 ^{o}C) indicates that the aggregates eventually fall out of solution. At pH 3 and 4, mAb-A manifests blue-shifted Trp peak positions, an increase in ANS intensity and decreases in CD signal which indicates conformational alterations at much lower temperatures compared to higher pH conditions. Nevertheless, the

protein remains aggregation resistant under these conditions. In contrast, a single cooperative transition was observed in the case of mAb-B[120] between 60 – 70 ^{o}C at pH values ranging from 5 – 8 based upon static measurements (Figure 1[120]). The unfolding event in mAb-B leads to the exposure of aromatic residues and the protein subsequently forms larger aggregates at pH 5 – 8 (Figure 1[120] e, f). Furthermore, mAb-B at pH 5 – 8 aggregates over a very narrow temperature range as detected by static light scattering. The T_{onset} of unfolding had no correlation with the T_{onset} of aggregation in this pH range (Figure 1[120] e, f). In this same study, mAb-B at pH 4 showed a broad unfolding transition and aggregated to a lesser extent than at pH 5 – 8, while the protein at pH 3 was found to be resistant to formation of detectable aggregates. In summary, these results from a variety of biophysical measurements clearly show that IgG1 mAb-A and mAb-B have distinct patterns of conformational alterations and aggregation behavior in response to changes in pH and temperature.

Antibodies by virtue of their multi-domain structure routinely display multiple conformational transitions due to environmental stresses such as changes in pH and temperature which can be detected by DSC. A number of previous DSC studies have assigned these different transitions to the unfolding of antigen binding (F_{ab}) region, crystallizable (F_c) region or individual domains within F_{ab} and F_c regions[204-206]. The presence of three transitions detected by DSC for mAb-A (Figure 4a, b) over a wide range of pH (3 – 7) correlated with spectroscopic measurements, which also showed multiple transitions (Figure 1b, c, and f). The highest T_{onset} of unfolding for mAb-A (Figure 1b, c) and the lowest T_{onset} of aggregation (Figure 1d, e) at pH 8 indicate that the protein aggregates rapidly upon unfolding. Such a concerted phenomenon may explain only two major transitions that are apparent at pH 8. In contrast, mAb-B was found to have two major transitions at higher pH except for pH 3, 4 (Figure 4c, d). Our previous

spectroscopic results[120] using mAb-B have shown that it undergoes a single cooperative unfolding transition at pH 5 – 8. Therefore, the two main structural transitions (compared to three transitions for mAb-A) detected by DSC for mAb-B may suggest that the unfolding of one domain leads to an immediate subsequent unfolding of other domains within the mAb-B molecule. The additional transition detected at pH 3 and 4 by DSC (Figure 4d) was also observed by other spectroscopic methods at similar temperatures (Ramsey JD et al.[120]; Figure 1b, f). The thermal behavior and aggregation data for mAb-B suggests that no detectable stable intermediates are formed and that the protein undergoes concerted thermal unfolding and subsequent aggregation under these solution conditions.

In addition, comparison of structural features and thermal stability profiles of the two mAbs can be compared by their differences in the static and dynamic EPDs, i.e., mAb-A (Figure 3 in this work) and mAb-B (Ramsey JD et al.[120], Figure 3). The static EPDs generated for mAb-A and mAb-B[120] were both able to detect differences in conformational stability as a function of temperature and pH. The dynamic EPD containing the additional compressibility results for mAb-A (Figure 3b) was able to detect changes in dynamic behavior in the pre-transition region at a broader pH range (pH 4 – 8) than mAb-B (Ramsey JD et al.[120], Figure 3), where the dynamic EPD was found to contain additional regions in the pH range of 6 – 8. This difference in the EPDs of mAb-A and mAb-B may potentially be due inherent differences between the two IgGs or due to experimental differences such as: (1) the dynamic properties of mAb-B were studied above 20 ^{o}C rather than 10 ^{o}C for mAb-A. Therefore, the conformational fluctuations that may exist at lower temperatures could be incompletely represented in the EPD for mAb-B, and/or (2) ANS fluorescence results for mAb-B (Ramsey JD et al.,[120] Figure 1f) at lower pH values show a broad unfolding transition with a T_{onset} of ~37.5 ^{o}C. The smaller magnitude of dynamic

fluctuations may therefore be obscured during the mathematical data processing used to construct the EPD.

2.4.2 Effects of arginine and sucrose on the conformational stability and pre-transition dynamics of mAb-A and mAb-B

Arginine was found to be a destabilizer, whereas sucrose was a stabilizer for both mAb-A and mAb-B in a concentration dependent manner, albeit at different effective concentrations as determined by DSC measurements. Arginine was a more potent destabilizer for mAb-A compared to mAb-B, and sucrose was more potent at stabilizing mAb-B than mAb-A (Figure 5b, Supplementary Table 2a). Arginine, however, did not perturb the tertiary structure stability of mAb-A. Potential reasons for the destabilizing effect of arginine on mAb-A could either be the suppression of intermolecular β-structure rich oligomer formation and/or promotion of its dissociation[207]. The destabilization of such β-structure rich intermediates structures, that potentially stabilize partially altered structures of mAb-A, may increase the propensity of mAb-A to form larger aggregates. Furthermore, the blue-shift observed in Trp peak position as a function of temperature for mAb-A in the presence of sucrose suggests that this sugar may be stabilizing the intermolecular β-structure rich structures, thus shielding the aromatic residues from the solvent. Both of these excipients, however, influenced the tertiary structure stability of mAb-B. Thus the effect of arginine and sucrose on the global thermal stability and tertiary structure suggest that both mAb-A and mAb-B interact with the same excipients in a different manner and at different effective concentrations. This may in part be due to the inherent differences in the physico-chemical properties and the unfolding processes between the two proteins, where mAb-A appears to have a greater propensity to form β-structure rich structures that stabilize the partially altered native structure before any global unfolding/aggregation event.

In contrast, mAb-B undergoes a more cooperative unfolding process starting with disruption of its tertiary structure followed by an immediate aggregation of the structurally altered protein.

It is generally accepted that experimentally determined adiabatic compressibility values are comprised of positive contributions from the intrinsic compressibility of a protein and a negative contribution from a hydration component[200]. Depending upon the magnitude of the intrinsic compressibility and the hydration contribution, the apparent adiabatic compressibility values may either be positive or negative. The lower (negative at lower temperatures) adiabatic compressibility values in the pre-transition region for mAb-B compared to mAb-A (Figure 7a) suggest a combined effect of lower intrinsic compressibility and/or higher hydration contribution to mAb-B. Such a combined effect may result in stronger coupling of mAb-B conformational fluctuations to the fluctuations in the surrounding hydration water and/or the proteins' environment compared to mAb-A. Sucrose did not affect the compressibility of mAb-A in the pre-transition region. This result may be related to the lower potency of sucrose as a stabilizer of mAb-A. Arginine marginally lowered the compressibility of mAb-A resulting in negative values in the pre-transition region suggesting an increased contribution of hydration to the apparent adiabatic compressibility values. In contrast, arginine marginally increased the compressibility of mAb-B in the pre-transition region. These mAb-B compressibility values go from negative to positive at lower temperatures suggesting either an increase in intrinsic compressibility and/or decrease in the hydration contribution. These effects, however, may not be mutually exclusive. Arginine was found to destabilize mAb-B by influencing its tertiary structure stability. Such a destabilization effect may require perturbation of the structure of water in the protein's hydration layer, potentially due to the chaotropic nature of guanidinium group in arginine, resulting in a lower hydration contribution to the apparent compressibility of mAb-B. This could explain the

marginal increase in compressibility in the presence of arginine at lower temperatures. Sucrose, however, significantly decreased the compressibility of mAb-B especially in the pre-transition region. The negative values of mAb-B compressibility in the presence of sucrose indicate that the hydration component has a greater contribution to the experimentally determined compressibility values. This suggests that solvent fluctuations around the protein's surface may have a significant effect on the dynamic behavior of mAb-B in the presence of sucrose. Overall, these compressibility measurements suggest that mAb-B exists in a less dynamic or a more compact form due to the potent stabilizing effect of sucrose, which may increase the ordering of water in the hydration layer due to a preferential hydration mechanism. In summary, HR-US results show that effective concentrations of arginine and sucrose did not significantly influence the dynamic behavior of mAb-A in the pre-transition region. Similarly, arginine did not appreciably affect the pre-transition dynamics of mAb-B. Sucrose, however, significantly reduced the dynamic behavior of mAb-B as indicated by the lower compressibility values in the pre-transition region.

Such a reduction in mAb-B pre-transition dynamics was also observed by increases in the magnitude of the red edge excitation shifts (REES) in the presence of stabilizing concentrations of sucrose. The increase in magnitude of the red edge effect suggests that solvent relaxation contributions in the environment around the Trp residues in mAb-B were reduced. This in turn suggests that the environment around the Trp residues is rigidified in the presence of sucrose, especially at lower temperatures, potentially due to a reduction in the internal dynamics of mAb-B. The inability of both arginine and sucrose to affect the magnitude of red edge effects for mAb-A at different temperatures suggests that excipients did not alter the dynamics of mAb-A in the immediate environment of aromatic residues. Because the conformational fluctuations in

mAb-A and mAb-B are differently coupled to solvent fluctuations, it is possible that excipients which modulate solvation properties can influence the pre-transition dynamics of proteins whose conformational fluctuations are strongly coupled to the surrounding solvent.

Figure 1

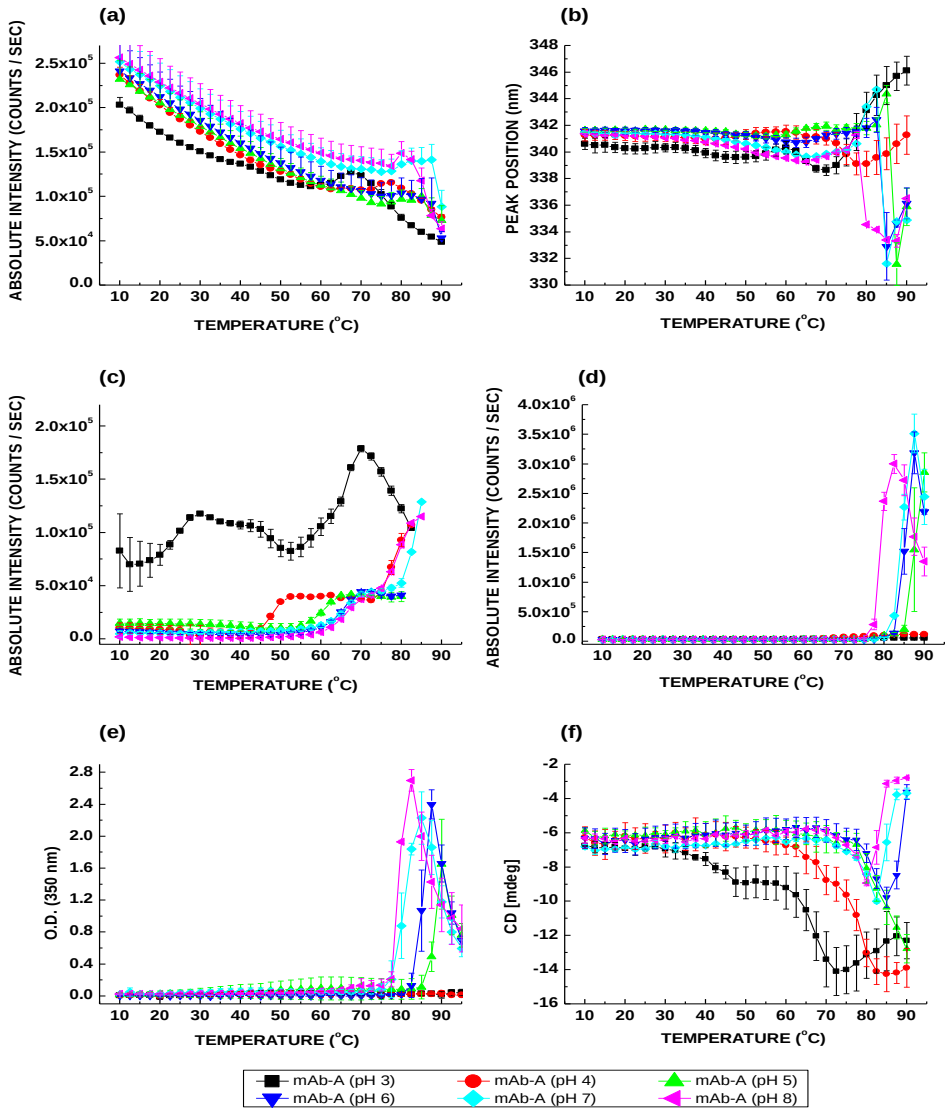

Effect of pH and temperature on conformational stability of an IgG1 monoclonal antibody (mAb-A) as measured by a variety of biophysical techniques: (a) Intrinsic tryptophan fluorescence intensity, (b) intrinsic tryptophan fluorescence peak position shifts, (c) ANS fluorescence intensity, (d) static light scattering, (e) $OD_{(350\ nm)}$, and (f) CD signal at 217 nm.

Figure 2

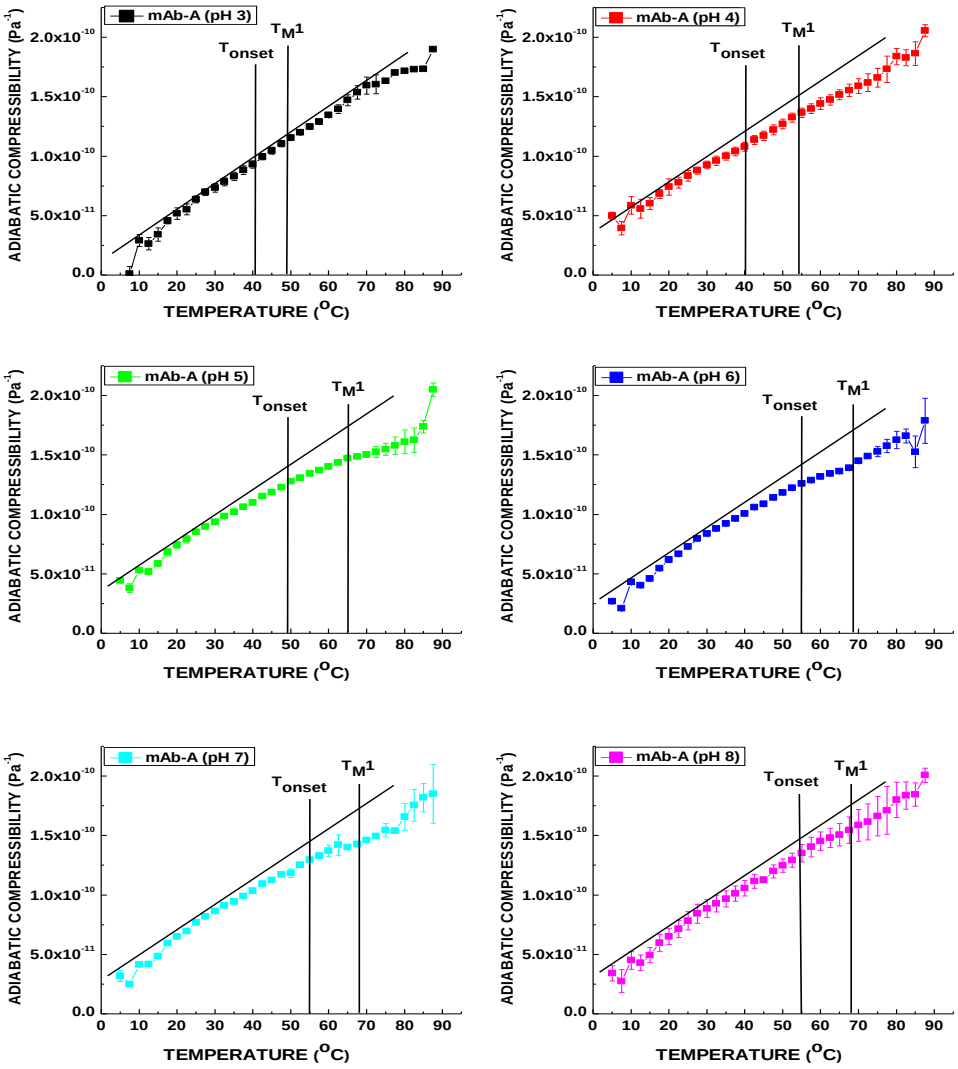

Adiabatic compressibility of mAb-A as a function of pH and temperature as measured by HR-US. The straight lines along the data points are a visual aid for comparison of pre-transition regions. The T_{onset} and T_M values represent the initiation and peak maximum for the first thermal transition as determined separately by DSC.

Figure 3

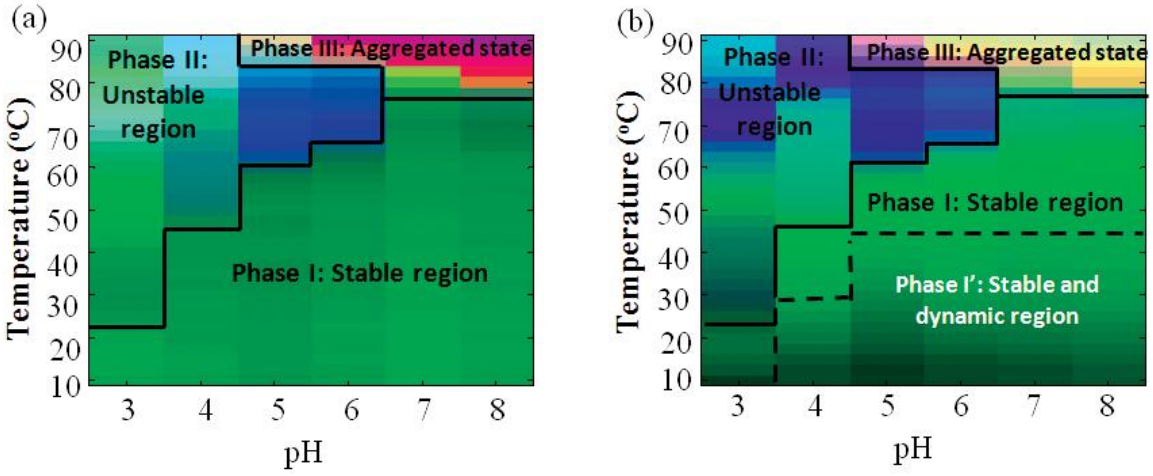

Empirical phase diagrams for mAb-A as a function of pH and temperature using (a) Static (time-averaged) biophysical techniques alone, and (b) data from static techniques in (a) in conjunction with HR-US data. Static biophysical techniques data from intrinsic tryptophan fluorescence intensity and peak position shifts, static light scattering intensity, extrinsic ANS fluorescence intensity, circular dichroism at 217 nm, and OD_{350nm} values. A continuous color in the phase diagram represents a single structural state of the protein. Transitions in the protein's structure are manifested by changes in color.

Figure 4

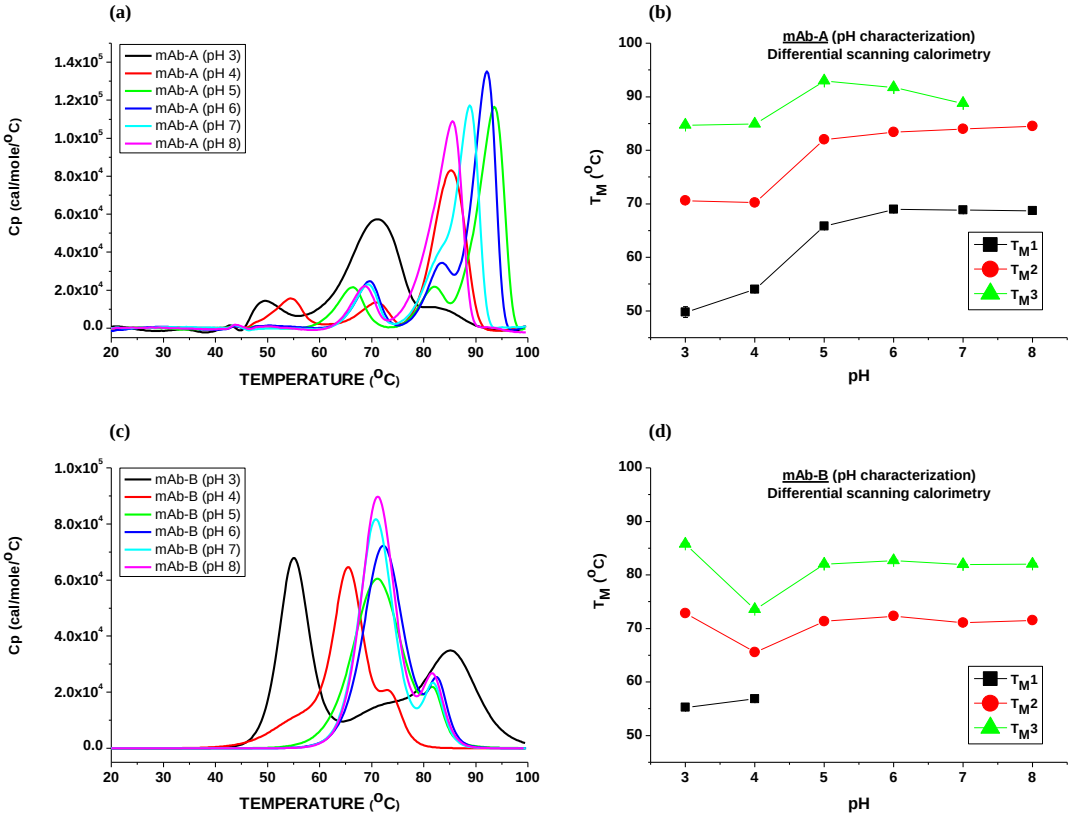

Representative differential scanning calorimetric thermograms for mAb-A (a) and mAb-B (c) over pH 3 – 8 and 10 – 100 ^{o}C (shown only above 30 ^{o}C); and plot of midpoint of thermal unfolding values (T_M1, T_M2, T_M3) for mAb-A (b) and mAb-B (d) as a function of pH. Error bars cannot be seen in (b) and (d) because they are within the symbols. The summary of T_M results and their corresponding SD values are presented in supplementary Table 1.

Figure 5

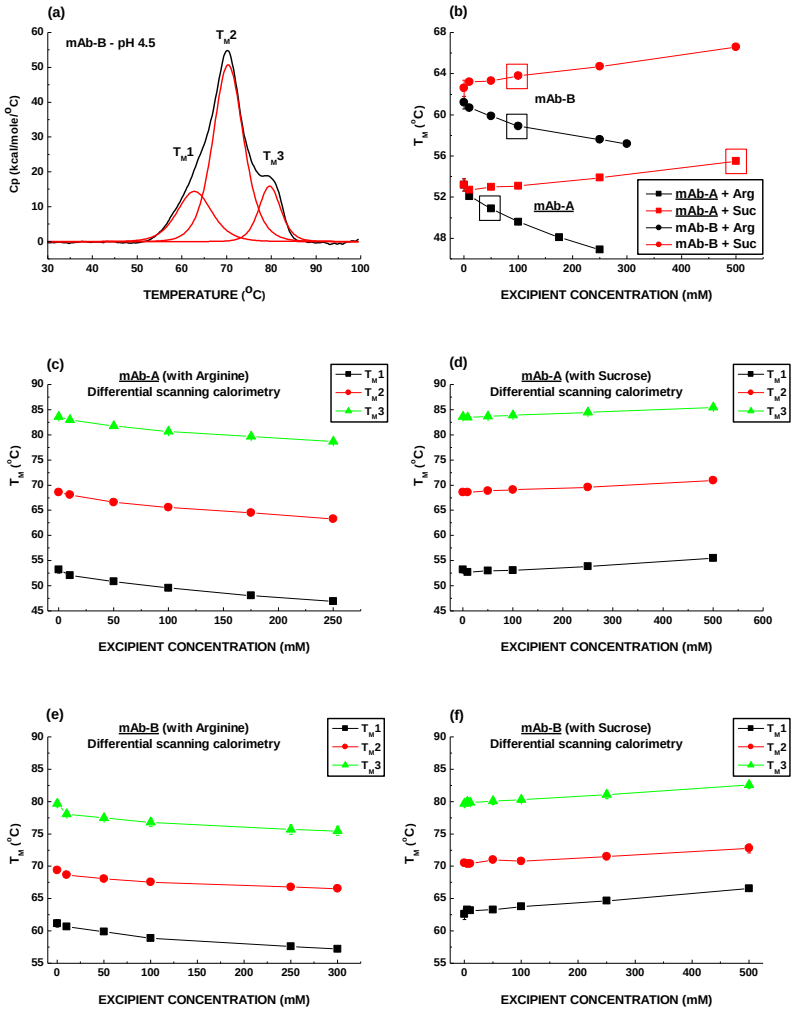

Effect of sucrose and arginine on conformation stability of mAb-A and mAb-B as measured by DSC: (a) Representative DSC thermograms for mAb-B (pH 4.5) with T_M1, T_M2 and T_M3; (b) effect of different concentrations of excipients on T_M1 for mAb-A and mAb-B. The box represents the effective concentration of excipient required to have ~ 2.5 °C of effect. Plots of T_M values for mAb-A (c, d) and mAb-B (e, f) in the presence of varying concentrations of arginine (c, e) and sucrose (d, f). Error bars often cannot be seen because they fall within the dimensions of the data points.

Figure 6

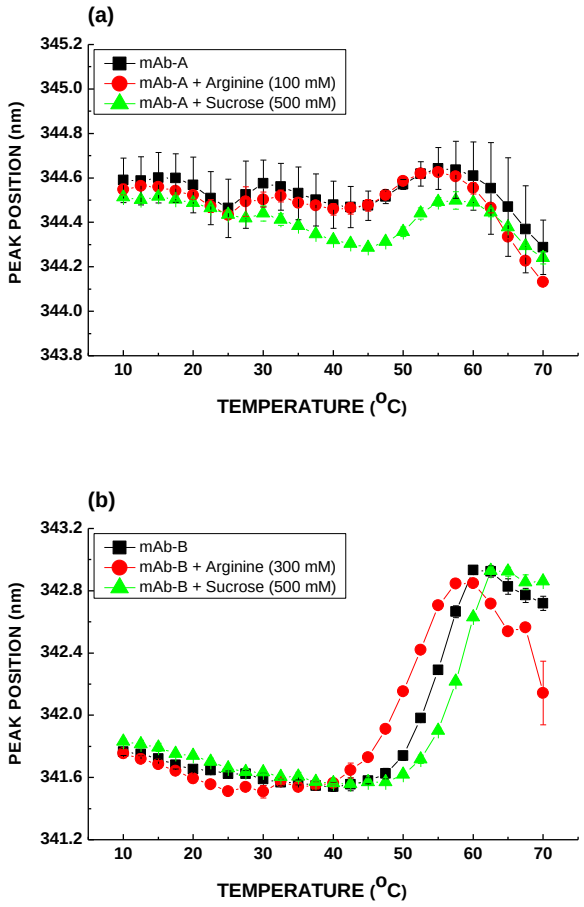

Effect of sucrose and arginine on Trp peak position shifts for (a) mAb-A and, (b) mAb-B as a function of temperature using fluorescence spectroscopy.

Figure 7

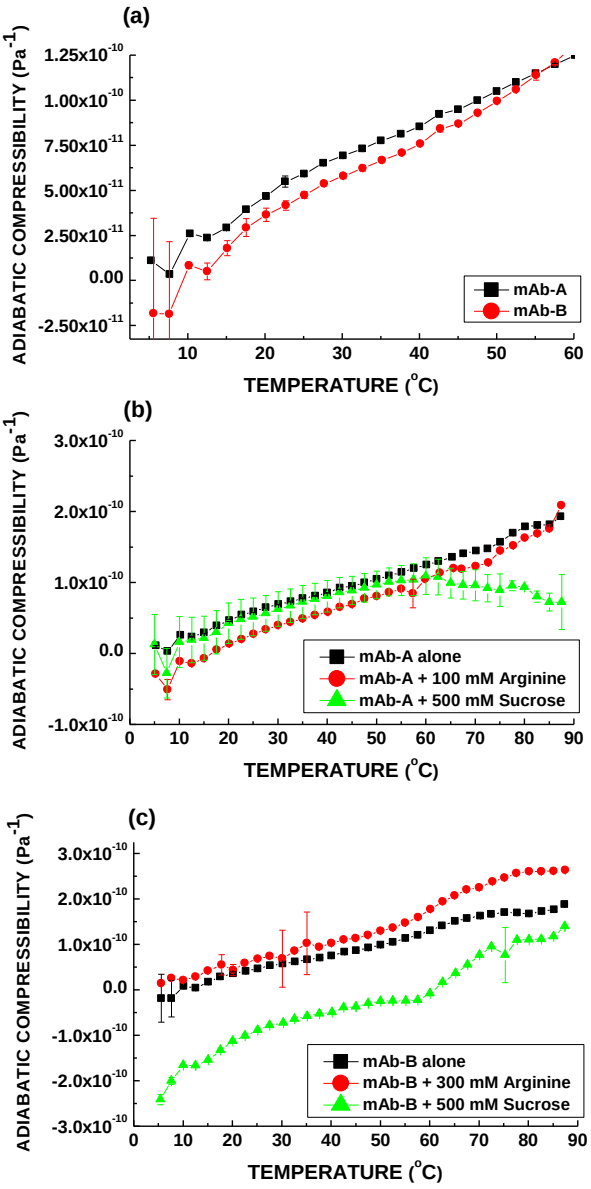

Effect of sucrose and arginine on adiabatic compressibility of mAb-A and mAb-B as measured by HR-US: (a) comparison of compressibility of mAb-A and mAb-B in the pre-transition region, (b) effect of arginine and sucrose on adiabatic compressibility of mAb-A, and (c) effect of arginine and sucrose on adiabatic compressibility of mAb-B.

Figure 8

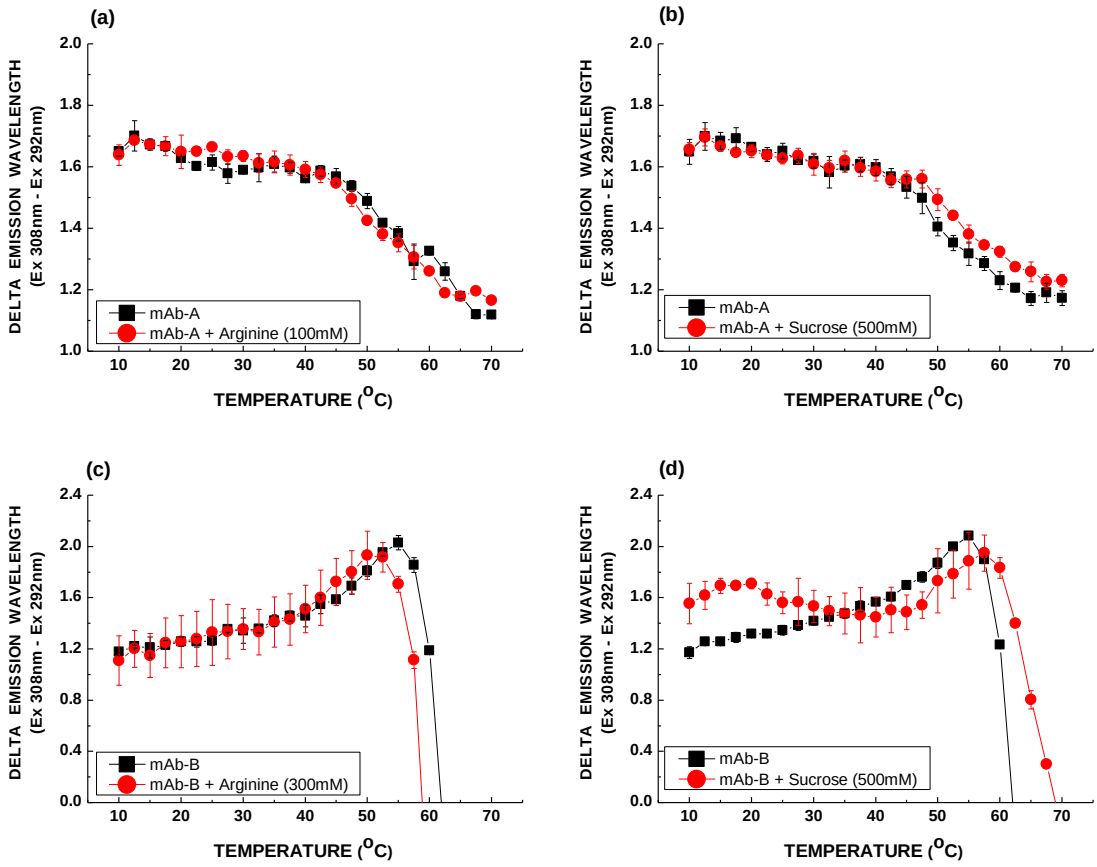

Red edge excitation shifts (REES) fluorescence measurements with mAb-A (a, b) and mAb-B (c, d) in the presence and absence of sucrose (b, d) and arginine (a, c).

Supplementary figure S1

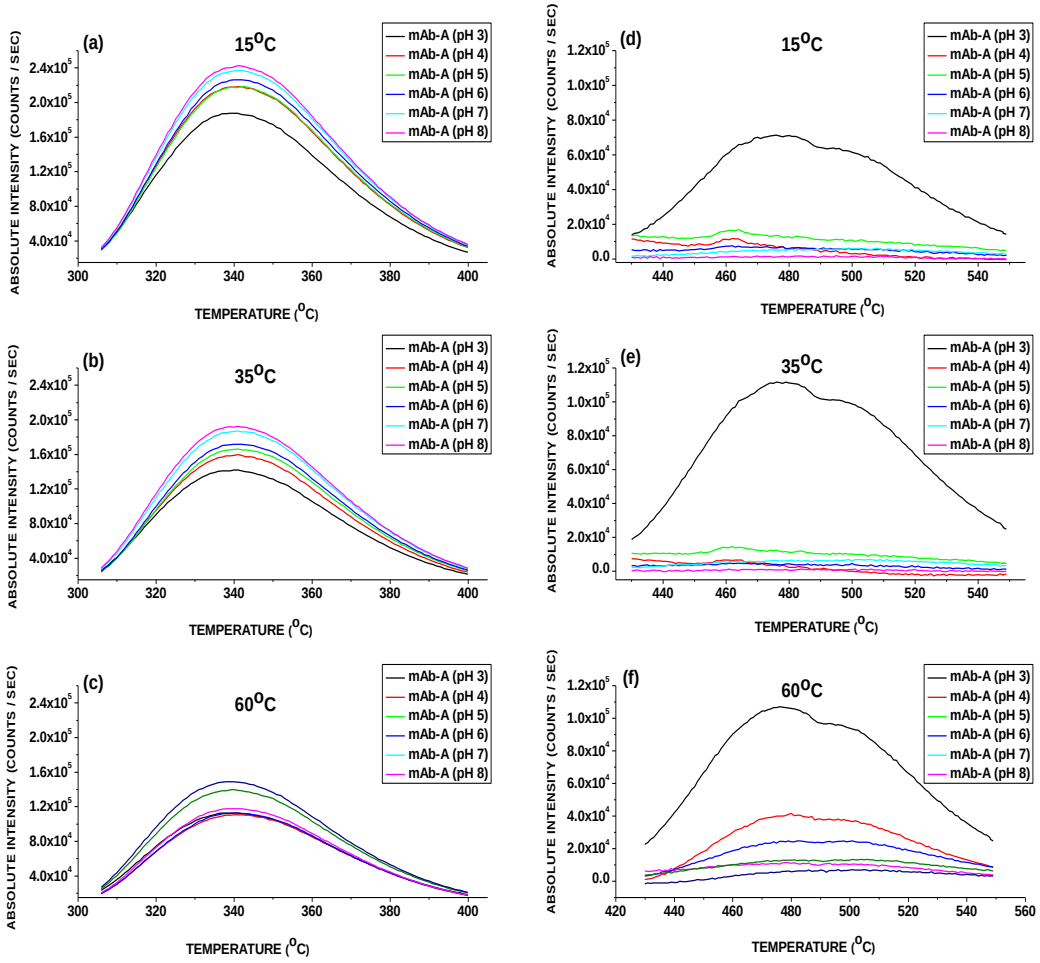

Fluorescence emission spectra for mAb-A as a function of pH (3 – 8). Intrinsic Trp (a – c) and ANS (d – f) fluorescence were monitored at 15 °C (a, d), 35 °C (b, e) and 60 °C (c, f).

Table 1: Effect of excipients on thermal unfolding temperature (T_M) of mAb-B as monitored by intrinsic tryptophan fluorescence spectroscopy using 0.1 mg/mL protein at pH 4.5 in 20 mM citrate-phosphate buffer (containing NaCl, I=0.1 and indicated level of excipients). ΔT_M and aggregation inhibition (%) columns represent the change in midpoint of thermal unfolding and change in aggregation, respectively for mAb-B in presence of excipients.

Category	Name	Concentration*	T_M (°C)[a]	ΔT_M (°C)[a]	Aggregation inhibition (%)
Protein	IgG1 (mAb-B)	0.1 mg/mL	59.9		
Stabilizer	Lactose	10%	62.5	2.6	75.7
	Trehalose	10%	61.8	1.9	30.5
	Dextrose	10%	63.1	3.2	63.8
	Sucrose	10%	62.4	2.5	81.9
	Mannitol	10%	62.2	2.3	NC
	Sorbitol	10%	61.9	2.0	59.7
	Malic acid	0.30 M	62.7	2.8	ND
Destabilizer	α-cyclodextrin	2.5%	57.2	-2.7	NC
	2-hydroxypropyl-β-cyclodextrin	10%	56.8	-3.1	NC
	Aspartic acid	0.075 M	58.5	-1.4	NC
	Lactic acid	0.15 M	58.2	-1.7	NC
	Arginine	0.30 M	55.9	-4.0	61.7
	Diethanolamine	0.30 M	57.5	-2.4	NC
	Guanidine	0.30 M	57.9	-2.0	NC
	Histidine	0.21 M	54.1	-5.8	NC
	Pluronic F-68	0.1%	56.7	-3.2	ND
Neutral	Sodium Citrate	0.1 M	58.9	-1.0	NC
	Brij 35	0.1%	60.0	0.1	57.8
	Tween 20	0.1%	59.7	-0.2	NC
	Tween 80	0.1%	58.9	-1.0	NC
	Glycine	0.30 M	61.1	1.2	62.5
	Proline	0.30 M	59.6	-0.3	NC
	Glycerol	10%	58.9	-1.0	64.7
	Dextran T40	0.0075 mM	59.4	-0.5	53.1
	2-hydroxypropyl-γ-cyclodextrin	10%	58.9	-1.0	NC
	Glutamic acid	0.30 M	60.7	0.8	ND
	Lysine	0.30 M	58.9	-1.0	ND

*Excipient concentrations are higher than those commonly used in formulations to facilitate excipient screening. [a]The T_M measurements were made within the standard error of ± 0.5 °C. [b]The aggregation inhibition (%) represents a mean of three measurements with a standard deviation of ± 2.5% for excipients that inhibited mAb-B aggregation. NC is a group of excipients that resulted in no change (±10%) in the aggregation behavior of mAb-B. ND is a group of excipients that increased mAb-B aggregation.

Supplementary Table 1: Mid-point of thermal transitions (T_M) for mAb-A (a) and mAb-B (b) studied over pH range 3-8 in 20 mM citrate-phosphate buffer (containing NaCl, I=0.1) as measured by differential scanning calorimetry (DSC). Error is SD of three measurements. NA represents the experimental condition where no corresponding transition could be detected.

(a)						
pH	**3**	**4**	**5**	**6**	**7**	**8**
T_M1	49.8 ± 1.0	54.1 ± 0.1	65.8 ± 0.1	69.0 ± 0.3	68.9 ± 0.1	68.7 ± 0.1
T_M2	70.7 ± 0.1	70.3 ± 0.1	82.1 ± 0.1	83.4 ± 0.2	84.0 ± 0.1	84.5 ± 0.1
T_M3	84.7 ± 0.4	84.9 ± 0.00	93.0 ± 0.1	91.7 ± 0.1	88.8 ± 0.1	NA

(b)						
pH	**3**	**4**	**5**	**6**	**7**	**8**
T_M1	55.3 ± 0.1	56.9 ± 0.2	NA	NA	NA	NA
T_M2	72.8 ± 0.2	65.6 ± 0.0	71.4 ± 0.2	72.4 ± 0.1	71.1 ± 0.2	71.5 ± 0.0
T_M3	85.8 ± 0.1	73.6 ± 0.1	82.0 ± 0.0	82.7 ± 0.0	82.0 ± 0.0	82.1 ± 0.1

Supplementary Table 2: Effect of varying excipient concentrations on midpoints of thermal transitions (T_M) for mAb-A at pH 4 [arginine (a) and sucrose (b)]; and mAb-B at pH 4.5 [arginine (c) and sucrose (d)] in 20 mM citrate-phosphate buffer (containing NaCl, I=0.1) as measured by DSC. Error is SD of three measurements.

(a)						
Arginine conc. (mM)	**T_M1 (^oC) ± SD**	**ΔT_M1 (^oC)**	**T_M2 (^oC) ± SD**	**ΔT_M2 (^oC)**	**T_M3 (^oC) ± SD**	**ΔT_M3 (^oC)**
0	53.2 ± 0.6		68.6 ± 0.1		83.6 ± 0.1	
10	52.1 ± 0.1	-1.1	68.1 ± 0.1	-0.5	83.0 ± 0.0	-0.6
50	50.9 ± 0.2	-2.3	66.6 ± 0.1	-2	81.8 ± 0.0	-1.8
100	49.6 ± 0.2	-3.6	65.6 ± 0.1	-3	80.7 ± 0.1	-2.9
175	48.1 ± 0.1	-5.1	64.5 ± 0.2	-4.1	79.7 ± 0.1	-3.9
250	46.9 ± 0.1	-6.3	63.3 ± 0.1	-5.3	78.7 ± 0.2	-4.9

(b)						
Sucrose conc. (mM)	**T_M1 (^oC) ± SD**	**ΔT_M1 (^oC)**	**T_M2 (^oC) ± SD**	**ΔT_M2 (^oC)**	**T_M3 (^oC) ± SD**	**ΔT_M3 (^oC)**
0	53.2 ± 0.6		68.6 ± 0.1		83.6 ± 0.1	
10	52.7 ± 0.1	-0.5	68.6 ± 0.1	0.0	83.5 ± 0.0	-0.1
50	53.0 ± 0.1	-0.2	68.9 ± 0.0	0.3	83.7 ± 0.1	0.1
100	53.1 ± 0.1	-0.1	69.1 ± 0.1	0.5	83.9 ± 0.2	0.3
250	53.9 ± 0.2	0.7	69.6 ± 0.1	1.0	84.5 ± 0.1	0.9
500	55.5 ± 0.1	2.3	71.0 ± 0.2	2.4	85.5 ± 0.2	1.9

(c)						
Arginine conc. (mM)	**T_M1 (^oC) ± SD**	**ΔT_M1 (^oC)**	**T_M2 (^oC) ± SD**	**ΔT_M2 (^oC)**	**T_M3 (^oC) ± SD**	**ΔT_M3 (^oC)**
0	61.2 ± 0.6		69.4 ± 0.4		79.7 ± 0.5	
10	60.7 ± 0.2	-0.5	68.7 ± 0.2	-0.7	78.1 ± 0.5	-1.6
50	59.9 ± 0.1	-1.3	68.1 ± 0.2	-1.3	77.5 ± 0.4	-2.2
100	58.9 ± 0.2	-2.3	67.6 ± 0.3	-1.8	76.8 ± 0.6	-2.9
250	57.6 ± 0.2	-3.6	66.8 ± 0.2	-2.6	75.7 ± 0.7	-4.0
300	57.2 ± 0.2	-4.0	66.6 ± 0.2	-2.8	75.5 ± 0.7	-4.2

(d)						
Sucrose conc. (mM)	**T_M1 (^oC) ± SD**	**ΔT_M1 (^oC)**	**T_M2 (^oC) ± SD**	**ΔT_M2 (^oC)**	**T_M3 (^oC) ± SD**	**ΔT_M3 (^oC)**
0	61.2 ± 0.2		69.4 ± 0.3		79.7 ± 0.5	
10	63.2 ± 0.2	2.0	70.4 ± 0.4	1.0	79.9 ± 0.5	0.2
50	63.3 ± 0.2	2.1	71.0 ± 0.4	1.6	80.1 ± 0.5	0.4
100	63.8 ± 0.1	2.6	70.8 ± 0.4	1.4	80.3 ± 0.4	0.6
250	64.7 ± 0.2	3.5	71.5 ± 0.5	2.1	81.1 ± 0.6	1.4
500	66.6 ± 0.2	5.4	72.8 ± 0.7	3.4	82.6 ± 0.5	2.9

Chapter 3

Effect of excipients on local dynamics of a monoclonal antibody and correlations with its global conformational stability

3.1 Introduction

The three-dimensional structure of native, functionally active proteins is considered to be a large ensemble of dynamic intra-convertible microstates that are stable in solution[208,209]. Proteins typically exhibit a wide variety of molecular motions ranging on the timescale from 10^{-15} to 10^{4} seconds. These fluctuations are comprised of local motions (10^{-15}–10^{-1} s; 0.01–5 Å) such as atomic and side chain fluctuations, rigid body motions (10^{-9}–1 s; 1–10 Å) such as helix or hinge bending deflections, or larger-scale movements (10^{-7}–10^{4} s; >5 Å) such as helix-coil or folding/unfolding transitions[210]. Protein dynamics can be influenced by both equilibrium fluctuations and non-equilibrium effects[208]. Equilibrium fluctuations strongly influence the biological function of a wide variety of proteins, including immunoglobulins[211]. The complex inter-relationships between protein dynamics, function and stability, however, are still being established[29,36-41,100]. A better understanding of the effect of micro-scale and large-scale conformational motions on the overall physical stability of pharmaceutically relevant proteins such as monoclonal antibodies (mAbs) will potentially aid in addressing challenges involved in the development of stable and efficacious formulations[127,212,213].

Proteins such as immunoglobulins can exhibit motions with different magnitudes of spatial and temporal scales which may arise from distinct regions within the protein. The thermodynamic and kinetic implications of such distinct dynamic regions in proteins have been previously studied[214-216]. These regions may have different degrees of exposure to the solvent in their immediate vicinity primarily involving water of hydration. This bound water is believed to play an important role in maintaining the stability and dynamics of the nonpolar core as well as the hydrophilic surface of proteins[53,190,192,217]. Many compounds such as osmolytes are known to influence the hydration potential of proteins by modulating protein-solvent interactions in

solution[74,218-220]. It is therefore of interest to study the effect of different solution variables such as pH, temperature and the presence of excipients not only on a global time-averaged scale but also on the local motions of different regions with distinct solvent exposures.

Polar fluorophores in environments with reduced mobility in which the solvent relaxation time (τ_R) is either equal to or higher than the lifetime (τ_F) of the fluorophore, exhibit an excitation wavelength dependent shift in their emission maxima towards higher wavelengths, a phenomenon known as red-edge excitation shift (REES)[201,221-225]. The concept of red-edge excitation can be used for site-selection and thus monitor the fraction of fluorophores (in this case Tryptophan; Trp) in different environments of immunoglobulins, instead of studying the averaged entire fluorophore population. The conserved Trp residues in immunoglobulins are generally categorized into at least two different environments. The solvent-exposed Trp populations are generally located between individual domains while the more buried Trp residues are located close to the intra-domain disulfide bond and in the proximity of other apolar side chains[226-231]. The two antigen binding domains (F_{ab}) comprise a total of 12 conserved Trp residues, while 8 Trp residues are contained in the crystallizable fragment (F_c) of immunoglobulins[232,233]. The Trp residues located in and between different domains constitute ~90% of the tryptophans present in the molecule[234]. A few additional Trp residues may also be present in the variable regions of an antibody[235].

Although the majority of conserved Trp residues can be categorized into these two defined environments (solvent-exposed and solvent-shielded), immunoglobulin fluorescence has diverse contributions arising from many distinct fluorophores with differences in their individual fluorescence spectra, lifetimes and anisotropies[236] indicative of differences in their microenvironments. Thus, selectively exciting a population of these Trp residues in

immunoglobulins (where $\tau_R \geq \tau_F$) with radiation containing progressively lower energy quanta (i.e., increasing excitation wavelength towards the red edge of an absorption band) should enable selective excitation of different average populations of fluorophores that have an increasing ability to interact strongly with solvent molecules in the excited state. Solvent molecules orient around these excited state fluorophores similar to that in a solvent-relaxed state, thus lowering electronic transition energies. The degree of fluorophore sampling upon red-edge excitation will be determined by the magnitude of a fluorophore's electronic transition energy, in which fluorophores with progressively lower electronic transition energies would be preferably excited upon red-edge excitation. It should be noted, however, that the observed fluorescence emission is still an average signal from more than one tryptophan residues.

It has been previously shown that techniques sensitive to the dynamic properties of immunoglobulins are able to detect minor transitions within the pre-unfolding transition region[120]. This region is defined as a range of temperature and pH over which the experimental parameters routinely used to evaluate a protein's higher-order structure and conformational stability do not demonstrate any evidence of a cooperative structural change. Such ambient temperatures and near neutral solution pH values comprising the pre-unfolding transition range are commonly encountered with formulated protein therapeutics. Solution parameters, however, such as pH, ionic strength, and the presence of salts and other excipients critically influence the stability of proteins in solution[47,237]. A recent study evaluating the effect of two different formulation excipients on the conformational stability and dynamics of immunoglobulins determined that sucrose and arginine differentially influenced the conformational stability and pre-transition dynamics of two IgG1 monoclonal antibodies in a concentration dependent manner[86]. Interestingly, the excipients influenced the global dynamics of one antibody and not

the other mAb within the pre-transition temperature range. These distinct effects on pre-transition dynamics were attributed to inherent differences in the two IgG1 mAbs potentially due to their thermal unfolding patterns, aggregation behavior, and/or levels of hydration. Stabilizing concentrations of sucrose were found to decrease, while destabilizing concentrations of arginine marginally increase, the global dynamics of mAb-B as studied by a combination of differential scanning calorimetry, ultrasonic spectroscopy and red-edge excitation spectroscopy.

The ability to selectively excite and monitor intrinsic Trp fluorophores in regions with different degrees of solvent exposure within mAb-B, as a function of temperature and/or the presence of excipients, should therefore provide valuable insights into changes in conformational stability and dynamics of different regions within the protein. The current study is thus aimed at (1) evaluating the conformational stability, dynamics and excipient effects on regions with distinct solvent-exposures in mAb-B as a function of temperature, as measured by fluorescence spectroscopy using red-edge excitation (REE) and, (2) better understanding correlations between local dynamics and global conformational stability of mAb-B, both in the absence and presence of stabilizing or destabilizing excipients.

3.2 Experimental

3.2.1 Materials

The IgG1 monoclonal antibody (mAb-B) was supplied by MedImmune (Gaithersburg, MD) and stored in its formulation buffer at 2 – 8 ^{o}C. The protein was dialyzed into 20 mM citrate phosphate buffer at pH 4.5 and the final ionic strength was maintained at 0.1 using NaCl. All chemicals, including the buffer components, were purchased either from Sigma (St. Louis,

MO) or Fisher Scientific (Pittsburgh, PA). Sucrose from Ferro Pfanstiehl Laboratories was used in these studies.

3.2.2 Methods

Intrinsic tryptophan fluorescence spectra were acquired using a two-channel, peltier controlled four-position PTI Quanta Master Spectrophotometer (Lawrenceville, NJ). The sample temperature was precisely controlled from 10.0 to 70.0 ^{o}C at 2.5 ^{o}C intervals with an equilibration time of 4 min. An IgG1 concentration of 0.1 mg/mL (~ 6.7 x 10^{-4} mM) was used in a 1 cm quartz cuvette. Excitation and emission slit widths were set at 3 nm. Samples were excited from 292 to 308 nm at 4 nm intervals to insure samplings of tryptophan residues with different degrees of solvent exposure. Emission spectra were collected from 310 – 400 nm for each of the excitation wavelengths. The spectra were corrected for background fluorescence and contributions from solvent Raman scattering by subtraction of a corresponding buffer. The emission maxima and peak intensity were determined by a mean spectral center of mass (MSM) method, since the scattering peak at 308 nm limits the application of derivative analysis in a few cases. Such emission maxima are usually higher by ~ 8 – 10 nm than that obtained by derivative analysis (the actual peak position). The relative change in peak position, however, can be measured with increased precision and reproducibility by MSM. This is especially the case for Trp fluorescence at the red edge of an absorption band due to poor signal to noise ratio (low emission).

Experiments were performed in the absence and presence of excipients. Sucrose (500 mM) and arginine (250 mM; as hydrochloride salt) were used as a stabilizing and destabilizing excipient, respectively[86]. The midpoints of thermal unfolding transitions (T_M) were determined

by fitting tryptophan peak position versus temperature plots using a Sigmoidal-Boltzmann function, in which the half transition point was considered as the T_M value.

To provide further insights into local dynamic behavior of mAb-B, Trp fluorescence quenching experiments were performed using different concentrations of acrylamide as a neutral quencher[238-240]. The peak intensities at various acrylamide concentrations (0 – 0.5 M) were used for constructing Stern-Volmer plots at different excitation wavelengths, in the absence and presence of excipients and at different temperatures (10, 20, 45 and 60 ^oC). The temperatures were selected to monitor the pre-transition range (10 and 20 ^oC), onset temperature (T_{onset}; 45 ^oC) and the melting temperature (T_M; 60 ^oC) of mAb-B thermal unfolding[86,120]. Inner filter effects produced by acrylamide were corrected using the following equation[241]:

$$F_{corrected} = F_{observed} \text{ antilog } [(Abs_{EX} + Abs_{EM})/2]$$

where $F_{corrected}$ and $F_{observed}$ are the corrected and background subtracted fluorescence intensities of the sample. Abs_{EX} and Abs_{EM} are the measured absorbance at excitation and emission wavelengths, respectively.

3.3 Results

3.3.1 Intrinsic tryptophan fluorescence, thermal melting temperature and excipient effects as a function of fluorescence excitation wavelength

Changes in mAb-B higher-order structure and conformational stability with temperature and excitation wavelength are illustrated in Figure 1, in which the tryptophan emission maximum (peak position) is plotted as a function of temperature at different excitation wavelengths. At 10

^{o}C and throughout the pre-transition temperature range (10 – 35 ^{o}C), the Trp emission maxima for mAb-B have shifted to a higher wavelength upon red-edge excitation from 292 to 308 nm (Figure 1A, 1D). This observation suggests that the sampled fluorophores exist in an environment with reduced mobility in which a red-edge effect is observed. Similar trends in the red-edge shifts in mAb-B were also observed in the presence of arginine and sucrose, albeit to different extents (Figure 1B, 1C, 1D). Since Trp fluorophores in immunoglobulins can exist in distinct microenvironments with differences in their solvent exposures, the higher initial peak positions (Figure 1A to 1D) and decrease in fluorescence intensity (Figure 1E) indicate that regions with a greater degree of solvent exposure in mAb-B are monitored by progressively increasing excitation wavelengths. The change in peak position with temperature in the absence and presence of excipients and at different excitation wavelengths can thus be used to study alterations in tertiary structure and conformational stability of different regions within mAb-B. mAb-B undergoes structural transitions with increases in temperature above 40 ^{o}C such that the intrinsic protein fluorophores are more exposed to solvent as suggested by red-shifts in the Trp peak position. The thermal melting temperature (T_M), however, was found to inversely correlate with excitation wavelength (i.e., T_M values were lower when the protein was probed with higher excitation wavelengths). For example, the melting temperature for mAb-B was determined to be 55.2 ± 0.0 when excited at 292 nm, while the T_M was lowered to 52.7 ± 0.2 when the peak position shifts were monitored upon excitation at 308 nm (Table 1).

The unfolding pattern as a function of excitation wavelength was not, however, altered in the presence of the excipients (Figure 1B and 1C). Figure 2 (2A to 2D) shows a comparison of the same data set in terms of peak position shifts in mAb-B as a function of temperature in the absence and presence of arginine and sucrose at different excitation wavelengths. Arginine

lowered the T_M, whereas sucrose increased the melting temperature of mAb-B at all excitation wavelengths. The trend of decreasing T_M values as a function of increasing excitation wavelength was retained in the presence of arginine and sucrose, albeit possessing lower and higher T_M values, respectively (Figure 2E; Table 1). In the pre-transition temperature range (< 35 ^oC), sucrose caused an increase in Trp peak position in mAb-B regions with relatively higher degrees of solvent exposure as probed by excitation at 304 and 308 nm (Figure 2C and 2D). This result suggests an expected increased hydration of fluorophore environments closer to the surface of the protein, and is consistent with the well-known preferential hydration mechanism of protein stabilization by sucrose[105]. Both arginine and sucrose influenced the stability of the more solvent-exposed versus more solvent-shielded Trp containing regions in mAb-B to different extents, in which the trend and magnitude of stabilizing or destabilizing effects were greater for regions that were excited at 304 and 308 nm compared to those excited at 292 nm and 296 nm (Figure 2F, Table 2).

It was also found that the tryptophan peak positions in the pre-transition temperature range (10 – ~35 ^oC; prior to any major structural transitions as evidenced by a red-shift with temperature) were sensitive to increases in solution temperature (Figure 1A, 1B, 1C). As shown in Figure 3, for mAb-B in the absence of excipients, these peak positions versus temperature plots demonstrated a measurable negative slope for lower excitation wavelengths. This slope was found to increase (become more positive) as the excitation wavelength was raised (as observed with two separate controls in Figure 3A and 3B, respectively). Since arginine and sucrose were found to influence the dynamics of mAb-B in its pre-transition temperature range[86], the effect of these excipients on mAb-B was evaluated by assessing their effects on the pre-transition slope as a function of excitation wavelength. Figure 3 displays the magnitude of pre-

transition slopes (10 – 27.5 ^{o}C) for mAb-B in the absence and presence of both sucrose and arginine at various excitation wavelengths. For the protein in the absence of excipients, the negative slope of peak position versus temperature data remained unchanged when the excitation wavelength was increased from 292 nm up to 300 nm. The peak position shifts for Trp fluorophores excited with > 300 nm radiation, however, were found to have greater slopes as a function of temperature compared to those at lower excitation wavelengths. Arginine and sucrose both increased the magnitude of negative slopes seen for mAb-B. The prominent effect of arginine was on pre-transition slopes at lower excitation wavelength (from 292 – 300 nm), while sucrose primarily influenced the slopes when probed by higher excitation wavelengths (304 and 308 nm). The significance of these results is discussed later.

3.3.2 Acrylamide quenching studies using mAb-B at various excitation wavelengths and temperatures: Evaluation of excipient effects.

Acrylamide quenching of tryptophan fluorescence is routinely used to monitor changes in tryptophan environment in proteins as well as the dynamic properties of protein matricies[238,239]. Figure 4 (A to I) shows Stern-Volmer plots for acrylamide quenching of tryptophan residues in mAb-B at 20 ^{o}C (Figure 4A, 4D, 4G), 45 ^{o}C (Figure 4B, 4E, 4H) and 60 ^{o}C (Figure 4C, 4F, 4I) and at excitation wavelengths ranging from 292 – 308 nm. These experiments were performed in the absence and presence of arginine and sucrose as described above. The slopes of these individual plots are related to the accessibility of Trp residues to the quencher (which in turn is related to the dynamics of the fluorophore environment), wherein a more positive slope is indicative of a higher degree of Trp exposure. For example, the Stern-Volmer plots were found to deviate from linearity (towards the X-axis) at 20 ^{o}C, when the Trp residues with a higher degree of solvent-shielding (excitation at 292 nm) were examined. Such well-defined curvature,

indicative of heterogeneous Trp environments, was less apparent for more solvent-exposed Trp residues (excitation at 308 nm). Excipients did not alter these non-linear curves in their respective Stern-Volmer plots (Figure 6A, 6B, 6C; see text below) suggesting that a heterogeneous environment of Trp fluorescence exists in mAb-B even in the presence of excipients.

The standard Stern-Volmer equation[234] is valid only for homogenous fluorescence and in the absence of static quenching. Heterogeneity due to the multiple microenvironments of tryptophan(s) residues in immunoglobulins thus precludes fitting of the data to the Stern-Volmer equation. This limits our ability to extract quantitative static and dynamic components from the data. Furthermore, a meaningful bimolecular quenching constant could not be determined since it was not possible to deconvolute the intensity decay into its components to obtain individual lifetimes. Processes such as configurational relaxation and/or contributions from heterogeneous microenvironments are also known to cause complex time dependence in excited-state interactions resulting in non-exponential fluorescence decay[242]. All of the plots, however, can be qualitatively compared based on the trends in the magnitude of the quenching by acrylamide. This trend analysis can be used to evaluate the effect of excipients on potential changes in dynamics of different regions within mAb-B.

At 20 ^{o}C, the slopes in the Stern-Volmer plots were found to increase with increases in excitation wavelength (Figure 4A, 4D, 4G). The largest and smallest slope was found for 308 nm (solvent-exposed regions) and 292 nm (solvent-shielded regions) excitation respectively. The dependence of these slopes on excitation wavelength was influenced by temperature. For instance, the trend in the magnitude of the slopes and/or the extent of quenching as a function of excitation wavelength were reversed when the temperature of a mAb-B solution was raised from

20 to 45 ^{o}C (Figure 4A compared to Figure 4B). This effect of temperature on the extent of quenching at 292 nm and 308 nm in the absence and presence of excipients is plotted separately in Figure 5 (A – F). The extent of quenching was found to increase when the temperature was raised from 10 ^{o}C to 60 ^{o}C for mAb-B alone (Figure 5A) and in the presence of sucrose (Figure 5E) upon excitation at 292 nm. A similar temperature dependence was found for mAb-B in the presence of arginine only up to 45 ^{o}C while the trend in the magnitude of the Trp quenching was decreased at a higher temperature (Figure 5C). Upon an excitation at 308 nm, however, such trends in the magnitude of quenching were not observed until up to 45 ^{o}C for protein alone or in the presence of excipients (Figure 5B, 5D, 5F). At 60 ^{o}C, a smaller slope was observed for protein alone and in the presence of sucrose (Figure 5B, 5F). The magnitude of fluorescence quenching in the protein alone (Figure 5B) and in presence of arginine (Figure 5D) was found to be dependent upon acrylamide concentration at 60 ^{o}C. This acrylamide concentration dependence was not, however, observed in mAb-B solutions containing sucrose at 60 ^{o}C (Figure 5F).

The effect of excipients on the dynamics of mAb-B can be evaluated by monitoring trends in the Stern-Volmer plots upon excitation at 292 and 308 nm. These graphs, using the same data sets in Figure 4, are replotted at 20, 45 and 60 ^{o}C separately in Figure 6 to enable more effective comparison of the data. The slope of these plots for mAb-B was lowered in the presence of both sucrose and arginine when probed with excitation at 292 nm, albeit to different extents (Figure 6A, 6B, 6C). The magnitude of changes in slope values in the presence of arginine was sensitive to temperature while sucrose lowered mAb-B fluorescence quenching at all temperatures used in this study, especially notable at higher acrylamide concentrations

(Figure 6A, 6B, 6C). Upon 308 nm excitation, however, the differences in the slopes in the presence of excipients were only significant at 60 ^{o}C (Figure 6D, 6E, 6F).

3.4 Discussion

Excipients such as sugars and amino acids are frequently used to increase the conformational stability of therapeutic proteins' native structure and prevent aggregation both in solution and the dried state[47,78]. These excipients are known to influence the forces and interactions involved in maintaining the stability of protein(s)[47] in part by altering the organization of hydration water[243]. Our previous studies show that sucrose and arginine had distinct effects on the stability and global dynamics of two different mAbs[86]. It is now well accepted that changes in solvent properties by co-solutes not only influence proteins' inherent stability, but also have significant effect on their internal dynamics, which is thought to be coupled to the surrounding solvent[53,54,190]. The current study is directed toward a better understanding of the effects of these excipients on the stability of different regions within an antibody by site-selection (upon red-edge excitation) of Trp fluorophores within environments with differential extents of solvent exposure. The findings are further supported by acrylamide quenching studies to better understand excipient effects on the local dynamics of mAb-B.

3.4.1 Structure, conformational stability and excipient effects on different regions of mAb-B

As discussed earlier, excitation of Trp residues in mAb-B with a progressively higher excitation wavelength towards the red-edge of an absorption band should enable sampling of fluorophores within environments that are increasingly exposed to the solvent. For instance, excitation at 292 nm should monitor Trp fluorophore environments that are relatively more

shielded from the solvent (described as 'solvent-shielded' for rest of this discussion although these residues are still in polar environments as discussed below) compared to that at 308 nm which would sample more solvent-exposed Trp residues. A red-edge excitation shift was observed at all of the excitation wavelengths employed in this study with mAb-B, albeit to different extents. This result suggests that the indole sidechains of Trp residues in mAb-B are located in polar environments accessible to the solvent. This accessibility should be governed by the dynamics of both the global and local environments.

Higher peak positions as a function of excitation wavelength (Figure 1A, 1B, 1C) throughout the temperature range examined shows that fluorophores (Trp residues) with different degrees of solvent exposure are sampled in mAb-B. The peak position shifts with temperature, which indicates alterations in a protein's tertiary structure, demonstrates that the solvent-exposed regions (e.g., upon 308 nm excitation) in mAb-B unfold at lower temperatures than regions that are relatively more shielded (e.g., upon 292 nm excitation) from the solvent. This is evident from an inverse relationship between T_M values of these different regions as shown in Figure 2E and Table 1 (comparison of higher to a lower excitation wavelength). Although these observations seem intuitively reasonable, such results may be different for individual mAbs, since a similar pattern was not observed (unpublished data) for a different IgG1 antibody. Sucrose and arginine influenced the structural stability of the different solvent-exposed regions of Trp residues in mAb-B as monitored in these studies (Figure 2; Table 1). The trend and magnitude of stabilization and destabilization by both sucrose and arginine, respectively, was greater for solvent-exposed residues (monitored, for instance, by 308 nm excitation) compared to solvent-shielded ones (for example, upon 292 nm excitation) as shown in Figure 2F and Table 2.

In the pre-transition temperature range, however, arginine was found to significantly influence the solvent-shielded regions while sucrose effects were more prominent with solvent-exposed Trp residues in mAb-B (Figure 3). This result was supported by arginine and sucrose effects on the slope of peak position versus temperature plots in the pre-transition range. It is known that entropically governed apolar interactions generally increase with temperature[244-246] in the low temperature regime. Similar increases in apolar interactions in mAb-B may result in greater shielding of apolar residues with increases in temperature in the pre-transition range, consistent with the blue shifts in Trp peak position versus temperature (negative slope) results when probed, for example, at 292 nm. The trend in the magnitude of this slope was found to increase (become more positive) for more solvent-exposed residues in mAb-B (Figure 3), potentially reflecting limited participation of these different environments in apolar interactions that stabilize the native structure.

The effect of arginine on these pre-transition slopes was more pronounced for solvent-shielded regions, suggesting that arginine further increases the extent of apolar interactions in the protein's interior. One possible explanation for such an effect could arise from the fact that arginine can be involved in cation-π interactions and hydrogen bonding contacts with protein surface sidechains or have a direct or indirect effect on surface hydration[110,113,247,248]. Such effects may also strengthen compensatory stabilizing forces such as apolar interactions. Since solvent-exposed residues are expected to contribute less to apolar interactions, arginine does not appear to influence pre-transition slopes of such regions (Figure 3B; 304 and 308 nm excitation data). In contrast, the preferential hydration of proteins by sucrose stabilization is well known[105]. Such an effect would promote protein surface-solvent interactions and promote a significant effect of sucrose on solvent-exposed residues. These interactions would be expected to be more

effective at lower temperatures compared to room (or higher) temperatures. Such low temperature effects resulted in a red-shifted initial Trp peak position (Figure 1C), the magnitude of which decreases with increases in temperature, resulting in a negative pre-transition slope for solvent-exposed regions in mAb-B in the presence of sucrose (Figure 3A; 304 and 308 nm excitation data). This negative slope in the presence of sucrose should to a first approximation be a reflection of temperature effects on the interaction of the antibody surface with the surrounding solvent especially in the hydration layer.

3.4.2 Excipient effects on the dynamics of different regions in mAb-B with varying degrees of solvent exposure.

The dynamics of different tryptophan environments in mAb-B were studied in the absence and presence of excipients by monitoring acrylamide quenching of Trp fluorescence upon red-edge excitation. Acrylamide in solution acts as a neutral collisional quencher which can diffuse into proteins' interior and quench indole fluorescence. The accessibility of tryptophan residues, however, will depend upon the dynamic properties of its environment. A better understanding of local dynamics can therefore be obtained by performing quenching studies on distinct solvent-exposed Trp populations (and hence their environments). The quenching studies were performed at different temperatures to help evaluate the dynamic properties of mAb-B in the pre-transition temperature range (10 and 20 ^{o}C), at T_{onset} (45 ^{o}C) and at the melting temperature (60 ^{o}C) of thermal unfolding. Immunoglobulins such as mAb-B typically have ~20 conserved tryptophan residues, and although located in heterogeneous environments, can be generally grouped into two environments: solvent-exposed and solvent-shielded (see introduction).

When solvent-shielded environments in mAb-B were probed (for instance, by 292 nm excitation), a heterogeneous distribution of Trp residues results in a deviation of Stern-Volmer plots from linearity towards the X-axis (downward curvature). This effect was found at all temperatures (Figure 6A, 6B, 6C). Such heterogeneity was less apparent for surface-exposed regions (for instance, by 308 nm excitation as shown in Figure 6D, 6E, 6F). Deviations from simple Stern-Volmer behavior can also be a consequence of unresolved static and dynamic components in the data[234]. The static and dynamic (or collisional) quenching effects can be differentiated by decreases and increases in the magnitude of quenching upon increases in temperature, respectively. The magnitude of quenching for mAb-B Trp residues was found to increase when the temperature was raised from 10 to 20 ^{o}C (Figure 5A, 5C, 5E), both in the absence and presence of excipients, suggesting that the non-linearity in Stern-Volmer plots is due to a heterogeneous distribution of fluorophores rather than contributions from static quenching.

A greater magnitude of quenching is indicative of increased accessibility of Trp residues and thus a more dynamic nature of the fluorophore's environment. This is reflected in higher (more positive) slopes of Stern-Volmer plots. In the pre-transition range (at 20 ^{o}C), the solvent-exposed Trp containing regions of mAb-B (monitored, for instance, upon 308 nm excitation) were found to be more dynamically quenched compared to the solvent-shielded Trp containing regions (using 292 nm excitation), both in the absence and presence of arginine or sucrose (compare Figure 4D and 4G to 4A). Arginine and sucrose were found to rigidify the solvent-shielded regions to greater and lower extents, respectively, in the pre-transition range (Figure 6A). Such a rigidifying effect by arginine in the pre-transition temperature range can be explained by increases in apolar interactions involving solvent-shielded regions of mAb-B as

discussed earlier (Figure 3). The quenching data, however, could not distinguish such excipient effects for solvent-exposed regions (at 308 nm excitation) in the pre-transition range (Figure 6D).

At the T_{onset} temperature (~45 ^{o}C), however, it was determined that the dynamic nature of solvent-shielded regions of mAb-B (upon 292 excitation) was significantly increased relative to regions with more surface-exposed Trp residues (upon excitation at 308 nm) as shown in Figure 4B, 4E, 4H. No major change was observed in the dynamics of the surface exposed regions of mAb-B and in presence of sucrose when the temperature was raised from 20 ^{o}C to 45 ^{o}C (Figure 5B, 5F). The exception was protein in the presence of arginine where the dynamic behavior of the more surface-exposed regions of mAb-B seems to marginally decrease when the temperature was raised from 20 ^{o}C to either 45 or 60 ^{o}C (Figure 5D). These observations suggest that increases in dynamics of the more solvent-shielded regions presumably located in mAb-B's interior may predispose the protein to structural alterations such that it subsequently undergoes thermal unfolding.

The increase in internal dynamics (more solvent-shielded Trp containing regions monitored, for instance, by 292 nm) was further increased when observed at the thermal melting temperature (60 ^{o}C) of the protein alone and in the presence of sucrose (Figure 5A, 5E). The protein in the presence of arginine, however, showed a decrease in internal dynamics at 60 ^{o}C (Figure 5C). Since mAb-B is prone to formation of intermolecular β-sheet rich aggregates upon unfolding[86,120], arginine destabilization may result in shielding of tryptophan residues in such intermolecular species, thus lowering the magnitude of quenching by acrylamide. Such an apparent reduction in dynamics at 60 ^{o}C was also observed for solvent-exposed regions (probed by 308 nm excitation) in mAb-B in absence and presence of excipients (Figure 5B, 5D, 5F). This result may be due to the possibility that surface regions (more solvent-exposed Trp

residues) precede the internal regions (more solvent-shielded Trp residues) in their involvement during aggregate formation. Alternatively, the surface dynamics may be significantly dampened at the thermal melting temperature of the protein. For mAb-B alone and in the presence of arginine (Figure 5B, 5D), there exists a concentration dependent quenching of Trp residues in which higher concentrations of acrylamide seem to diffuse into more loosely formed mAb-B structures, suggesting the former mechanism is more likely in these scenarios. The protein in the presence of sucrose, however, does not show such concentration dependent acrylamide quenching trends suggesting that the surface dynamics of mAb-B are reduced dramatically by sucrose even at 60 ^{o}C. The preferential hydration of the protein in the presence of sucrose provides a potential reason for such a surface effect. Furthermore, it is apparent that at 60 ^{o}C, arginine decreases the dynamics of solvent-shielded Trp regions (probed using 292 nm excitation) as shown in Figure 6C, potentially due to aggregate formation upon mAb-B destabilization[120], while increasing the surface dynamics by influencing solvent-exposed Trp regions (Figure 6F). Sucrose, however, was found to decrease the dynamics of both regions at all temperatures examined (Figure 3 and Figure 6A – C, 6F). These results are consistent with our earlier results[86] in which sucrose decreased and arginine marginally increased global dynamics of mAb-B.

3.4.3 Correlation of excipient effects between conformational stability and the dynamics of different regions within mAb-B.

This study highlights some important relationships between protein dynamics and conformational stability within different solvent exposed regions of mAb-B, as monitored via the Trp residues in the protein. To summarize the results of changes in dynamics and conformational stability of mAb-B, in the absence and presence of excipients, it was initially

found that mAb-B thermal unfolding was a step-wise cascade of events that is initiated by transitions in the solvent-exposed regions of the protein. Secondly, arginine and sucrose influenced the conformational stability by decreasing and increasing the T_M, respectively, for both solvent-exposed and solvent-shielded regions. The magnitude of stabilization or destabilization of these excipients, however, was higher for solvent-exposed and less for solvent-shielded regions of mAb-B. Thirdly, the increase in internal dynamics (in the more solvent-shielded regions) of mAb-B was found to predispose the protein to unfolding structural transitions at the T_{onset}. Furthermore, this effect may increase the propensity of arginine to form cation-π or other interactions with solvent-shielded aromatic residues, leading to destabilization. The reduction in the pre-transition dynamics of mAb-B, however, observed in the presence of arginine for the solvent-shielded regions, within the pre-transition temperature range, could potentially be explained by increases in apolar interactions in mAb-B under these conditions. Furthermore, a reduction of mAb-B dynamics by sucrose, predominantly in the proteins' solvent-exposed regions, may better explain the greater magnitude of surface stabilization in the presence of sucrose (Figure 2F). Such an effect of sucrose on the more solvent-exposed regions of mAb-B may thus help prevent the step-wise, subsequent cascade of unfolding events that initiate upon surface destabilization (Figure 1A, 1C, 2F). Finally, the dampening of mAb-B surface dynamics (i.e., in the more solvent-exposed regions of mAb-B; Figure 5B, 5D) at the thermal melting temperature provide preliminary evidence that apolar amino acids in solvent-exposed regions could potentially initiate the formation of larger irreversible aggregates, as reported earlier[120], during thermal unfolding of mAb-B.

Figure 1

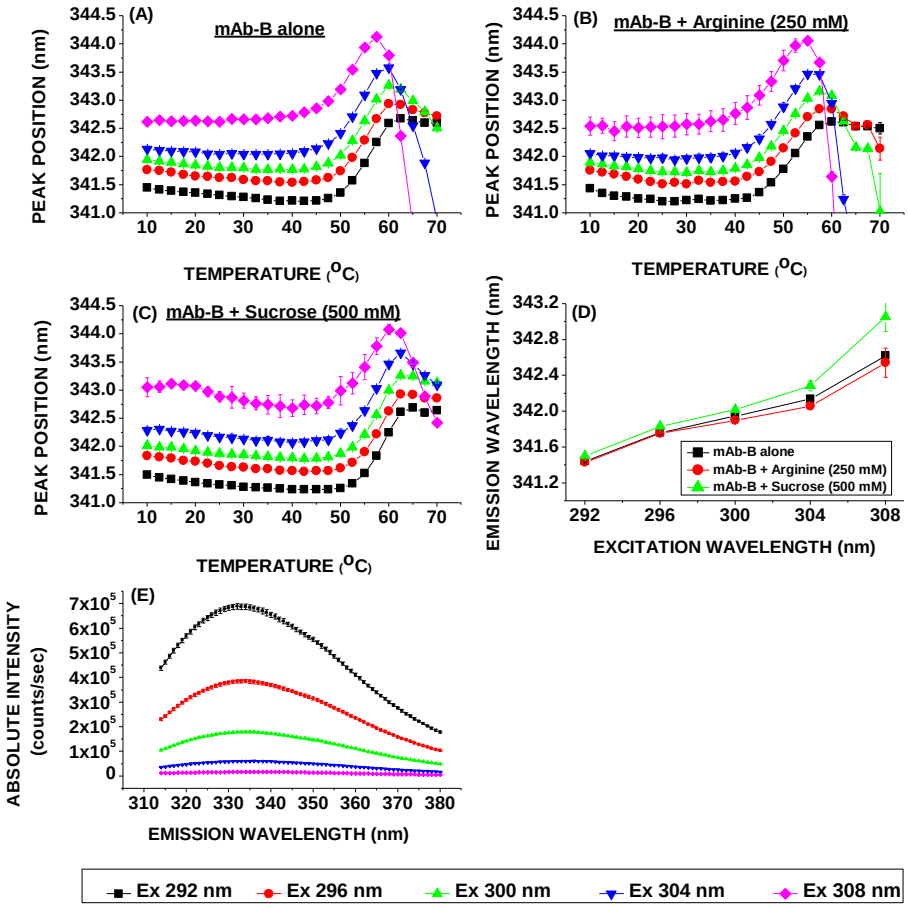

Tryptophan intrinsic fluorescence peak position as a function of temperature at different excitation wavelengths for (A) mAb-B alone, (B) mAb-B in the presence of arginine and, (C) mAb-B in the presence of sucrose. The emission maxima as a function of excitation wavelength at 10 ^{o}C is plotted in (D) for mAb-B in the absence and presence of arginine and sucrose. Representative emission spectra (E) are shown at 10 ^{o}C for different excitation wavelengths (292 – 308 nm) using mAb-B. Errors bars (n=3) that cannot be seen are encompassed within the symbols. Arginine and sucrose were used at 250 mM and 500 mM respectively in 20 mM citrate-phosphate buffer at pH 4.5 for all the studies.

Figure 2

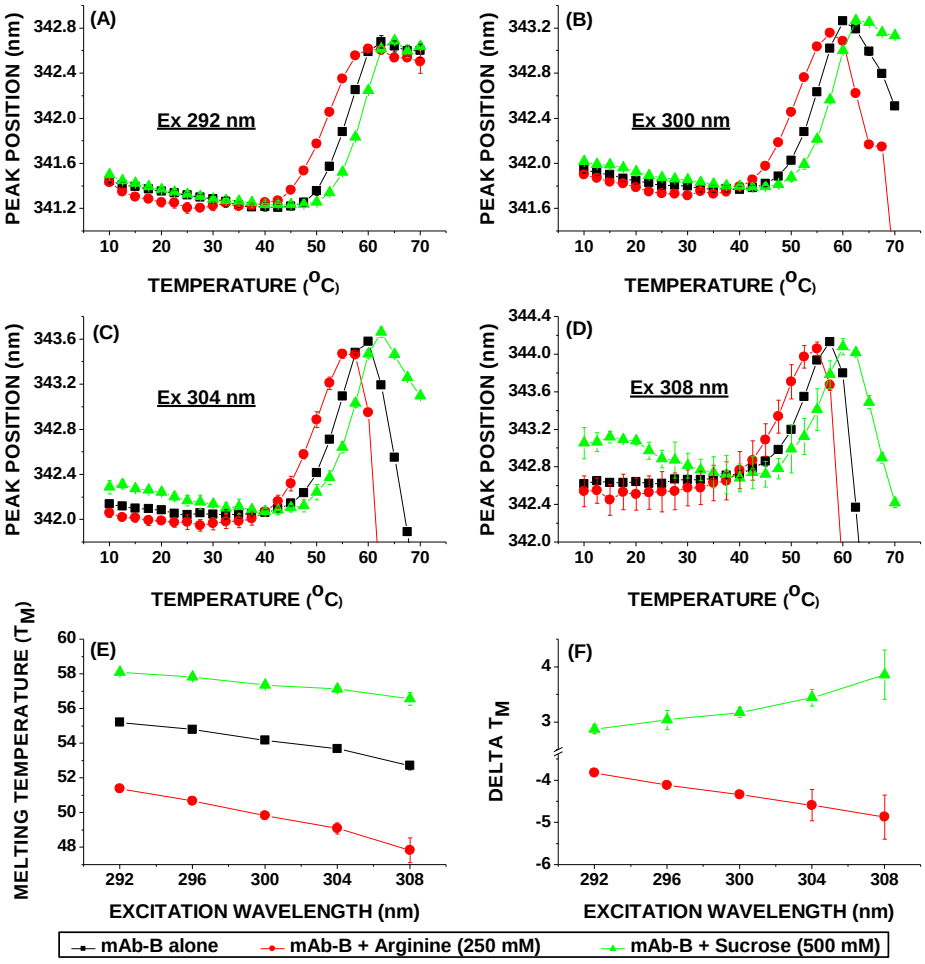

The effect of arginine and sucrose on the tertiary structure stability of mAb-B at pH 4.5 as measured by intrinsic fluorescence spectroscopy upon excitation at (A) 292 nm, (B) 300 nm, (C) 304 nm, and (D) 308 nm. Similar figure at 296 nm excitation has been presented previously[86]. The thermal melting temperature as a function of excitation wavelength is plotted in (E) for mAb-B in the absence and presence of arginine or sucrose. The change in thermal melting temperature (ΔT_M) of mAb-B produced by the excipients, compared to protein without excipients, is presented as a function of different excitation wavelengths (F).

Figure 3

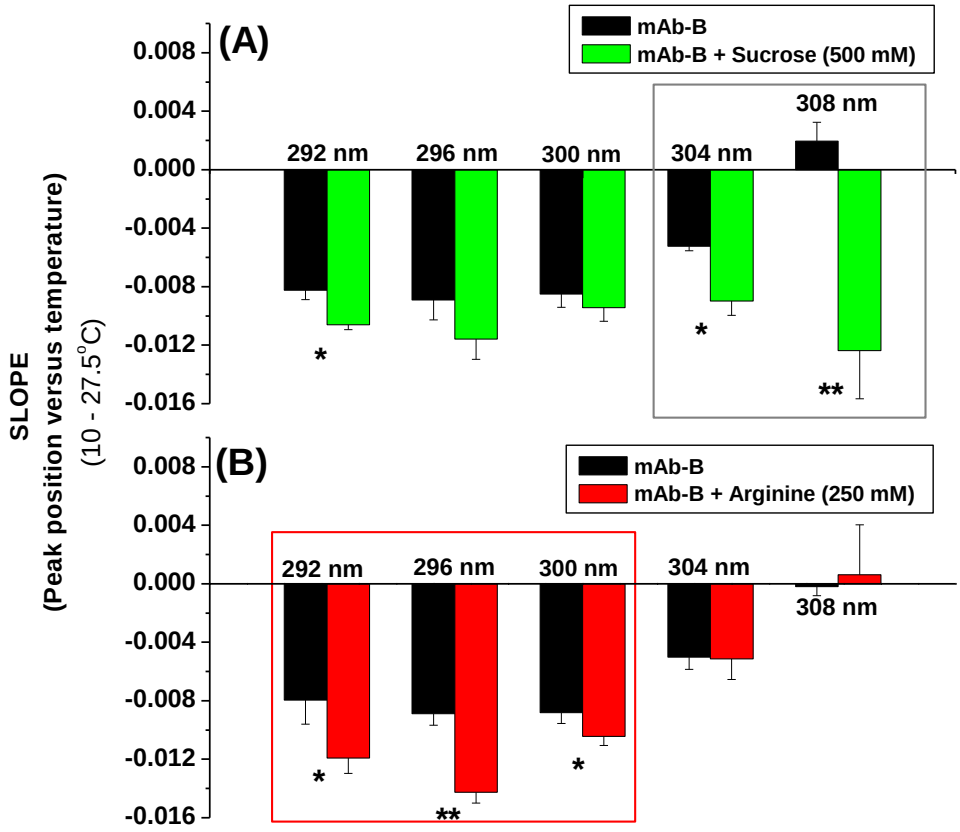

The slope of Trp peak position of mAb-B versus temperature in the pre-transition temperature range (10 – 27 ^{o}C) as measured by intrinsic fluorescence spectroscopy as a function of an excitation wavelength in the absence and presence of (A) sucrose or (B) arginine. The statistical significance of excipient effects on the measured slope were evaluated at p-values of <0.05 (*) and <0.01 (**).

Figure 4

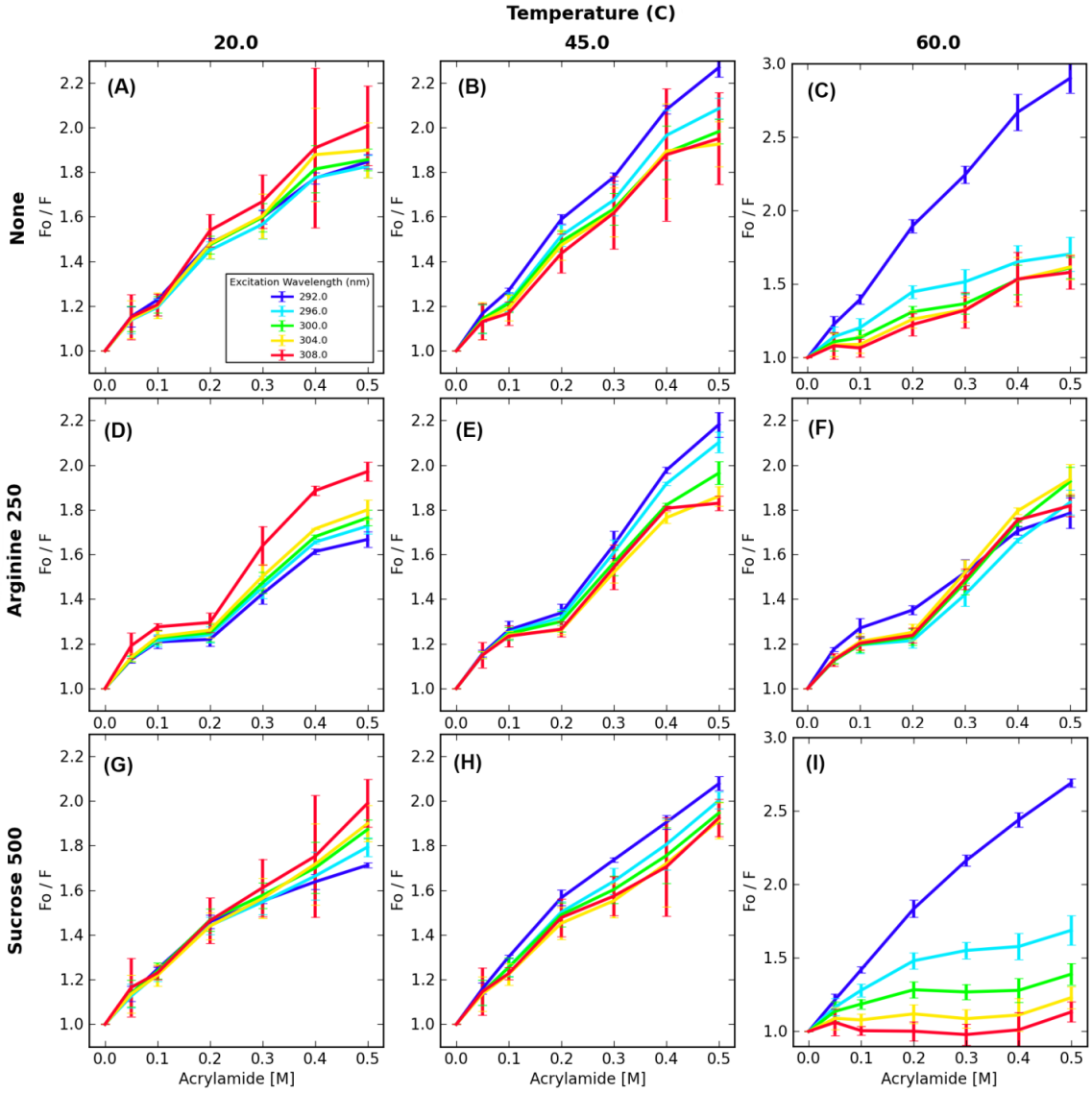

Stern-Volmer plots for acrylamide quenching of intrinsic tryptophan fluorescence in mAb-B at different excitation wavelengths for (A) mAb-B alone at 20 ^{o}C, (B) mAb-B alone at 45 ^{o}C, (C) mAb-B alone at 60 ^{o}C, (D) mAb-B with arginine at 20 ^{o}C, (E) mAb-B with arginine at 45 ^{o}C, (F) mAb-B with arginine at 60 ^{o}C, (G) mAb-B with sucrose at 20 ^{o}C, (H) mAb-B with sucrose at 45 ^{o}C and, (I) mAb-B with sucrose at 60 ^{o}C. Experimental details are given in the text. The line connecting data points are for visual aid only.

Figure 5

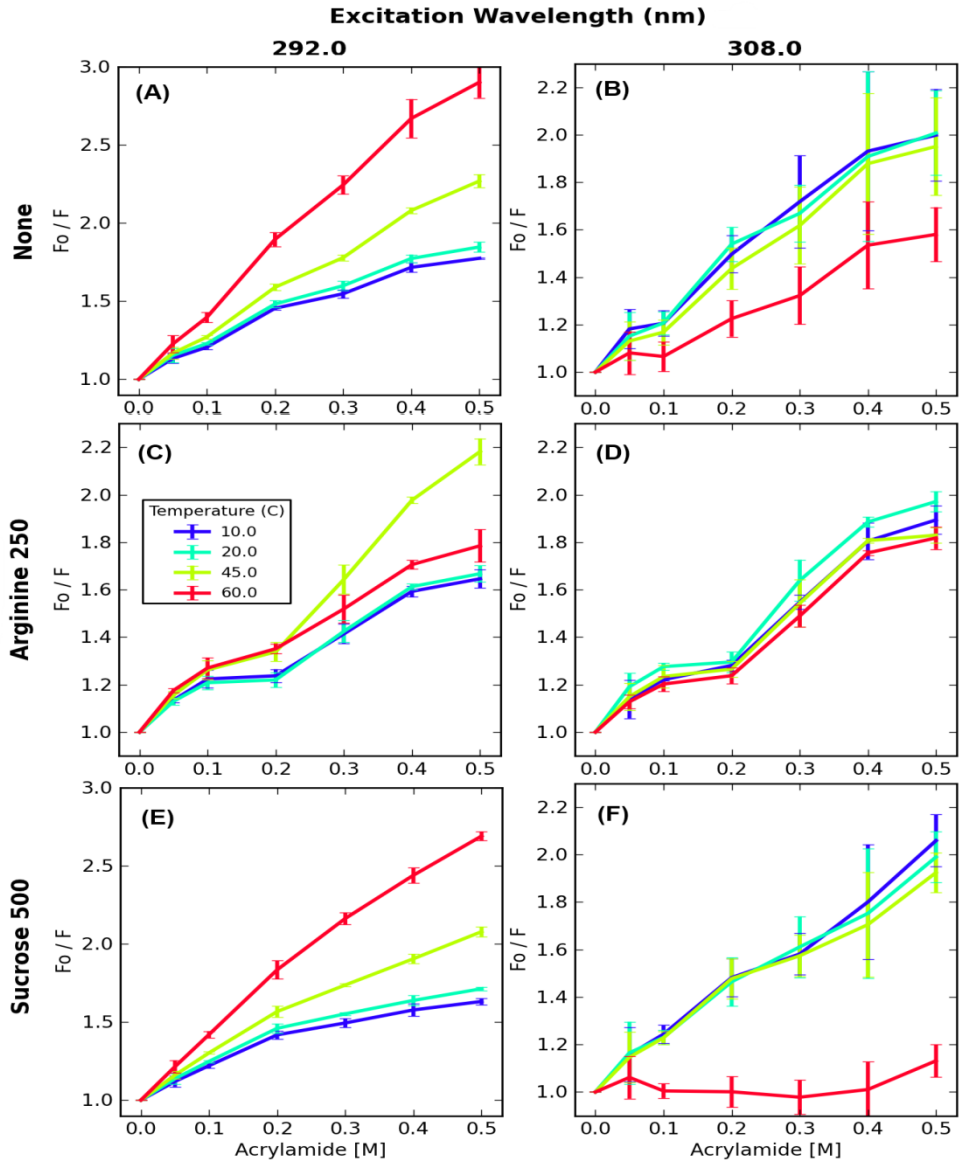

Stern-Volmer plots for acrylamide quenching of intrinsic tryptophan fluorescence of mAb-B at various temperatures upon an excitation at 292 nm (A, C, E) and 308 nm (B, D, F). The plots for mAb-B alone (A, B), mAb-B in presence of arginine (C, D) and, mAb-B in presence of sucrose (E, F) are presented separately for better representation and comparison of excipient effects. The line connecting data points are for visual aid only.

Figure 6

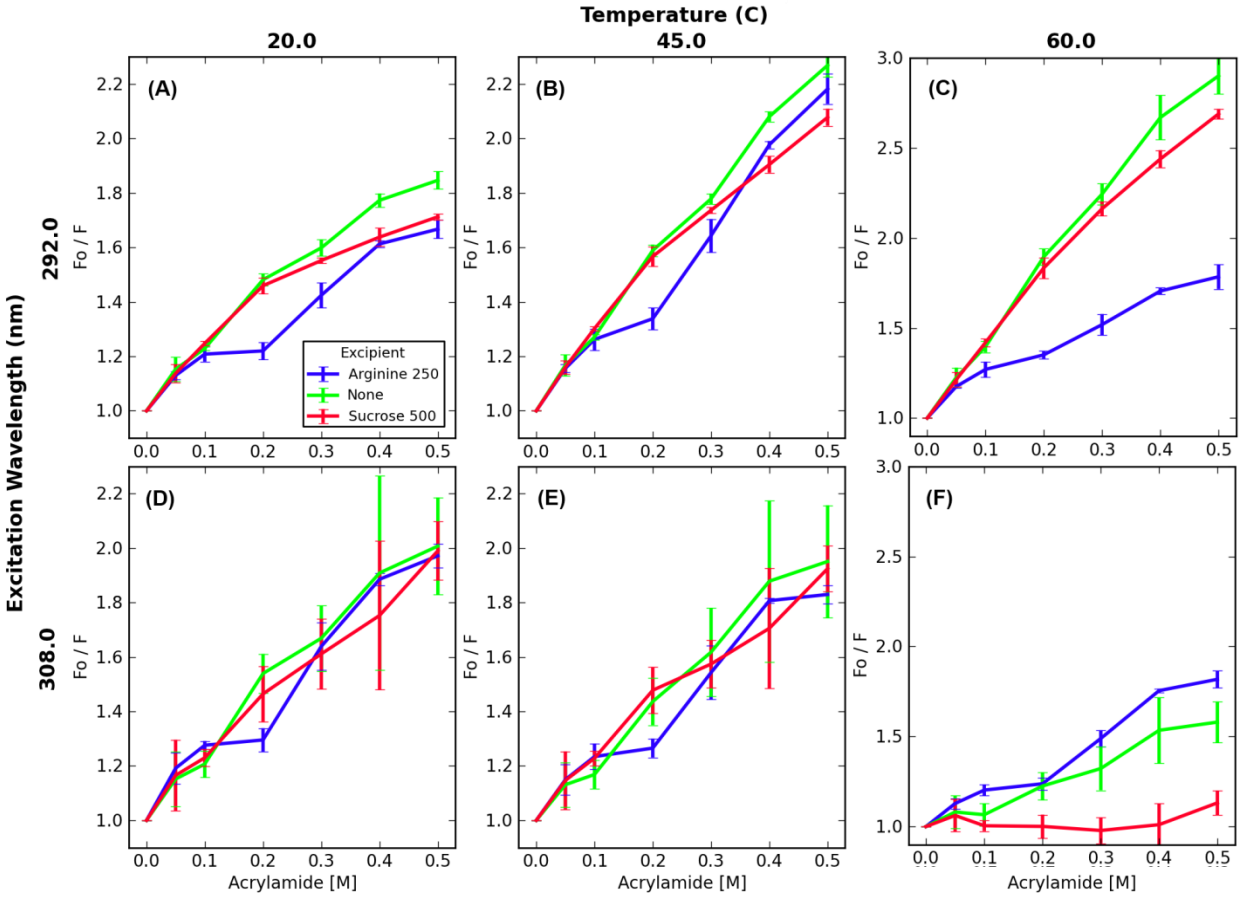

Stern-Volmer plots for acrylamide quenching of intrinsic tryptophan fluorescence of mAb-B in absence and presence of excipients (arginine or sucrose) upon an excitation at 292 nm (A, B, C) and 308 nm (D, E, F). Results at 20 ^{o}C (A, D), 45 ^{o}C (B, E) and 60 ^{o}C (C, F) are presented for better representation and comparison of temperature effects. The line connecting the data points is for visual aid only.

Table 1: Thermal melting temperature (T_M) values of mAb-B in presence and absence of excipients (arginine or sucrose) at pH 4.5 as measured by fluorescence spectroscopy at different excitation wavelengths. The melting temperature was determined by sigmoidal fitting of tryptophan peak position versus temperature plots above 30 ^oC. The mean and standard deviation (SD) are from three separate measurements. The change in T_M values due to excipients are significant with a p-value <0.01 (**) at all the excitation wavelengths.

Excitation wavelength (nm)	Melting Temperature (T_M); (^oC)		
	mAb-B alone (Mean ± SD)**	mAb-B + arginine (250mM) (Mean ± SD)**	mAb-B + sucrose (500mM) (Mean ± SD)**
292	55.2 ± 0.0	51.4 ± 0.0	58.1 ± 0.1
296	54.8 ± 0.0	50.7 ± 0.1	57.8 ± 0.2
300	54.2 ± 0.1	49.9 ± 0.0	57.4 ± 0.1
304	53.7 ± 0.1	49.1 ± 0.3	57.1 ± 0.2
308	52.7 ± 0.2	47.8 ± 0.7	56.6 ± 0.4

Table 2: Change in thermal melting temperature (ΔT_M) of mAb-B in presence and absence of excipients (arginine or sucrose) at pH 4.5 as measured by fluorescence spectroscopy at different excitation wavelengths. The mean and standard deviation (SD) represent data from three separate measurements. The ΔT_M, due to arginine and sucrose, at 292 nm was statistically compared for significant differences with ΔT_M at other excitation wavelengths with a p-value of <0.01(**), <0.05(*) and <0.1(‡).

Excitation wavelength (nm)	Change in Melting Temperature (ΔT_M); (^oC)	
	mAb-B + arginine (250mM) (Mean ± SD)	mAb-B + sucrose (500mM) (Mean ± SD)
292	-3.8 ± 0.1	2.9 ± 0.1
296	-4.1 ± 0.1**	3.0 ± 0.2
300	-4.3 ± 0.1**	3.2 ± 0.1*
304	-4.6 ± 0.4‡	3.4 ± 0.2**
308	-4.9 ± 0.5‡	3.9 ± 0.5‡

Chapter 4

Understanding interactions in high concentration protein solutions

4.1 Introduction

Biological processes largely are governed by macromolecular complexes and their interactions[249]. A plethora of qualitative and quantitative techniques have been developed and validated to understand the stoichiometry and strength of intermolecular interactions[250-261]. These interactions have generated significant interest in the context of better understanding the folding[262], solubility[263], osmolarity[264], crystallization[265-267], colloidal behavior[268], self-association[269], viscosity[213,270,271], and stability[128,203,272] of proteins and other macromolecular systems. With the appearance of an increasing number of high concentration protein therapeutic drugs (e.g., monoclonal antibodies), pharmaceutical challenges such as storage stability (conformational instability and aggregation), solution viscosity, and process optimization have also arisen[124].

A number of the analytical techniques used to study protein-protein interactions (such as light scattering, membrane osmometry, sedimentation equilibrium and self-interaction chromatography) determine the second virial coefficient (B_{22}), a thermodynamic parameter used to characterize non-ideality of solutions. B_{22} has traditionally been used as a guide to understand phenomena such as solubility[263], crystallization[267], and self-association[269]. Limited experimental data are currently available, however, that measure non-ideality effects in highly concentrated (>50 mg/mL or volume fraction >0.1) protein solutions or that employ non-hydrodynamic approaches. Experimental limitations of currently available methods such as low throughput, high protein requirements, increased viscosity or the need for prior immobilization of proteins encourage the development of complementary analytical technologies to better understand protein-protein interactions at high concentrations.

In this work, we present one such new approach that employs a variable-pathlength UV-Visible spectrophotometer to study interactions over a wide range of concentrations for three model proteins: bovine serum albumin (BSA), lysozyme and a monoclonal antibody (IgG2). We determine a unique parameter referred to as delta absorbance (ΔAbs), which is defined as the difference between the measured absorbance of proteins in solution at different protein concentrations and their corresponding theoretical/calculated absorbance values (determined by gravimetric dilution from a stock protein solution of known concentration). The origin of ΔAbs is hypothesized to be due to potential changes in the optical properties of interacting protein molecules in solution, rearrangement of water molecules around chromophores due to protein-protein interactions, and/or light scattering. Numerous studies[273-277] have been performed using either non-associating and/or self-associating proteins to study the effect of increasing protein concentrations (up to hundreds of milligrams per milliliter) on light scattering intensity. Concentration-dependent Raleigh scattering intensity was found to deviate from both ideal scattering and from the scattering values predicted by first-order corrections to non-ideality[273,276]. This non-linear dependence of light scattering on protein concentration has been attributed to repulsive interactions (excluded volume effects) and other short/long range effects that modulate the inter-molecular interactions in globular proteins[273,275]. Theoretical models using Rayleigh scattering theory, and subsequent experimental results, have quantitatively determined the magnitude of these contributions, which become especially significant at high concentrations. Various models such as simple hard-spheres, adhesive hard-spheres and effective hard-sphere mixture models have been employed to characterize different types of intermolecular interactions such as steric repulsion, short/long range interactions and equilibrium self-association[274-276]. The measurement of ΔAbs potentially provides complementary information to aid in the detection

and understanding of these protein-protein interactions. The unavailability of a convenient analytical technique to collect absorption spectra at high protein concentrations without prior sample handling and dilution, as well as challenges in obtaining a wide range of pathlength cuvettes, especially at very short pathlengths, have previously precluded such a study. Since increased solution viscosity is one of the most immediate consequences of high concentration protein solutions, we also evaluated the possibility that correlations might exist between ΔAbs and solution viscosity as a function of protein concentration.

The variable-pathlength (0.01 mm to 15 mm) tool that serves as a cuvette (the SoloVPE) used in these studies employs the principle of slope spectroscopy™ to reliably measure low and high protein concentrations without dilution using a coupled Cary 50™ UV-Visible spectrophotometer. This instrument is able to record and generate absorbance versus pathlength linear plots using its variable pathlength capability. The slope determined from absorbance versus pathlength relationships is further used to determine precise protein concentrations using the known extinction coefficients of proteins under investigation. This variable pathlength spectrophotometer is employed in the current studies to detect potential change(s) in optical properties of individual and/or interacting molecules for a wide range of protein concentrations. The absorbance values were computed using the Beer-Lambert law with experimentally determined protein concentrations and known values of extinction coefficients for BSA, lysozyme and IgG2. The theoretical absorbance was calculated after gravimetric dilution of a protein stock solution of known concentration. The calculation of theoretical absorbance was appropriately corrected for changes in density with protein concentration, which is especially significant at higher protein concentrations. The density measurements were performed at 20 ^{o}C using a DMA-5000 high precision densitometer (Anton Paar, Graz, Austria) with a precision of 1

$x10^{-6}$ g/cm^3 and 0.001 ^oC. This new analytical technique is simple, non-destructive and requires only small volumes (10–150 μL) of protein solution. It can potentially provide a simple and unique measure to study intermolecular interactions for a wide range of protein concentrations.

4.2 Experimental

4.2.1 Materials

Bovine serum albumin and lysozyme (chicken egg white) were obtained from Sigma-Aldrich. All chemicals and buffer components were purchased from Sigma-Aldrich. The monoclonal antibody (IgG2) was procured from a commercial source. The chemicals and protein samples were used without further processing or purification.

4.2.2 Sample preparation

Protein samples were extensively dialyzed into their respective, pH adjusted buffers and filtered through 0.22 μm Millipore filters prior to use. Stock solutions of BSA (250 mg/mL) and IgG2 (150 mg/mL) were prepared in 10 mM histidine buffer pH 6 with NaCl to produce a final ionic strength of 0.015. Lysozyme stock solution (240 mg/mL) was made by dissolving an appropriate amount of protein in 10 mM acetate buffer, pH 4 with NaCl to an ionic strength of 0.015. The ionic strength was kept low to minimize screening of electrostatic interactions. The pH of the final buffer solutions was determined post dialysis and found to be ± 0.05 units. The concentrations of the stock solutions were measured by the traditional dilution method and the absorbance was determined using a NanoDrop 2000 spectrophotometer and reconfirmed by an Agilent 8453 UV-Vis spectrophotometer. The series of solutions of varying protein concentrations were then prepared by gravimetric dilution of the stock solution, and the

theoretical absorbance was calculated using the extinction coefficients for BSA (0.66 mL mg^{-1} cm^{-1})[278], lysozyme (2.72 mL $mg^{-1}cm^{-1}$)[279] and IgG2 (1.45 mL $mg^{-1}cm^{-1}$)[280].

4.2.3 Optical density/absorbance measurements using a variable pathlength spectrophotometer

The SoloVPE (C. Technologies Inc., Bridgewater, NJ 08807, USA) takes advantage of its capability to change the optical pathlength (l), (which is held constant in traditional spectrophotometers using fixed pathlength cuvettes) and the linear Beer-Lambert Law to measure concentrations of solutions at higher concentrations than fixed pathlength spectrophotometers. The Beer-Lambert Law is expressed as

$$A = a \cdot l \cdot c \qquad (1)$$

where 'A' is the measured absorbance, 'a' is the molar absorption coefficient, 'l' is the pathlength, and 'c' is the sample concentration. Thus,

$$A / l = a \cdot c \qquad (2)$$

For absorbance versus pathlength measurements,

$$A = m \cdot l + b$$

where 'm' is the slope and 'b' is the y-intercept.

$$A / l \ \alpha \ m \qquad (3)$$

This dimensional equality allows direct replacement of the A/l term in eq (2) with the slope term (m) in eq (3),

$$m = a \cdot c \qquad (4)$$

where the concentration is : $c = m / a$ (if 'a' is known) (5)

and the molar absorptivity is : $a = m / c$ (if 'c' is known) . (6)

These measurements are acquired by capturing the light passing from a Varian Cary 50™ spectrophotometer through the sample solution onto a detector through an optical fiber (Fibrette™). The fibrette can be moved up and down relative to the bottom of the sample vessel, thus precisely and accurately controlling the pathlength (the distance between the lower tip of the fibrette and the bottom of the sample vessel). The light passing through the solution is monitored by a detector system housed below the sample vessel. The pathlength range achievable by this assembly is from 0.01 mm (10 microns) to 15 mm (1.5 cm) at pathlength intervals of 0.005 mm (5 microns). Absorption spectra (or individual wavelength specific absorbance measurements) can be collected for a range of predetermined pathlengths, and absorbance versus pathlength plots are then created and analyzed by linear regression analysis. The slope of this absorbance versus pathlength plots at a specific wavelength of interest (for example 280 nm for proteins) can be used to determine the concentration of protein in solution using eq 5. The smallest accessible pathlength of 10 microns allows this technology to conveniently measure protein concentrations of hundreds of milligrams per milliliter without dilution. The pathlength accuracy and concentration linearity of the SoloVPE was confirmed using a proprietary dye (CHEM013 VPE 1-mm standard, Lot # C141923) over a pathlength range of 0.01 – 1 mm.

The ‘Quick Slope’ software option provided by the manufacturer is a rapid method for measuring protein concentration without dilution or need to optimize data collection parameters. For the more systematic application of studying physical phenomena such as intermolecular interactions, however, the ‘Setup’ mode was used. The ‘setup’ option allows the user to tailor the experimental and data collection parameters, which may be required especially at higher protein concentrations. Absorbance measurements were acquired at room temperature for a

series of pathlengths spanning 10 μm to 3 mm by tailoring the data collection parameters in the 'Setup' mode of the software for BSA, lysozyme and IgG2. The step size for pathlength scanning was selected to obtain a maximum number of points (>5) to obtain a coefficient of determination (r^2) ≥ 0.999 for absorbance versus pathlength plots. To maintain the linear range of absorbance, an absorbance threshold of 1.0 (A_{280} = 1) was sufficient to derive the desired number of data points. For only a few cases was the absorbance threshold increased >1.0. This was required for lysozyme at higher protein concentrations due to the protein's relatively high extinction coefficient.

The measured absorbance values for proteins were corrected for scattering contributions (one-wavelength or two-wavelength corrections) at each of the pathlengths tested. The one-wavelength scattering correction subtracts the absorbance value at one specific wavelength in a non-absorbing region (for example, 350 nm) from the optical density spectrum through the absorbing region. The two-wavelength scattering option in the software corrects for scattering contribution by linear extrapolation of the non-absorbing region of the spectrum from 320 – 350 nm (these wavelengths can be selected by the user) through the absorbing region and subtracting the extrapolated scattering component to obtain protein specific absorbance values. These corrections are discussed in more detail later in the text.

4.2.4 Viscosity measurements

The viscosity of the protein samples was measured using mVROC, a Viscometer/Rheometer-on-a-Chip, (RheoSense Inc.) at 25 ± 0.1 ^{o}C after equilibration for 5 min. The mVROC determines shear-rate dependent viscosity of protein solutions by measuring the pressure drop of the solution when the liquid flows through a rectangular glass slit containing a monolithic Si pressure sensor array placed at different positions from the entrance. The pressure

drop as a function of the position of the pressure sensor is used to compute wall shear stress (τ) to determine the viscosity of Newtonian solutions. The viscosity of non-Newtonian solutions can also be determined using appropriate corrections available in the software. The instrument can determine the viscosity of the sample at either a fixed shear-rate (single-point measurement) or perform shear-rate sweeps (multi-point measurements)[281]. We performed shear-rate sweeps for BSA (240 mg/mL; Shear rate: 150 – 2250 s^{-1}), lysozyme (240 mg/mL; Shear rate: 500 – 5500 s^{-1}) and IgG2 (120 mg/mL; Shear rate: 50 – 850 s^{-1}) to determine the Newtonian and/or non-Newtonian behavior of these protein solutions at the highest concentration used in these studies. The measurement was made for 20 seconds with a wait time of 3 seconds before each shear-rate determination. The shear rate range used in the study was optimized based on acceptable criteria (i.e., 5% < x <90% of the maximum limit) to monitor pressure by the instrument. The flow/shear rate at lower protein concentrations was selected (where x ~20% of the maximum pressure limit) from the respective shear rate range mentioned above to avoid potential shear-thinning of the protein samples.

4.2.5 Dynamic light scattering

Dynamic light scattering (DLS) was used to evaluate IgG2 self-association as a function of protein concentration. The DLS measurements were carried out at 20 ^{o}C using a DynaPro™ Plate reader DLS system from Wyatt Technology (Santa Barbara, CA) with a data acquisition time of 30 s and an average of 10 acquisitions per measurement.

4.3 Result and discussion

4.3.1 Optical density measurements and scattering correction

Figure 1 shows plots of the theoretical and measured absorbance versus protein concentration for BSA (a), lysozyme (b) and IgG2 (c). The theoretical absorbance was calculated from the gravimetric dilution of protein stock solution at known concentrations while the measured absorbance at each concentration point was determined using the measured protein concentration (without further dilution by SoloVPE) and the extinction coefficient of the protein. The measured absorbance values for all the three proteins show a positive deviation from the theoretical values, the magnitude of which increases as the protein concentration rises. The deviation from linearity observed in the theoretical plot for BSA is due to small dilution errors at higher concentrations. The measured absorbance values were corrected for light scattering contributions using the two-wavelength scatter correction method available in the instrument software. To determine the suitability of this method to appropriately correct for scattering, we compared (Figure 2) the two-wavelength scatter correction method (linear extrapolation, Figure 2b) with the standard multi-wavelength method[282] which employs a log-log extrapolation (Figure 2c) using a 120 mg/mL IgG2 solution. This concentration of IgG2 was chosen because it showed the highest deviation among the samples. The variability in the concentration of IgG2 solution obtained at 280 nm and 0.05 mm pathlength (Abs ~1.0) was found to be <0.5%. This variability in the measured concentration values was even smaller at lower concentrations. Furthermore, the inter-sample variability (~2.5 percent standard deviation) found by analysis of five replicate measurements was higher than the variability (<0.5%) in measured concentration between linear and log-log scatter correction of 120 mg/mL IgG2. In addition, the effectiveness of the linear and log-log scatter correction methods was further studied using 1 mg/mL of IgG2 in the absence and presence of an external scatterer (polystyrene beads) at different pathlengths. A sufficient amount of external scatterer was added to increase the apparent absorbance of 1 mg/mL IgG2

solution by 20% (comparable to the difference observed for IgG2 at concentrations exceeding 120 mg/mL) at 280 nm using a 1 mm pathlength. Figure 3a shows that both the linear and log-log correction methods were able to correct for scattering in the IgG2 solution (1 mg/mL) with no added scatter (the non-scattering control). At 1 mm pathlength, the log-log scatter correction method, however, was more efficient in retrieving the spectrum corresponding to the non-scattering control from the protein solutions containing an external scatterer. In contrast, as the pathlength of absorbance measurement was lowered (for instance to 0.25 mm, Figure 3c), both the linear and log-log correction methods were equally effective in correcting for light scattering. Because a majority of absorbance measurements at high protein concentrations were made at pathlengths below 0.25 mm, the choice of the light scattering correction method should not influence the measurement of intermolecular interactions described in these studies.

Light scattering intensity generally increases with increases in protein concentration. An effective hard particle model based on Raleigh scattering theory for single and multicomponent systems can accurately describe this concentration dependence of light scattering for single non-associating, non-associating mixture and self-associating proteins[273-276]. Thus, the log-log extrapolation (or the two-wavelength scatter correction) method described above, to a first approximation, should account for the concentration dependent increase in Raleigh scattering intensity for the different protein systems. The small differences in the measured and calculated absorbance values may therefore qualitatively represent some form of weak interactions at both low and high protein concentrations. The magnitude of these deviations, which is a function of protein concentration, suggests that the variable-pathlength spectrophotometer is sensitive enough to detect subtle spectral changes arising from the interactions between protein molecules as a function of protein concentration (see below).

The characteristics and behavior of proteins in aqueous solutions are governed by both long and short-range interactions between protein molecules as well as their interactions with solvent and other co-solute molecules[126]. These interactions are known to be a function of protein concentration with long-range, repulsive charge-charge interactions dominating at low protein concentrations, while short-range interactions such as van der Waals attraction and dipole-dipole interactions are significant at higher concentrations. These interactions along with excluded volume effects are known to increase the probability of protein-protein interactions[128,283,284], especially at high protein concentrations. A variety of analytical techniques such as light scattering (static and dynamic) and analytical ultracentrifugation are used to study protein-protein interactions by determining either the second virial coefficient (B_{22}) from SLS or an interaction parameter (kD) from DLS. The B_{22} and kD parameters are now well established as measurements of solute interactions with each other or with the solvent. These parameters, however, are generally studied in dilute solution conditions (<50 mg/mL). A qualitative correlation of ultrasonic storage modulus (G') at high protein concentration was observed with B22 (or kD) measured at low protein concentration[284]. The authors, however, discuss differences in attractive and repulsive behavior of the protein in dilute and concentrated solutions as measured by G', B22 and kD.

It has been pointed out[284] that the inter-particle distance between monoclonal antibody molecules is reduced from 22 to 12 nm as the protein concentration increases from 20 to 120 mg/mL. Similarly, concentrated protein solutions with fractional volume occupancy >0.1 increase the propensity for protein-protein interactions[285]. The basis of the current work is the hypothesis that these protein-protein interactions might affect the optical characteristics of interacting protein molecules and/or cause fluctuations in hydrating water molecules around one

or more aromatic amino acid residues. This may cause either an increase or decrease in the measured ultraviolet absorbance (extinction coefficient) compared to that of the theoretical absorbance which assumes a linear relationship between absorbance and protein concentration. The theoretical absorbance was computed from gravimetric dilution of protein stock solution of known concentration using the Beer-Lambert law and is highly accurate with an error less than 1.5%. The capability of the variable-pathlength technology to measure a wide range of protein concentrations without dilution enabled the accurate direct measurement of absorbance at both low and high protein concentrations, which in turn could potentially detect change(s) in optical characteristics of interacting macromolecules.

4.3.2 Delta absorbance measurements (ΔAbs)

Figure 4 represents these deviations in the form of ΔAbs, which is the difference in measured and theoretical absorbance, for the three proteins. The average ratio of ΔAbs to total absorbance was found to be ~4% for BSA (5 – 240 mg/mL), ~3% for lysozyme (5 – 220 mg/mL) and ~17% for IgG2 (5 – 140 mg/mL). The magnitude of ΔAbs should represent a measure of weak association arising from the various types of interactions undergone by proteins under conditions of increasing thermodynamic activity. The ΔAbs values were not found to vary significantly below 100 mg/mL for BSA and 40 mg/mL for lysozyme. Similar low concentration (<50 mg/mL) behavior was reported[286] for both BSA and lysozyme where the second virial coefficient measured by an osmotic pressure method showed little change as a function of protein concentration over this low concentration range. Another study[274] based on hard particle approximation models used to describe concentration dependent scattering that treats attractive intermolecular interactions as association equilibria, reported repulsive, short-range interactions and no significant self-association (or attractive intermolecular interactions) up

to ~100 mg/mL for BSA, which should further explain the lower magnitude of ΔAbs observed in dilute BSA solutions. The magnitude of ΔAbs, however, clearly increases at higher BSA and lysozyme concentrations (>100 mg/mL) suggesting that at these concentrations protein-protein interactions may result in non-ideal solution behavior of these two proteins. Furthermore, self-interaction chromatographic studies of a peptide[287] and light scattering measurements using model proteins[275,276] suggests attractive interactions to be predominant at higher (>100 mg/mL) concentrations. Similarly, the increase in magnitude of ΔAbs values observed at high (>100 mg/mL) BSA and lysozyme concentrations may therefore represent increases in the extent of attractive interactions between protein molecules.

Various symmetric potentials such as hard-sphere or excluded-volume effects, van der Waals dispersion, charge-charge repulsion, attractive interactions due to presence of salts, square-well interactions representing specific self-association and dipole interactions potentially contribute to interactions between globular proteins and affect the center-to-center distance, r[288], between molecules in solution. The interplay of these contributions will govern the overall interactions of a solute in solution and therefore may influence an experimentally measured parameter such as ΔAbs in any number of different ways. The repulsive charge-charge interactions, known to predominate at low protein and low salt concentrations, might increase the inter-particle distance, r, and thus fail to affect optical properties such that the measured absorbance of the molecules in solution does not deviate significantly from the theoretical absorbance. This would explain the low magnitude of ΔAbs at low BSA and lysozyme concentrations. At high BSA and lysozyme concentrations, the van der Waals and dipolar potentials (among others) could have a larger contribution to the sum of potentials of the mean force (W_{22}) between interacting particles, thus lowering the inter-particle distance. This

lowering of ‘r’ may significantly perturb the spectral properties of interacting molecules compared to individual non-interacting molecules and therefore increase the magnitude of ΔAbs at higher concentration.

In the case of the IgG2 (Figure 1c and Figure 4), however, the ΔAbs values deviate from theoretical absorbance values even at the lower protein concentrations of ~20 mg/mL, and the magnitude of the effect increases markedly at >40 mg/mL. The magnitude of ΔAbs reached a plateau at >100 mg/mL. An increase in ΔAbs at lower (~20 mg/mL) IgG2 concentration could potentially be due to increases in the square-well interaction and account for weak self-association. Jimenez M. et al.[289] not only reported weak self-association of IgG2 molecules at ~30 mg/mL for the antibody of their study but also suggested formation of ~33% trimers at 100 mg/mL and ~50% at 200 mg/mL due to predominant attractive interactions. Recent work[276] provides a detailed account of such interactions, using different hard-sphere models and light scattering data, successfully accounting for the self-association of monoclonal antibodies. The steep increase in ΔAbs at IgG2 concentration greater than ~100 mg/mL (Figure 4) may thus be a consequence of the formation of higher order reversible oligomeric species in solution. In addition, the markedly different behavior of ΔAbs for each of the model proteins as a function of concentration argues strongly that the apparent observed changes in ultraviolet absorbance or extinction coefficient are not due to an instrumental artifact (Figure 4).

Nonetheless, orthogonal methods to study these types of interactions are needed to validate these possibilities and to correlate the change in magnitude of ΔAbs with the physical phenomenon occurring for IgG2. DLS was therefore employed to see if IgG2 self-association could be detected as the protein concentration was raised. It was found that the average diameter of the monoclonal antibody increased from 9.8 ± 0.1 to 10.9 ± 0.03 nm (n=3) as the protein

concentration was increased from 0.5 to 10 mg/mL. Measurements could not be performed above 10 mg/mL due to multiple scattering (data not illustrated). These results suggest association of the IgG2 and this effect may thus be responsible for the observed changes in ΔAbs even at lower concentrations.

Why should the absorbance (or extinction coefficient) change at higher protein concentration? Aromatic residues are known to be dispersed throughout the structure of most proteins. While Phe residues are typically buried, both Trp and Tyr side chains are often at least partially accessible to solvent. Furthermore, the dynamic nature of protein structure is known to permit significant solvent penetration into protein interiors and potentially increase the hydration of these aromatic residues. It seems probable that this phenomenon would be enhanced at higher protein concentrations due to a corresponding increase in the thermodynamic activity of either the hydrating or bulk water. Whichever is the case, small changes in absorbance are not necessarily unexpected at higher protein concentrations.

Three other potential sources of the observed deviation from the theoretical absorbance values at higher protein concentration are absorption flattening, opalescence and constructive interference. Absorption flattening arises from shadowing of one particle by another and is accompanied by red shifts in the absorption spectrum[290]. This effect should become more pronounced as the pathlength is increased. Because neither of these phenomena is seen at the pathlengths used for concentration measurement, it is unlikely to be the source of the deviations manifested by positive ΔAbs. Opalescence is a form of micro-phase separation and is characterized by a unique shimmering appearance of solutions[291,292]. This optical effect was not observed by visual examination for the three model proteins, even at the highest protein concentrations examined. A third possibility is the constructive interference that is observed

when a low degree of periodic order is present in liquids containing large solutes as has been observed in the mammalian lens[293-295]. Since this phenomenon is known to produce increases in the transmittance of light, such a phenomenon cannot be responsible for the deviations in absorbance observed in the present study. We cannot, however, entirely exclude a contribution from light scattering to these deviations, which is not adequately compensated for by the methods employed. Light scattering effects would appear, however, to provide only a small contribution to the spectral changes as described above. The positive ΔAbs values observed in this study at low and high protein concentrations can therefore be taken as a reflection of the complex interplay of intermolecular interactions in solution.

4.3.3 Viscosity measurements and correlation with ΔAbs

Protein-protein interactions in aqueous solution are known to have a direct effect on viscosity, especially with significant self-association at higher protein concentrations[126,296]. We therefore studied the effect of protein concentration on the viscosity and compared the changes in magnitude of ΔAbs to see if they correlated with changes in viscosity as a function of BSA, lysozyme and IgG2 concentrations. Figure 5 illustrates the effect of shear rate (or flow rate) on the viscosity of BSA, lysozyme and IgG2 at the highest concentrations tested. Dilute protein solutions are known to behave like Newtonian fluids in which the viscosity of the solution is independent of shear rate. In contrast, non-Newtonian (viscosity dependent on shear rate) behavior is often observed at higher protein concentrations. We therefore tested the effect of shear rate on viscosity of solutions containing 240 mg/mL BSA and lysozyme, and 120 mg/mL IgG2. The shear rates employed in this experiment were selected based on a predetermined criteria (i.e., 5% < x <90%) of the maximum limit of the instrument to monitor pressure. BSA and lysozyme were found to behave like Newtonian fluids under the conditions tested in which

the viscosity of the solution did not markedly change with shear rate. IgG2 viscosity, however, was found to undergo shear-thinning upon an increase in shear rate, suggesting non-Newtonian behavior (Figure 5).

Figure 6 shows a correlation of ΔAbs with viscosity for BSA (a), lysozyme (b) and IgG2 (c) as a function of protein concentration. The change in magnitude of ΔAbs for BSA and lysozyme was found to correlate with increases in viscosity as a function of protein concentration. The change in magnitude of ΔAbs for the IgG2 (Figure 6c), however, correlated with an exponential increase in viscosity as a function of IgG2 concentration. A similar exponential increase in viscosity was reported earlier for other monoclonal antibodies[296]. The differences in correlation of ΔAbs with viscosity change between BSA, lysozyme and IgG2 are intriguing and require further investigation to better understand the contributions of the different intermolecular forces that dictate solute viscosity.

Because ionic strength is one of the key parameters that affect viscosity, flow behavior and interactions in proteins solutions[297,298], we studied the effect of varying ionic strength on ΔAbs and the viscosity of IgG2 (Figure 7). The viscosity of IgG2 solutions was reduced with increases in ionic strength from 0.015 to 0.15. This viscosity mitigating effect was more pronounced at higher protein concentrations (≥ 40 mg/mL). A similar effect of ionic strength was observed in terms of the magnitude of experimentally measured ΔAbs value. The ΔAbs was lowered significantly at higher IgG2 concentrations in higher ionic strength solutions. These trends of change in ΔAbs at different IgG2 concentrations correlated well with the changes observed in viscosity in low and high ionic strength solutions. Increases in ionic strength are believed to screen both net attractive (electrostatic component) and net repulsive (excluded volume) interactions in immunoglobulins consistent with both electrostatic and excluded volume

effects affecting the properties of high concentration protein solutions[276]. The correlation between solution viscosity and ΔAbs value (measured by ultraviolet spectroscopy) may therefore reflect the interplay of the factors responsible for protein-protein interactions at higher protein concentrations.

The measurement of ΔAbs values represents a new approach to characterize the relationship between intermolecular interactions and viscosity in low and high concentration protein solutions, the magnitude of which is a function of protein concentration. ΔAbs values were monitored for three model proteins of varying size and molecular weight (lysozyme, BSA, and IgG2) over a wide range of protein concentrations. The observed change in ΔAbs correlated with measured changes in solution viscosity for all three model proteins at different protein concentrations. The correlation between ΔAbs and solution viscosity for the IgG2 monoclonal antibody solution, observed at different protein concentrations and ionic strengths, suggests that the spectral changes detected by the deviations in the optical characteristics of protein molecules at high concentration represent changes in the intermolecular forces governing protein-protein interactions. A more detailed analysis of such protein-protein interactions under these conditions should further clarify the origin of the spectral changes detected by ultraviolet spectroscopy in this study. This type of measurement offers a new analytical probe for monitoring protein interactions in concentrated solutions and studying the effect of solution variables on protein-protein and protein-solvent interactions.

Figure 1

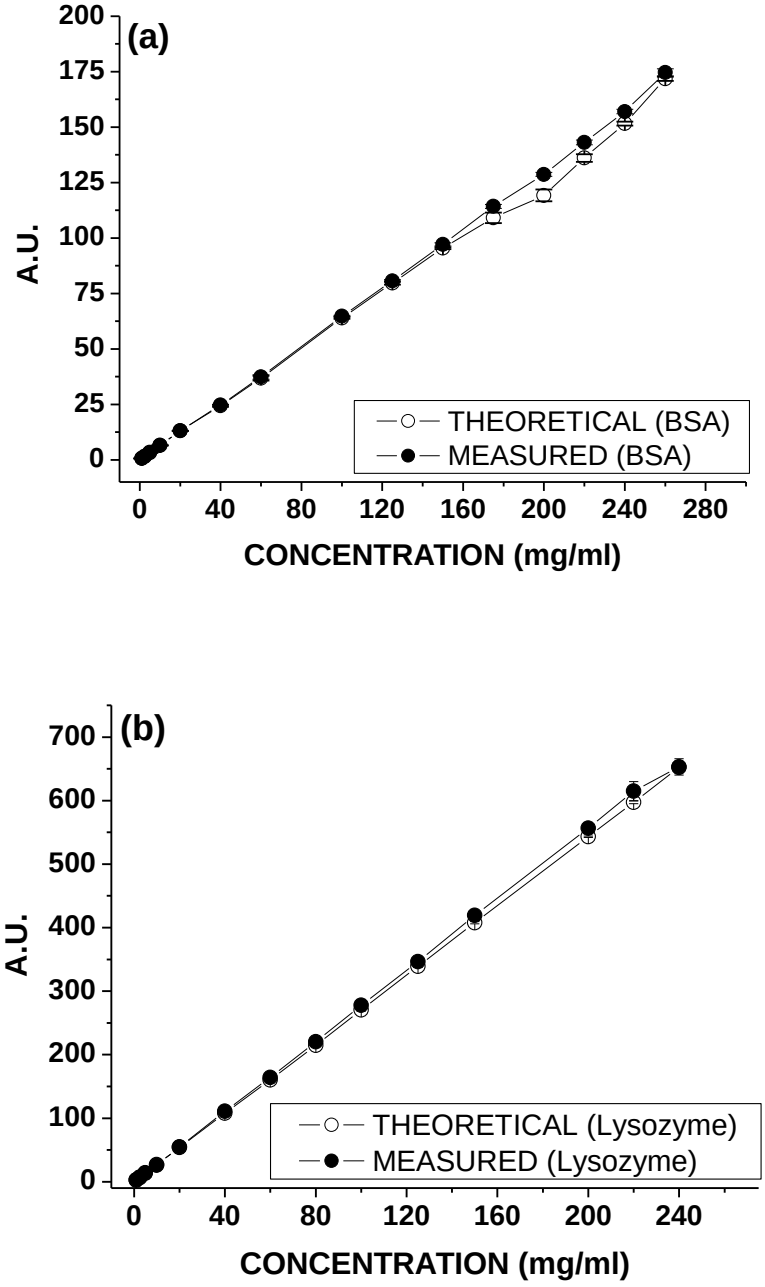
(a)
A.U.
CONCENTRATION (mg/ml)
THEORETICAL (BSA)
MEASURED (BSA)
(b)
A.U.
CONCENTRATION (mg/ml)
THEORETICAL (Lysozyme)
MEASURED (Lysozyme)

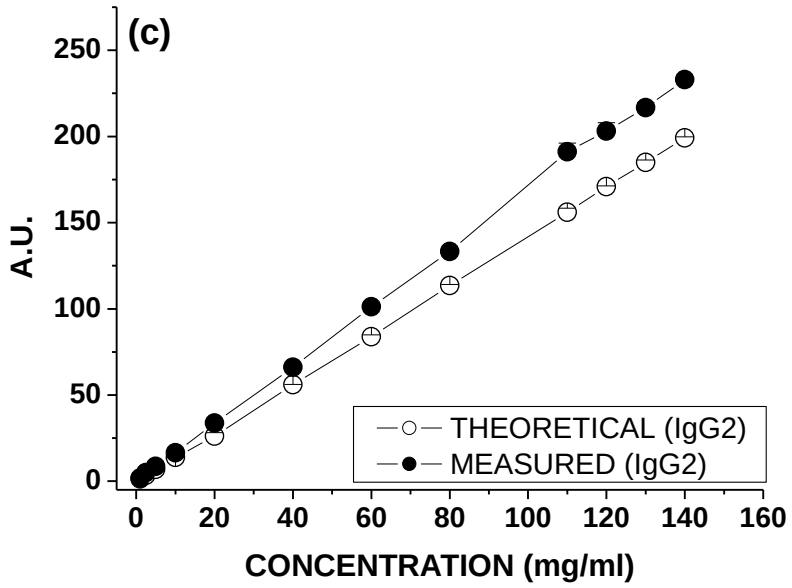

Theoretical and measured absorbance of proteins: (a) BSA in 10 mM histidine buffer pH 6 (I=0.015), (b) lysozyme in 10 mM acetate buffer pH 4 (I=0.015), and (c) IgG2 mAb in 10 mM histidine buffer pH 6 (I=0.015) as a function of protein concentration. The theoretical absorbance was calculated from the gravimetric dilution of protein stock solutions of known concentration. The measured absorbance at each concentration was determined at room temperature using the extinction coefficient of the protein and the measured protein concentration, respectively. The measured concentration was appropriately corrected for light scattering as described in the text. The line connecting the data points is for visual aid only. When error bars (representing standard deviation of five replicate measurements) cannot be seen, they are encompassed within the individual symbols.

Figure 2

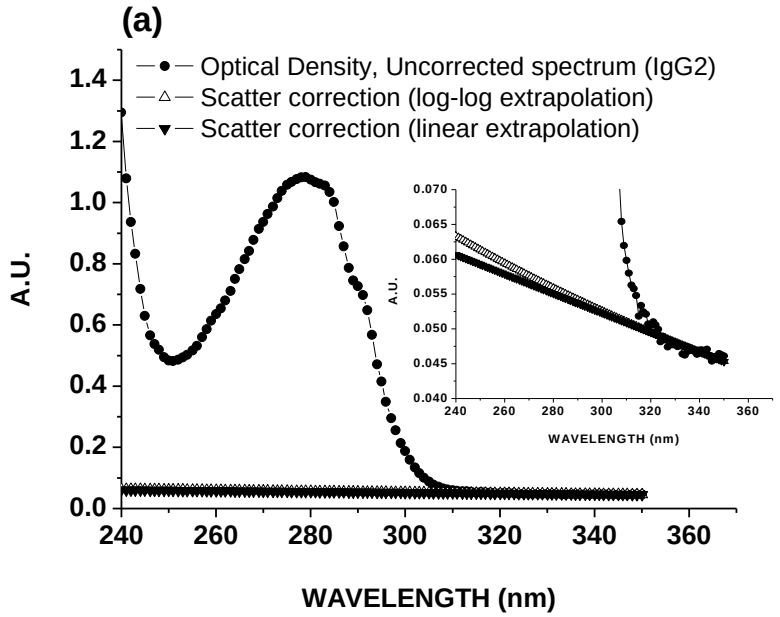
(a)
Optical Density, Uncorrected spectrum (IgG2)
Scatter correction (log-log extrapolation)
Scatter correction (linear extrapolation)
A.U.
WAVELENGTH (nm)
(b)
Optical Density, Uncorrected spectrum (IgG2)
Scatter correction (log-log extrapolation)
Absorbance (after log-log scatter correction)
A.U.
WAVELENGTH (nm)

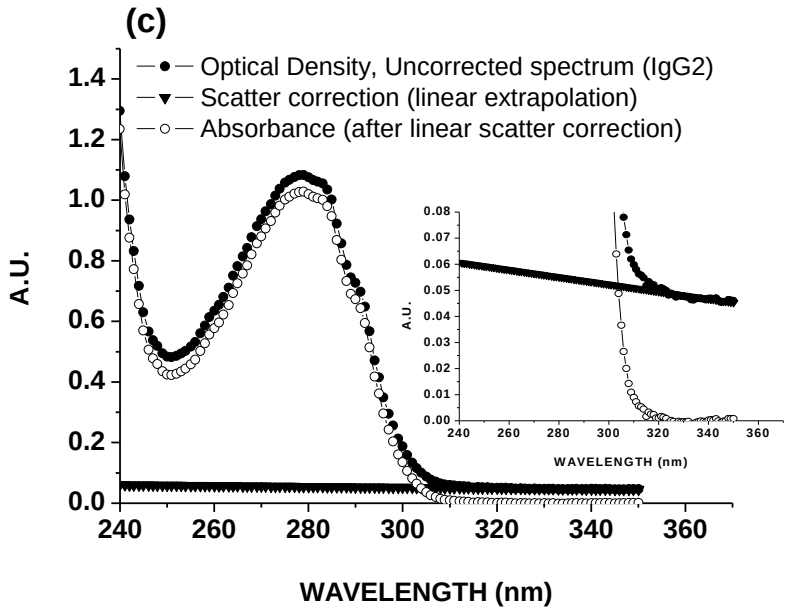

Representative absorption spectra of the IgG2 monoclonal antibody (a) uncorrected along with extrapolated scatter signal for linear and log-log correction method, (b) corrected using linear extrapolation of the non-absorbing (320 – 350 nm) region and, (c) corrected using log-log extrapolation of non-absorbing (320 – 350 nm) region. Protein sample contained IgG2 (10 mM histidine buffer pH 6, I=0.015) at 120 mg/mL and measurements employed a pathlength of 50 microns.

Figure 3

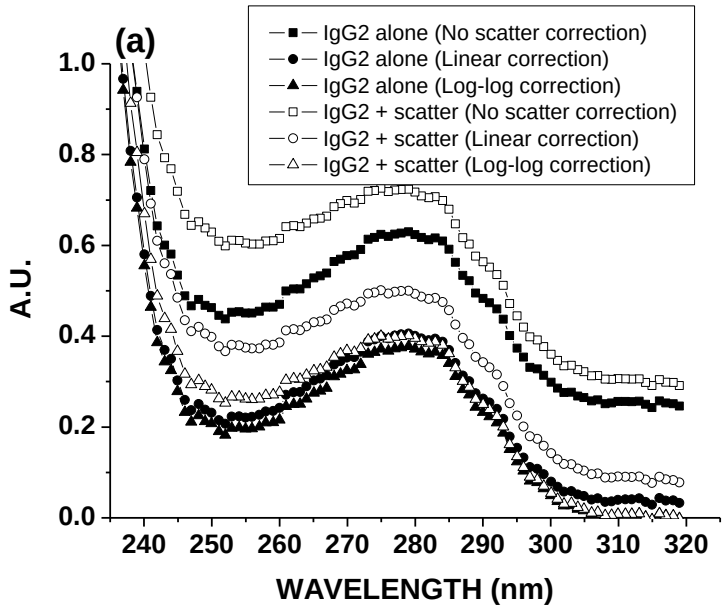
(a)
IgG2 alone (No scatter correction)
IgG2 alone (Linear correction)
IgG2 alone (Log-log correction)
IgG2 + scatter (No scatter correction)
IgG2 + scatter (Linear correction)
IgG2 + scatter (Log-log correction)
A.U.
1.0
0.8
0.6
0.4
0.2
0.0
240
250
260
270
280
290
300
310
320
WAVELENGTH (nm)

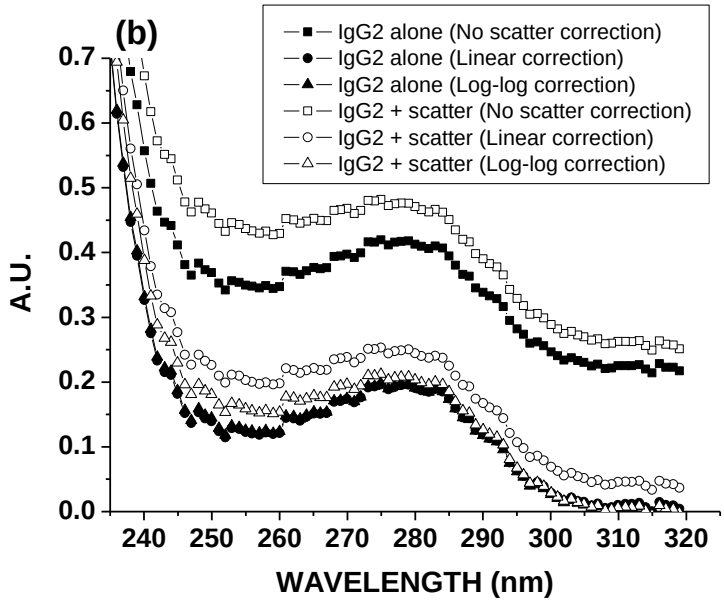
(b)
IgG2 alone (No scatter correction)
IgG2 alone (Linear correction)
IgG2 alone (Log-log correction)
IgG2 + scatter (No scatter correction)
IgG2 + scatter (Linear correction)
IgG2 + scatter (Log-log correction)
A.U.
0.7
0.6
0.5
0.4
0.3
0.2
0.1
0.0
240
250
260
270
280
290
300
310
320
WAVELENGTH (nm)

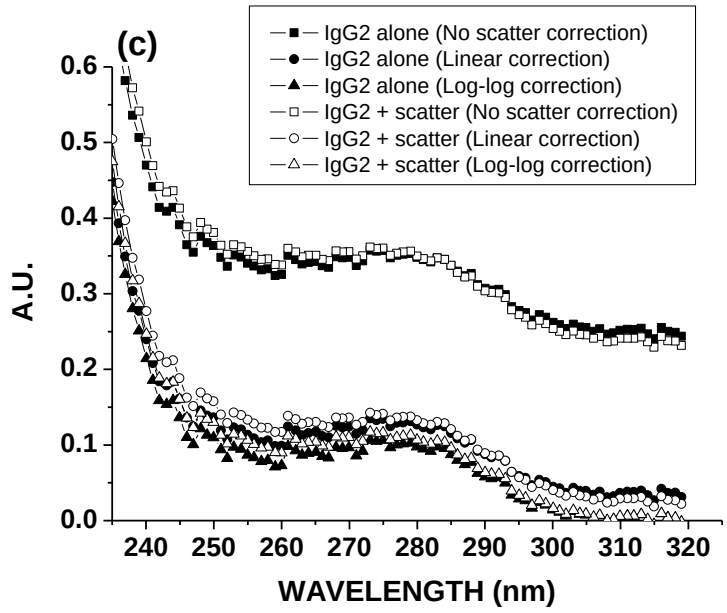

Absorption spectra of the IgG2 monoclonal antibody (1 mg/mL) in absence and presence of an external scatter (polystyrene beads) corrected for scattering using linear and log-log scatter correction methods. The spectra were collected at pathlength of (a) 1 mm, (b) 0.5 mm and, (c) 0.25 mm.

Figure 4

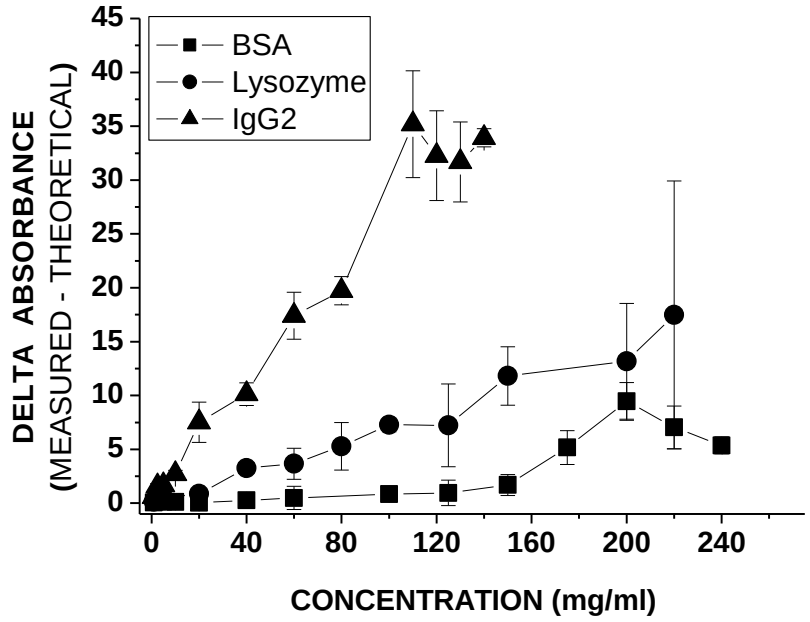

Delta absorbance (ΔAbs), the difference between measured and theoretical absorbance, for BSA, lysozyme and IgG2 mAb solutions as a function of protein concentration. The error bars represent the standard deviation for five replicate measurements. Experimental conditions are listed in Figure 1.

Figure 5

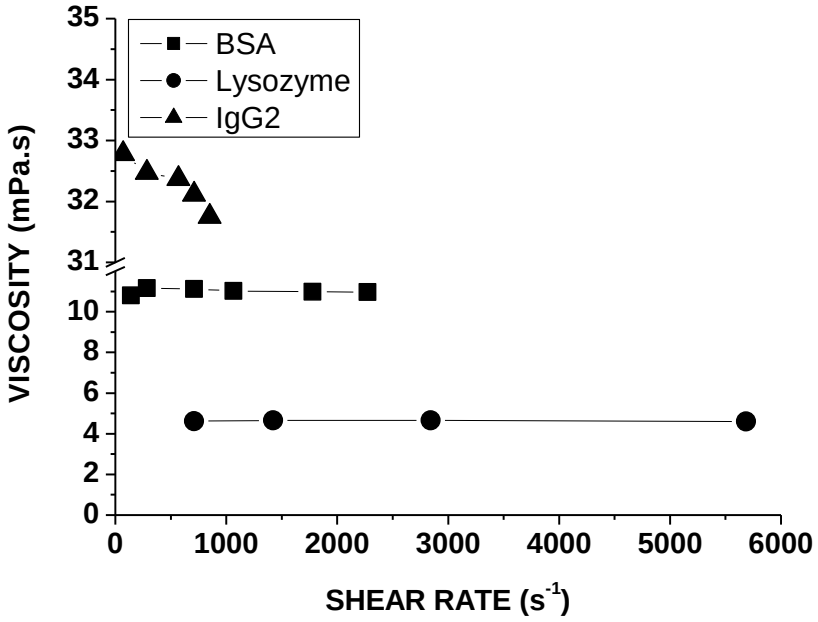

Viscosity measurements of solutions containing BSA, lysozyme and IgG2 mAb as a function of shear-rate (s^{-1}). Shear-rate sweeps were performed at 150 – 2250 s^{-1} for BSA (240 mg/mL), 500 – 5500 s^{-1} for lysozyme (240 mg/mL) and 50 – 850 s^{-1} for IgG2 (120 mg/mL).

Figure 6

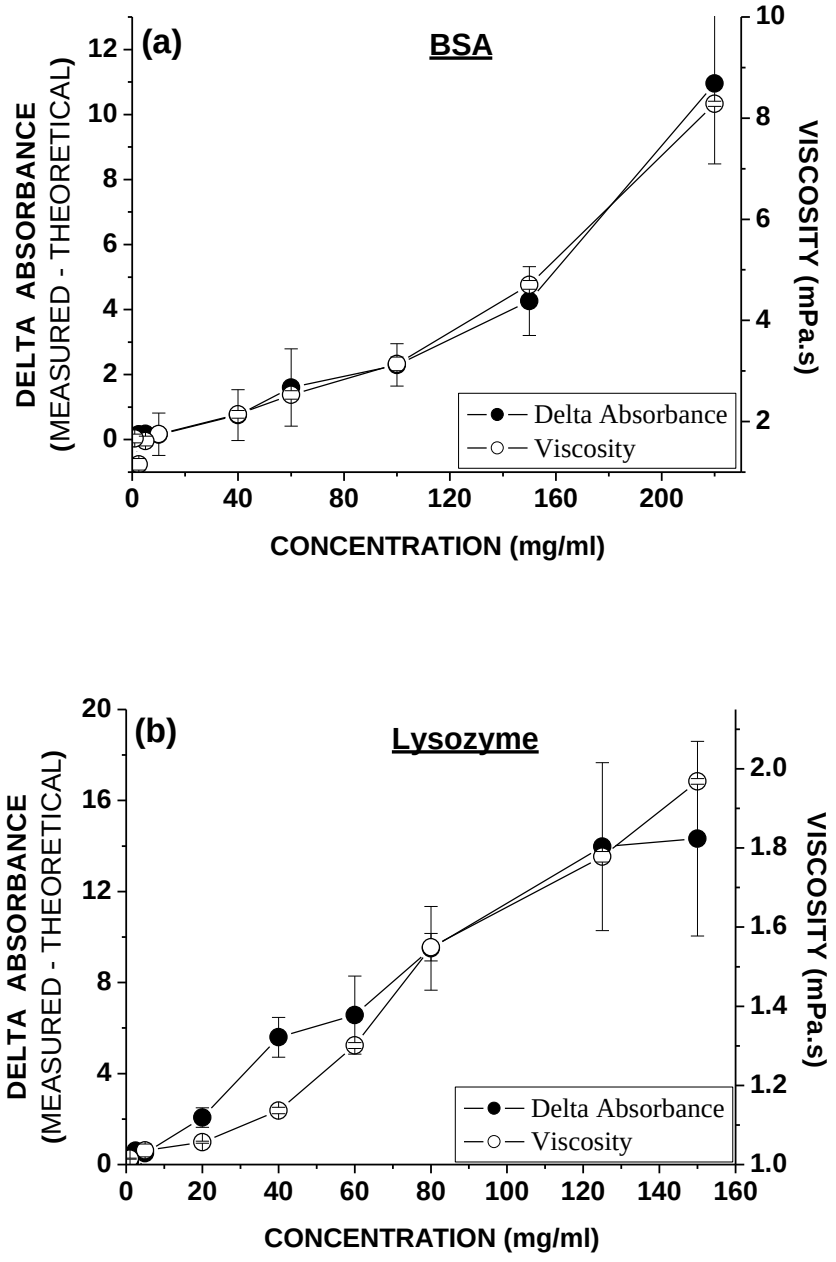
(a)
BSA
DELTA ABSORBANCE
(MEASURED - THEORETICAL)
VISCOSITY (mPa.s)
CONCENTRATION (mg/ml)
Delta Absorbance
Viscosity
0
2
4
6
8
10
12
40
80
120
160
200
(b)
Lysozyme
DELTA ABSORBANCE
(MEASURED - THEORETICAL)
VISCOSITY (mPa.s)
CONCENTRATION (mg/ml)
Delta Absorbance
Viscosity
0
4
8
12
16
20
1.0
1.2
1.4
1.6
1.8
2.0
20
40
60
80
100
120
140
160

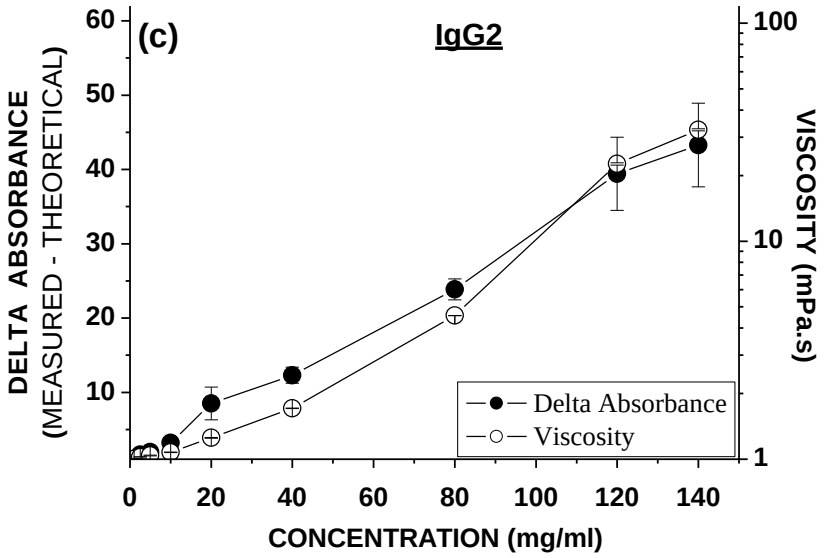

Comparison of changes in ΔAbs and viscosity (mPa.s) as function of protein concentration for solutions containing (a) BSA, (b) lysozyme and (c) IgG2 mAb. The ΔAbs values are plotted on the Y-axis and viscosity values on Y'-axis. The error bars represent the standard deviation of five replicate measurements.

Figure 7

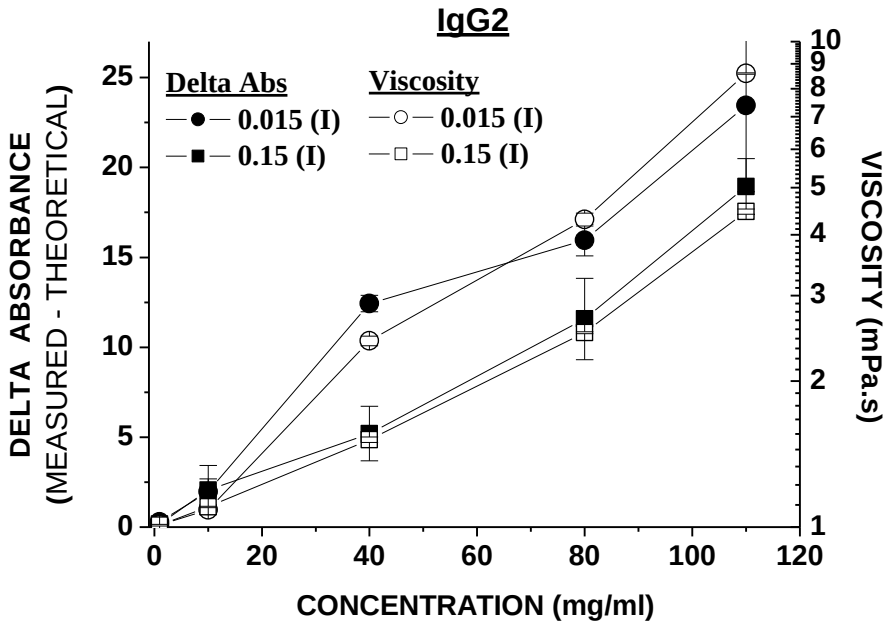

Effect of ionic strength on ΔAbs and viscosity (mPa.s) for solution containing IgG2 mAb as function of protein concentration. An ionic strength (I) of 0.015 (low) and 0.15 (high) was attained using NaCl. The ΔAbs values are plotted on Y-axis and viscosity on the Y'-axis. The error bars represent the standard deviation of five replicate measurements.

Chapter 5

Summary, conclusions and future directions

5.1 Summary and conclusions

Protein dynamics and flexibility has been extensively investigated in the context of understanding their role in regulating biological functions such as enzyme catalysis and ligand recognition by macromolecules[57-61]. The functional properties of native proteins are often attributed to their unique ability to interconvert between energetically equivalent conformational microstates and a role for solvent in such processes is well recognized[299]. The interplay between protein dynamics, stability and aqueous solvent, however, is less well understood. To better understand these relationships, the studies presented in this dissertation evaluate the effect of varying solution characteristics (i.e., alterations in pH, temperature, protein concentration and excipients) on protein dynamics, conformation stability, protein-protein interactions and aggregation. A variety of experimental methods and their underlying physical principles were combined to better understand the correlations between global and/or local dynamics and the conformational stability at a molecular level of two IgG1 monoclonal antibodies. In addition, such correlations were also evaluated in the absence and presence of stabilizing and destabilizing excipients at different pH values and temperatures, both of which can affect a protein's intrinsic stability.

Proteins in solution at high concentrations are known to have unique properties as compared to that at lower concentrations. One of the major consequences of interactions governing the properties of proteins in highly concentrated solutions is increases in solution viscosity[126,213,270,276,300,301]. Such increases in viscosity can consequently influence the dynamics[302] and conformational properties[303] of proteins. Findings of studies aimed at a better understanding of such interactions in high concentration protein solutions using a new ultraviolet absorption spectroscopy based approach are presented in *Chapter 4.*

Chapter 2 characterizes the conformational properties and 'global' dynamics of an IgG1 monoclonal antibody (mAb-A) and compares these characteristic with another antibody (mAb-B) of the same heavy-chain subtype. A variety of biophysical, hydrodynamic and thermodynamic techniques such as fluorescence spectroscopy, circular dichroism, static light scattering, ultraviolet absorption spectroscopy, high resolution ultrasonic spectroscopy, red-edge excitation shift spectroscopy and differential scanning calorimetry were employed to characterize these two antibodies. The effects of sucrose (a stabilizer) and arginine (a destabilizer) on the conformational stability and global dynamics of mAb-A and mAb-B were evaluated using a combination of ultrasonic spectroscopy, red-edge excitation shift spectroscopy and differential scanning calorimetry[86].

The two IgG1 mAbs used in this study exhibited notable differences in their conformational stability and dynamic properties as a function of pH, temperature and presence of solutes. Using the experimental techniques mentioned above, differences in the conformational properties, global dynamics and aggregation were summarized using an empirical phase diagram (EPD) approach. The EPD generated using techniques sensitive to global dynamic properties of mAb-A was able to detect additional structural alterations when compared to the static (time-averaged) EPD. These differences were detectable at lower temperatures and at pH values commonly used to formulate proteins. A similar observation was published earlier using mAb-B[120]. In addition, a pH dependent inverse correlation of the T_M of unfolding and T_M of aggregation was observed for mAb-A. Circular dichroism studies suggested formation of intermolecular β-sheet rich species. Formation of such species was postulated to be a potential mechanism explaining an inverse correlation between the unfolding and aggregation observed in mAb-A. No such correlation between unfolding and aggregation was seen for mAb-B.

Furthermore, structural transitions apparent in differential scanning calorimetric data showed differences between mAb-A and mAb-B at pH 3 – 8 (unit intervals). Three transitions were observed for mAb-A while only two apparent transitions were determined for mAb-B. Finally, apparent adiabatic compressibility measurements suggest that mAb-A and mAb-B may differ in their hydration characteristics, wherein mAb-B was either more hydrated and/or more rigid compared to mAb-A, especially in the pre-unfolding transition region.

Sucrose and arginine were identified as candidate stabilizer and a destabilizer, respectively, based on a screening of a GRAS library of excipients. These excipients influenced the conformational stability of mAb-A and mAb-B to varying extents and at different effective concentrations. Both sucrose and arginine, however, did not significantly influence the pre-transition dynamics of mAb-A as determined by both HR-US and REES studies. In contrast, in the case of mAb-B, the effects of stabilizing concentrations of sucrose on the compressibility and the magnitude of red-edge effects suggest that both the internal dynamics and the surrounding solvent dynamics of mAb-B are influenced by sucrose. The conformational stability and global dynamics results reported in this work highlight some of the key differences in physical behavior between two generally similar IgG mAbs. The molecular origin of these effects for mAb-B is discussed in *Chapter 3*, while the studies using mAb-A are ongoing (work in progress).

These results show that formulation components can have unique effects on the dynamics of individual proteins within a single IgG1 subclass, especially in the pre-transition region. Such distinct effects of excipients on dynamics of therapeutic proteins may thus profoundly influence the long-term storage stability and efficacy of biopharmaceutical products and thus require evaluation during preformulation and formulation activities.

Chapter 3 is focused on a molecular understanding of excipient effects on the inter-relationship(s) between 'local' dynamics and the conformational stability of mAb-B. Such an understanding may potentially provide insights into the development of better biopharmaceuticals, such as monoclonal antibodies. In these studies, stabilizing and destabilizing effects of excipients were examined on the conformational stability and local dynamics of distinct solvent-exposed regions within mAb-B. The conformational stability of different regions was evaluated by selectively sampling distinct Trp-containing environments upon red-edge excitation and subsequently monitoring their thermal unfolding. Furthermore, the local dynamic behavior of these environments was studied by acrylamide quenching of Trp-fluorescence as a function of increasing excitation wavelengths.

It was determined that mAb-B thermal unfolding was a step-wise cascade of events that is initiated by transitions in the solvent-exposed regions of the protein. Arginine and sucrose influenced the conformational stability by decreasing and increasing the T_M, respectively, for both solvent-exposed and solvent-shielded regions. The magnitude of stabilization or destabilization of these excipients, however, was higher for solvent-exposed and lower for more solvent-shielded regions of mAb-B. In addition, an increase in internal dynamics (in the more solvent-shielded regions) of mAb-B was found to predispose the protein to unfolding structural transitions at the T_{onset}. Such an effect may increase the propensity of arginine to form cation-π or other interactions with solvent-shielded aromatic residues, subsequently leading to the protein's destabilization. In the pre-transition temperature range, however, arginine was found to increase the extent of apolar interactions within the solvent-shielded regions of mAb-B. Such an increase may explain the reduction in pre-transition dynamics of solvent-shielded regions in the presence of arginine. Furthermore, a reduction of mAb-B dynamics by sucrose at all

temperatures, predominantly in the proteins' solvent-exposed regions, may better explain the greater magnitude of surface stabilization in the presence of sucrose. Such an effect of sucrose on the more solvent-exposed regions of mAb-B may thus help prevent the step-wise, subsequent cascade of unfolding events that initiates upon surface destabilization. Finally, surface dynamics (i.e., in the more solvent-exposed regions) was found to be dampened at the thermal melting temperature, and this may provide preliminary evidence that apolar amino acids in solvent-exposed regions of mAb-B could potentially initiate the formation of larger irreversible aggregates, as reported earlier[120], during its thermal unfolding.

These results suggest that local dynamics in mAb-B are intimately correlated to its conformational stability in the pre-transition region, as well as at the onset and melting temperature. Furthermore, alterations in these dynamic properties by excipients at various temperatures were found to modulate the global conformational stability of mAb-B. These results indicate that the mechanisms by which excipients exert their stabilizing and/or destabilizing effects on proteins profoundly influences their global and/or local dynamic properties at a molecular level. It is therefore proposed that the dynamic properties of proteins such as immunoglobulins may strongly influence their stability and thermal unfolding properties.

Since aqueous proteins can exist in dilute and concentrated forms, *Chapter 4* presents a new ultraviolet absorption spectroscopy based approach to study interactions in both dilute and concentrated solutions of bovine serum albumin (BSA), lysozyme and a monoclonal antibody (IgG2). A variable pathlength UV-Visible spectrophotometer was employed for these studies. Delta absorbance (ΔAbs), which is a difference between the measured absorbance of proteins in solution and their corresponding theoretical/calculated absorbance, was determined for the three model proteins as a function of protein concentration. It was found that ΔAbs, which potentially

represent changes in molar extinction coefficient, increased with increases in protein concentration. The magnitude of change in ΔAbs was different for all the three model proteins examined in these studied. It was hypothesized that interacting protein molecules in solution and/or rearrangement of water molecules around chromophores due to protein-protein interactions may be responsible for the magnitude of ΔAbs observed for these different protein systems. Since intermolecular interactions are known to modulate solution viscosity[126,213,270,276,300,301], the magnitude of ΔAbs was compared with changes in apparent viscosity as a function of protein concentration. The changes in ΔAbs were highly correlated with changes in viscosity for BSA, lysozyme and the monoclonal antibody as the protein concentration in solution was raised. Such a correlation may suggest that ΔAbs measurements can be used as a complementary analytical approach to evaluate factors, such as excipients or salts, which can potentially modulate interactions and viscosity in high concentration protein solutions.

5.2 Ongoing studies and future work

The outcome of the research presented in Chapters 2 – 4 of this dissertation highlights a few major findings; (1) Antibody molecules belonging to the same IgG subclass can have inherent differences in their conformational properties, protein dynamics and aggregation behavior, (2) external perturbations such as changes in solution pH, temperature and the presence of stabilizing or destabilizing solutes can uniquely influence the conformational stability and protein dynamics of closely related proteins, (3) global and/or local protein dynamics and their alterations by excipients can have a profound influence on the conformational stability and aggregation properties of monoclonal antibodies and, (4) interactions and factors modulating

solution viscosity in high concentration protein solutions may result in changes in extinction coefficients of proteins, which can be monitored by determining ΔAbs in such solutions.

The effect of local dynamics and their alterations by excipients has been evaluated on the conformational stability of mAb-B (Chapter 3). Excipients (sucrose or arginine), however, did not have a major influence on the global dynamics of mAb-A (Chapter 2) as monitored by ultrasonic spectroscopy and red-edge excitation shift spectroscopy. In addition, mAb-A showed a unique pH-dependent inverse correlation between its unfolding and aggregation. Furthermore, preliminary evidence for the presence of intermolecular interactions was observed with mAb-A. Finally, excipients differentially influenced the conformational stability of mAb-A in comparison to mAb-B. A molecular understanding of these inherent differences in the conformational stability and protein dynamics between mAb-A and mAb-B should provide valuable insights into interactions (intra- and inter-) governing the folding, stability and dynamics of these proteins. Furthermore, evaluating excipient effect on the conformational stability and local protein dynamics of mAb-A should help better understand modulation of the protein characteristics due to alterations in solution properties at a molecular level.

These studies are currently ongoing and will be continued as a part of future research. The site-selective fluorescence approach accompanied by acrylamide quenching, infrared spectroscopy and differential scanning calorimetry is being employed for mAb-A at different pH values and temperatures comprising the pre-transition range, onset temperature and at the midpoints of thermal unfolding and aggregation. Since sucrose and arginine have distinct effective concentrations for mAb-A compared to mAb-B, the excipient effects are being evaluated on the intermolecular interactions and local protein dynamics to help unravel the complex pH dependent relationship between conformational stability and aggregation.

Furthermore, a combination of analytical approaches, including but not limited to fluorescence spectroscopy and calorimetry, are being developed to better understand these excipient effects on distinct domains in immunoglobulins. In addition, amide hydrogen/deuterium exchange coupled with mass spectrometry is being currently employed in the laboratory to further investigate the effect of excipients on local flexibility of mAb-B and correlate the effects on the protein's overall conformational and accelerated storage stability. Finally, the application of ΔAbs as an analytical probe is being further evaluated using two (IgG1 and IgG2) antibody candidates with known differences in their viscosity behavior at high concentrations. The effect of viscosity modulating excipients will be tested to gain an insight into intermolecular interactions governing the characteristics of these proteins at high concentrations. These studies should validate the newly developed method of determining potential changes in extinction coefficient of high concentration proteins using a variable-pathlength ultraviolet spectrophotometer.

All of these ongoing and future studies taken together should eventually help define any molecular connection between protein dynamics, conformational stability and intra- and intermolecular interactions governing proteins in solution, both at low and high concentrations.

References

(1) Fersht, A. R. *Nat Rev Mol Cell Biol* **2008**, *9*, 650.

(2) Fink, A. L. *Curr Opin Struct Biol* **2005**, *15*, 35.

(3) Karplus, M. *Fold Des* **1997**, *2*, S69.

(4) Brockwell, D. J.; Radford, S. E. *Curr Opin Struct Biol* **2007**, *17*, 30.

(5) Onuchic, J. N.; Wolynes, P. G. *Curr Opin Struct Biol* **2004**, *14*, 70.

(6) Bryngelson, J. D.; Onuchic, J. N.; Socci, N. D.; Wolynes, P. G. *Proteins* **1995**, *21*, 167.

(7) Ferreiro, D. U.; Hegler, J. A.; Komives, E. A.; Wolynes, P. G. *Proc Natl Acad Sci U S A* **2007**, *104*, 19819.

(8) Haustein, E.; Schwille, P. *Annu Rev Biophys Biomol Struct* **2007**, *36*, 151.

(9) Royer, C. A. *Chem Rev* **2006**, *106*, 1769.

(10) Schuler, B.; Eaton, W. A. *Curr Opin Struct Biol* **2008**, *18*, 16.

(11) Kelly, S. M.; Jess, T. J.; Price, N. C. *Biochim Biophys Acta* **2005**, *1751*, 119.

(12) Balakrishnan, G.; Weeks, C. L.; Ibrahim, M.; Soldatova, A. V.; Spiro, T. G. *Curr Opin Struct Biol* **2008**, *18*, 623.

(13) Fabian, H.; Naumann, D. *Methods* **2004**, *34*, 28.

(14) Lipfert, J.; Doniach, S. *Annu Rev Biophys Biomol Struct* **2007**, *36*, 307.

(15) Dyson, H. J.; Wright, P. E. *Methods Enzymol* **2005**, *394*, 299.

(16) Krishna, M. M.; Hoang, L.; Lin, Y.; Englander, S. W. *Methods* **2004**, *34*, 51.

(17) Maier, C. S.; Deinzer, M. L. *Methods Enzymol* **2005**, *402*, 312.

(18) Zarrine-Afsar, A.; Davidson, A. R. *Methods* **2004**, *34*, 41.

(19) Bustamante, C.; Cheng, W.; Mejia, Y. X. *Cell* **2011**, *144*, 480.

(20) Ferguson, N.; Sharpe, T. D.; Johnson, C. M.; Schartau, P. J.; Fersht, A. R. *Nature* **2007**, *445*, E14.

(21) Dill, K. A. *Biochemistry* **1990**, *29*, 7133.

(22) Pace, C. N.; Shirley, B. A.; McNutt, M.; Gajiwala, K. *FASEB J* **1996**, *10*, 75.

(23) Laue, T. *J Mol Recognit* **2012**, *25*, 165.

(24) Zhong, D.; Pal, S. K.; Zewail, A. H. *Chemical Physics Letters* **2011**, *503*, 1.

(25) Qiu, W.; Kao, Y. T.; Zhang, L.; Yang, Y.; Wang, L.; Stites, W. E.; Zhong, D.; Zewail, A. H. *Proc Natl Acad Sci U S A* **2006**, *103*, 13979.

(26) Meersman, F.; Smeller, L.; Heremans, K. *Biochim Biophys Acta* **2006**, *1764*, 346.

(27) Daniel, R. M.; Dines, M.; Petach, H. H. *Biochem J* **1996**, *317 (Pt 1)*, 1.

(28) Bjelic, S.; Brandsdal, B. O.; Aqvist, J. *Biochemistry* **2008**, *47*, 10049.

(29) Hernandez, G.; Jenney, F. E., Jr.; Adams, M. W.; LeMaster, D. M. *Proc Natl Acad Sci U S A* **2000**, *97*, 3166.

(30) Roca, M.; Liu, H.; Messer, B.; Warshel, A. *Biochemistry* **2007**, *46*, 15076.

(31) Chalikian, T. V. *J Phys Chem B* **2008**, *112*, 911.

(32) Cooper, A. *Proc Natl Acad Sci U S A* **1976**, *73*, 2740.

(33) Kamerzell, T. J.; Middaugh, C. R. *Biochemistry* **2007**, *46*, 9762.

(34) Krishnamurthy, H.; Munro, K.; Yan, H.; Vieille, C. *Biochemistry* **2009**, *48*, 2723.

(35) Houde, D.; Arndt, J.; Domeier, W.; Berkowitz, S.; Engen, J. R. *Anal Chem* **2009**, *81*, 2644.

(36) Jaenicke, R. *Proc Natl Acad Sci U S A* **2000**, *97*, 2962.

(37) Jaenicke, R.; Bohm, G. *Curr Opin Struct Biol* **1998**, *8*, 738.

(38) Kamerzell, T. J.; Middaugh, C. R. *J Pharm Sci* **2008**, *97*, 3494.

(39) Yesylevskyy, S. O.; Kharkyanen, V. N.; Demchenko, A. P. *Biophys J* **2006**, *91*, 3002.

(40) Shoichet, B. K.; Baase, W. A.; Kuroki, R.; Matthews, B. W. *Proc Natl Acad Sci U S A* **1995**, *92*, 452.

(41) Tang, K. E.; Dill, K. A. *J Biomol Struct Dyn* **1998**, *16*, 397.

(42) Despa, F. *Ann N Y Acad Sci* **2005**, *1066*, 1.

(43) Kauzmann, W. *Adv Protein Chem* **1959**, *14*, 1.

(44) Levy, Y.; Onuchic, J. N. *Annu Rev Biophys Biomol Struct* **2006**, *35*, 389.

(45) Young, R. D.; Fenimore, P. W. *Biochim Biophys Acta* **2011**, *1814*, 916.

(46) Wang, W. *Int J Pharm* **1999**, *185*, 129.

(47) Kamerzell, T. J.; Esfandiary, R.; Joshi, S. B.; Middaugh, C. R.; Volkin, D. B. *Adv Drug Deliv Rev* **2011**, *63*, 1118.

(48) Ball, P. *Chem Rev* **2008**, *108*, 74.

(49) Gregory, R. B. *Protein-solvent interactions*; Marcel Dekker: New York, N.Y., 1995.

(50) Burling, F. T.; Weis, W. I.; Flaherty, K. M.; Brunger, A. T. *Science* **1996**, *271*, 72.

(51) Levitt, M.; Park, B. H. *Structure* **1993**, *1*, 223.

(52) Otting, G.; Liepinsh, E.; Wuthrich, K. *Science* **1991**, *254*, 974.

(53) Fenimore, P. W.; Frauenfelder, H.; McMahon, B. H.; Parak, F. G. *Proc Natl Acad Sci U S A* **2002**, *99*, 16047.

(54) Frauenfelder, H.; Fenimore, P. W.; McMahon, B. H. *Biophys Chem* **2002**, *98*, 35.

(55) Frauenfelder, H.; Fenimore, P. W.; Young, R. D. *IUBMB Life* **2007**, *59*, 506.

(56) Teilum, K.; Olsen, J. G.; Kragelund, B. B. *Biochim Biophys Acta* **2011**, *1814*, 969.

(57) Kumar, S.; Ma, B.; Tsai, C. J.; Sinha, N.; Nussinov, R. *Protein Sci* **2000**, *9*, 10.

(58) Freire, E. *Proc Natl Acad Sci U S A* **1999**, *96*, 10118.

(59) Rejto, P. A.; Verkhivker, G. M. *Proc Natl Acad Sci U S A* **1996**, *93*, 8945.

(60) Tsai, C. J.; Kumar, S.; Ma, B.; Nussinov, R. *Protein Sci* **1999**, *8*, 1181.

(61) Volkman, B. F.; Lipson, D.; Wemmer, D. E.; Kern, D. *Science* **2001**, *291*, 2429.

(62) Barron, L. D.; Hecht, L.; Wilson, G. *Biochemistry* **1997**, *36*, 13143.

(63) Tarek, M.; Tobias, D. J. *Phys Rev Lett* **2002**, *88*, 138101.

(64) Ansari, A.; Jones, C. M.; Henry, E. R.; Hofrichter, J.; Eaton, W. A. *Science* **1992**, *256*, 1796.

(65) Dunn, R. V.; Daniel, R. M. *Philos Trans R Soc Lond B Biol Sci* **2004**, *359*, 1309.

(66) Finney, J. L. *Faraday Discuss* **1996**, 1.

(67) Mattos, C. *Trends Biochem Sci* **2002**, *27*, 203.

(68) Priev, A.; Almagor, A.; Yedgar, S.; Gavish, B. *Biochemistry* **1996**, *35*, 2061.

(69) Parak, F. G. *Curr Opin Struct Biol* **2003**, *13*, 552.

(70) Shukla, D.; Schneider, C. P.; Trout, B. L. *Adv Drug Deliv Rev* **2011**, *63*, 1074.

(71) Teixeira, J. *Gen Physiol Biophys* **2009**, *28*, 168.

(72) Frank, H. S.; Evans, M. W. *The Journal of Chemical Physics* **1945**, *13*, 507.

(73) Privalov, P. L.; Gill, S. J. *Adv Protein Chem* **1988**, *39*, 191.

(74) Timasheff, S. N. *Annu Rev Biophys Biomol Struct* **1993**, *22*, 67.

(75) Timasheff, S. N. *Adv Protein Chem* **1998**, *51*, 355.

(76) Timasheff, S. N. *Biochemistry* **2002**, *41*, 13473.

(77) Timasheff, S. N. *Proc Natl Acad Sci U S A* **2002**, *99*, 9721.

(78) Ohtake, S.; Kita, Y.; Arakawa, T. *Adv Drug Deliv Rev* **2011**, *63*, 1053.

(79) Traube, J. *The Journal of Physical Chemistry* **1909**, *14*, 452.

(80) Traube, J. *The Journal of Physical Chemistry* **1909**, *14*, 471.

(81) Stumpe, M. C.; Grubmuller, H. *J Am Chem Soc* **2007**, *129*, 16126.

(82) Vagenende, V.; Yap, M. G.; Trout, B. L. *Biochemistry* **2009**, *48*, 11084.

(83) Mason, P. E.; Dempsey, C. E.; Neilson, G. W.; Kline, S. R.; Brady, J. W. *J Am Chem Soc* **2009**, *131*, 16689.

(84) Moelbert, S.; Normand, B.; De Los Rios, P. *Biophys Chem* **2004**, *112*, 45.

(85) Collins, K. D.; Washabaugh, M. W. *Q Rev Biophys* **1985**, *18*, 323.

(86) Thakkar, S. V.; Joshi, S. B.; Jones, M. E.; Sathish, H. A.; Bishop, S. M.; Volkin, D. B.; Middaugh, C. R. *J Pharm Sci. 2012 May 11. doi: 10.1002/jps.23187.* **2012**.

(87) Bennion, B. J.; Daggett, V. *Proc Natl Acad Sci U S A* **2004**, *101*, 6433.

(88) Butler, S. L.; Falke, J. J. *Biochemistry* **1996**, *35*, 10595.

(89) Cioni, P.; Bramanti, E.; Strambini, G. B. *Biophys J* **2005**, *88*, 4213.

(90) DePaz, R. A.; Barnett, C. C.; Dale, D. A.; Carpenter, J. F.; Gaertner, A. L.; Randolph, T. W. *Arch Biochem Biophys* **2000**, *384*, 123.

(91) Doan-Nguyen, V.; Loria, J. P. *Protein Sci* **2007**, *16*, 20.

(92) Jamal, S.; Poddar, N. K.; Singh, L. R.; Dar, T. A.; Rishi, V.; Ahmad, F. *FEBS J* **2009**, *276*, 6024.

(93) Kendrick, B. S.; Chang, B. S.; Arakawa, T.; Peterson, B.; Randolph, T. W.; Manning, M. C.; Carpenter, J. F. *Proc Natl Acad Sci U S A* **1997**, *94*, 11917.

(94) Kim, D. H.; Jang, D. S.; Nam, G. H.; Yun, S.; Cho, J. H.; Choi, G.; Lee, H. C.; Choi, K. Y. *Biochemistry* **2000**, *39*, 13084.

(95) Kim, Y. S.; Jones, L. S.; Dong, A.; Kendrick, B. S.; Chang, B. S.; Manning, M. C.; Randolph, T. W.; Carpenter, J. F. *Protein Sci* **2003**, *12*, 1252.

(96) Mashino, T.; Fridovich, I. *Arch Biochem Biophys* **1987**, *258*, 356.

(97) Kamerzell, T. J.; Unruh, J. R.; Johnson, C. K.; Middaugh, C. R. *Biochemistry* **2006**, *45*, 15288.

(98) Buckin, V. A.; Kankiya, B. I.; Bulichov, N. V.; Lebedev, A. V.; Gukovsky, I.; Chuprina, V. P.; Sarvazyan, A. P.; Williams, A. R. *Nature* **1989**, *340*, 321.

(99) Chalikian, T. V.; Plum, G. E.; Sarvazyan, A. P.; Breslauer, K. J. *Biochemistry* **1994**, *33*, 8629.

(100) Kamerzell, T. J.; Ramsey, J. D.; Middaugh, C. R. *J Phys Chem B* **2008**, *112*, 3240.

(101) Sarvazyan, A. P.; Chalikian, T. V. *Ultrasonics* **1991**, *29*, 119.

(102) Cameron, D. L.; Jakus, J.; Pauleta, S. R.; Pettigrew, G. W.; Cooper, A. *J Phys Chem B* **2010**, *114*, 16228.

(103) Mitra, L.; Rouget, J. B.; Garcia-Moreno, B.; Royer, C. A.; Winter, R. *Chemphyschem* **2008**, *9*, 2715.

(104) Mitra, L.; Smolin, N.; Ravindra, R.; Royer, C.; Winter, R. *Phys Chem Chem Phys* **2006**, *8*, 1249.

(105) Lee, J. C.; Timasheff, S. N. *J Biol Chem* **1981**, *256*, 7193.

(106) Arakawa, T.; Ejima, D.; Tsumoto, K.; Obeyama, N.; Tanaka, Y.; Kita, Y.; Timasheff, S. N. *Biophys Chem* **2007**, *127*, 1.

(107) Arakawa, T.; Tsumoto, K.; Kita, Y.; Chang, B.; Ejima, D. *Amino Acids* **2007**, *33*, 587.

(108) Lange, C.; Rudolph, R. *Curr Pharm Biotechnol* **2009**, *10*, 408.

(109) Nakakido, M.; Kudou, M.; Arakawa, T.; Tsumoto, K. *Curr Pharm Biotechnol* **2009**, *10*, 415.

(110) Shukla, D.; Trout, B. L. *J Phys Chem B* **2010**, *114*, 13426.

(111) Baynes, B. M.; Trout, B. L. *Biophys J* **2004**, *87*, 1631.

(112) Schneider, C. P.; Trout, B. L. *J Phys Chem B* **2009**, *113*, 2050.

(113) Shukla, D.; Trout, B. L. *J Phys Chem B* **2011**, *115*, 1243.

(114) Mak, T. W.; Saunders, M. E. *The immune response : basic and clinical principles*; Elsevier/Academic: Amsterdam ; Boston, 2006.

(115) Hanson, D. C.; Yguerabide, J.; Schumaker, V. N. *Biochemistry* **1981**, *20*, 6842.

(116) Boehm, M. K.; Woof, J. M.; Kerr, M. A.; Perkins, S. J. *J Mol Biol* **1999**, *286*, 1421.

(117) Takahashi, H.; Suzuki, E.; Shimada, I.; Arata, Y. *Biochemistry* **1992**, *31*, 2464.

(118) Dangl, J. L.; Wensel, T. G.; Morrison, S. L.; Stryer, L.; Herzenberg, L. A.; Oi, V. T. *EMBO J* **1988**, *7*, 1989.

(119) Hanson, D. C. *Mol Immunol* **1985**, *22*, 245.

(120) Ramsey, J. D.; Gill, M. L.; Kamerzell, T. J.; Price, E. S.; Joshi, S. B.; Bishop, S. M.; Oliver, C. N.; Middaugh, C. R. *J Pharm Sci* **2009**, *98*, 2432.

(121) Kawata, Y.; Hamaguchi, K. *Biochemistry* **1991**, *30*, 4367.

(122) Kim, H.; Matsunaga, C.; Yoshino, A.; Kato, K.; Arata, Y. *J Mol Biol* **1994**, *236*, 300.

(123) Kozlowski, S.; Swann, P. *Adv Drug Deliv Rev* **2006**, *58*, 707.

(124) Shire, S. J. *Curr Opin Biotechnol* **2009**, *20*, 708.

(125) Wang, W.; Singh, S.; Zeng, D. L.; King, K.; Nema, S. *J Pharm Sci* **2007**, *96*, 1.

(126) Saluja, A.; Kalonia, D. S. *Int J Pharm* **2008**, *358*, 1.

(127) Shire, S. J.; Shahrokh, Z.; Liu, J. *J Pharm Sci* **2004**, *93*, 1390.

(128) Minton, A. P. *J Pharm Sci* **2005**, *94*, 1668.

(129) Joubert, M. K.; Luo, Q.; Nashed-Samuel, Y.; Wypych, J.; Narhi, L. O. *J Biol Chem* **2011**, *286*, 25118.

(130) Braun, A.; Kwee, L.; Labow, M. A.; Alsenz, J. *Pharm Res* **1997**, *14*, 1472.

(131) Demeule, B.; Gurny, R.; Arvinte, T. *Eur J Pharm Biopharm* **2006**, *62*, 121.

(132) Ryan, M. E.; Webster, M. L.; Statler, J. D. *Clin Pediatr (Phila)* **1996**, *35*, 23.

(133) Cleland, J. L.; Powell, M. F.; Shire, S. J. *Crit Rev Ther Drug Carrier Syst* **1993**, *10*, 307.

(134) Xie, M.; Schowen, R. L. *J Pharm Sci* **1999**, *88*, 8.

(135) Harris, R. J.; Kabakoff, B.; Macchi, F. D.; Shen, F. J.; Kwong, M.; Andya, J. D.; Shire, S. J.; Bjork, N.; Totpal, K.; Chen, A. B. *J Chromatogr B Biomed Sci Appl* **2001**, *752*, 233.

(136) Andya, J. D.; Maa, Y. F.; Costantino, H. R.; Nguyen, P. A.; Dasovich, N.; Sweeney, T. D.; Hsu, C. C.; Shire, S. J. *Pharm Res* **1999**, *16*, 350.

(137) Morales, A. A.; Nunez-Gandolff, G.; Perez, N. P.; Veliz, B. C.; Caballero-Torres, I.; Duconge, J.; Fernandez, E.; Crespo, F. Z.; Veloso, A.; Iznaga-Escobar, N. *Nucl Med Biol* **1999**, *26*, 717.

(138) Tous, G. I.; Wei, Z.; Feng, J.; Bilbulian, S.; Bowen, S.; Smith, J.; Strouse, R.; McGeehan, P.; Casas-Finet, J.; Schenerman, M. A. *Anal Chem* **2005**, *77*, 2675.

(139) Harris, R. J. *J Chromatogr A* **1995**, *705*, 129.

(140) Usami, A.; Ohtsu, A.; Takahama, S.; Fujii, T. *J Pharm Biomed Anal* **1996**, *14*, 1133.

(141) Kennedy, D. M.; Skillen, A. W.; Self, C. H. *Clin Exp Immunol* **1994**, *98*, 245.

(142) Querol, E.; Perez-Pons, J. A.; Mozo-Villarias, A. *Protein Eng* **1996**, *9*, 265.

(143) Baek, W. O.; Vijayalakshmi, M. A. *Biochim Biophys Acta* **1997**, *1336*, 394.

(144) Katre, N. V. *Advanced Drug Delivery Reviews* **1993**, *10*, 91.

(145) Matsumura, M.; Signor, G.; Matthews, B. W. *Nature* **1989**, *342*, 291.

(146) Zimmerman, S. B.; Trach, S. O. *J Mol Biol* **1991**, *222*, 599.

(147) Alford, J. R. *Physical Stability of a Therapeutic Protein in High Protein Concentration Aqueous Formulations*, 2007.

(148) Murphy, R. M.; Tsai, A. M. *Misbehaving proteins : protein (mis)folding, aggregation, and stability*; Springer: New York, 2006.

(149) Nezlin, R. *Immunol Lett* **2010**, *132*, 1.

(150) Mach, H.; Volkin, D. B.; Burke, C. J.; Middaugh, C. R. *Methods Mol Biol* **1995**, *40*, 91.

(151) Wiethoff, C. M.; Russell Middaugh, C. *Methods Mol Med* **2001**, *65*, 349.

(152) Esfandiary, R.; Hunjan, J. S.; Lushington, G. H.; Joshi, S. B.; Middaugh, C. R. *Protein Sci* **2009**, *18*, 2603.

(153) Lucas, L. H.; Ersoy, B. A.; Kueltzo, L. A.; Joshi, S. B.; Brandau, D. T.; Thyagarajapuram, N.; Peek, L. J.; Middaugh, C. R. *Protein Sci* **2006**, *15*, 2228.

(154) Bond, M. D.; Panek, M. E.; Zhang, Z.; Wang, D.; Mehndiratta, P.; Zhao, H.; Gunton, K.; Ni, A.; Nedved, M. L.; Burman, S.; Volkin, D. B. *J Pharm Sci* **2010**, *99*, 2582.

(155) Cardamone, M.; Puri, N. K. *Biochem J* **1992**, *282 (Pt 2)*, 589.

(156) LeVine, H., 3rd. *Protein Sci* **1993**, *2*, 404.

(157) Sreerama, N.; Manning, M. C.; Powers, M. E.; Zhang, J. X.; Goldenberg, D. P.; Woody, R. W. *Biochemistry* **1999**, *38*, 10814.

(158) Stryer, L. *J Mol Biol* **1965**, *13*, 482.

(159) Kueltzo, L. A.; Ersoy, B.; Ralston, J. P.; Middaugh, C. R. *J Pharm Sci* **2003**, *92*, 1805.

(160) Maddux, N. R.; Joshi, S. B.; Volkin, D. B.; Ralston, J. P.; Middaugh, C. R. *J Pharm Sci* **2011**.

(161) Ausar, S. F.; Foubert, T. R.; Hudson, M. H.; Vedvick, T. S.; Middaugh, C. R. *J Biol Chem* **2006**, *281*, 19478.

(162) Ausar, S. F.; Rexroad, J.; Frolov, V. G.; Look, J. L.; Konar, N.; Middaugh, C. R. *Mol Pharm* **2005**, *2*, 491.

(163) Brandau, D. T.; Joshi, S. B.; Smalter, A. M.; Kim, S.; Steadman, B.; Middaugh, C. R. *Mol Pharm* **2007**, *4*, 571.

(164) Cai, S.; He, F.; Samra, H. S.; de la Maza, L. M.; Bottazzi, M. E.; Joshi, S. B.; Middaugh, C. R. *Mol Pharm* **2009**, *6*, 1553.

(165) Fan, H.; Kashi, R. S.; Middaugh, C. R. *Arch Biochem Biophys* **2006**, *447*, 34.

(166) Fan, H.; Li, H.; Zhang, M.; Middaugh, C. R. *J Pharm Sci* **2007**, *96*, 1490.

(167) Fan, H.; Ralston, J.; Dibiase, M.; Faulkner, E.; Middaugh, C. R. *J Pharm Sci* **2005**, *94*, 1893.

(168) He, F.; Joshi, S. B.; Bosman, F.; Verhaeghe, M.; Middaugh, C. R. *J Pharm Sci* **2009**, *98*, 3340.

(169) He, F.; Joshi, S. B.; Moore, D. S.; Shinogle, H. E.; Ohtake, S.; Lechuga-Ballesteros, D.; Martin, R. A.; Truong-Le, V. L.; Middaugh, C. R. *Hum Vaccin* **2010**, *6*.

(170) Jiang, G.; Joshi, S. B.; Peek, L. J.; Brandau, D. T.; Huang, J.; Ferriter, M. S.; Woodley, W. D.; Ford, B. M.; Mar, K. D.; Mikszta, J. A.; Hwang, C. R.; Ulrich, R.; Harvey, N. G.; Middaugh, C. R.; Sullivan, V. J. *J Pharm Sci* **2006**, *95*, 80.

(171) Kissmann, J.; Ausar, S. F.; Rudolph, A.; Braun, C.; Cape, S. P.; Sievers, R. E.; Federspiel, M. J.; Joshi, S. B.; Middaugh, C. R. *Hum Vaccin* **2008**, *4*, 350.

(172) Kissmann, J.; Joshi, S. B.; Haynes, J. R.; Dokken, L.; Richardson, C.; Middaugh, C. R. *J Pharm Sci* **2011**, *100*, 634.

(173) Markham, A. P.; Jaafar, Z. A.; Kemege, K. E.; Middaugh, C. R.; Hefty, P. S. *Biochemistry* **2009**, *48*, 10353.

(174) Nonoyama, A.; Laurence, J. S.; Garriques, L.; Qi, H.; Le, T.; Middaugh, C. R. *J Pharm Sci* **2008**, *97*, 2552.

(175) Peek, L. J.; Brandau, D. T.; Jones, L. S.; Joshi, S. B.; Middaugh, C. R. *Vaccine* **2006**, *24*, 5839.

(176) Peek, L. J.; Brey, R. N.; Middaugh, C. R. *J Pharm Sci* **2007**, *96*, 44.

(177) Rexroad, J.; Evans, R. K.; Middaugh, C. R. *J Pharm Sci* **2006**, *95*, 237.

(178) Rexroad, J.; Martin, T. T.; McNeilly, D.; Godwin, S.; Middaugh, C. R. *J Pharm Sci* **2006**, *95*, 1469.

(179) Ruponen, M.; Braun, C. S.; Middaugh, C. R. *J Pharm Sci* **2006**, *95*, 2101.

(180) Salnikova, M. S.; Joshi, S. B.; Rytting, J. H.; Warny, M.; Middaugh, C. R. *J Pharm Sci* **2008**, *97*, 3735.

(181) Zeng, Y.; Fan, H.; Chiueh, G.; Pham, B.; Martin, R.; Lechuga-Ballesteros, D.; Truong, V. L.; Joshi, S. B.; Middaugh, C. R. *Hum Vaccin* **2009**, *5*, 322.

(182) Karplus, M.; McCammon, J. A. *Annu Rev Biochem* **1983**, *52*, 263.

(183) Kleckner, I. R.; Foster, M. P. *Biochim Biophys Acta* **2011**, *1814*, 942.

(184) Boehr, D. D.; Dyson, H. J.; Wright, P. E. *Chem Rev* **2006**, *106*, 3055.

(185) Loria, J. P.; Berlow, R. B.; Watt, E. D. *Acc Chem Res* **2008**, *41*, 214.

(186) Smock, R. G.; Gierasch, L. M. *Science* **2009**, *324*, 198.

(187) Gunasekaran, K.; Ma, B.; Nussinov, R. *Proteins* **2004**, *57*, 433.

(188) Teilum, K.; Olsen, J. G.; Kragelund, B. B. *Cell Mol Life Sci* **2009**, *66*, 2231.

(189) Fenimore, P. W.; Frauenfelder, H.; McMahon, B. H.; Young, R. D. *Proc Natl Acad Sci U S A* **2004**, *101*, 14408.

(190) Frauenfelder, H.; Fenimore, P. W.; Chen, G.; McMahon, B. H. *Proc Natl Acad Sci U S A* **2006**, *103*, 15469.

(191) Jiang, J. S.; Brunger, A. T. *J Mol Biol* **1994**, *243*, 100.

(192) Savage, H.; Wlodawer, A. *Methods Enzymol* **1986**, *127*, 162.

(193) Belton, P. S. *Prog Biophys Mol Biol* **1994**, *61*, 61.

(194) Denisov, V. P.; Jonsson, B. H.; Halle, B. *Nat Struct Biol* **1999**, *6*, 253.

(195) Halle, B.; Andersson, T.; Forsen, S.; Lindman, B. *Journal of the American Chemical Society* **1981**, *103*, 500.

(196) Kharakoz, D. P.; Sarvazyan, A. P. *Biopolymers* **1993**, *33*, 11.

(197) Zhai, Y.; Okoro, L.; Cooper, A.; Winter, R. *Biophys Chem* **2011**, *156*, 13.

(198) Shiio, H. *Journal of the American Chemical Society* **1958**, *80*, 70.

(199) Tamura, Y.; Gekko, K. *Biochemistry* **1995**, *34*, 1878.

(200) Chalikian, T. V.; Sarvazyan, A. P.; Breslauer, K. J. *Biophys Chem* **1994**, *51*, 89.

(201) Demchenko, A. P. *Biophys Chem* **1982**, *15*, 101.

(202) Demchenko, A. P. *Luminescence* **2002**, *17*, 19.

(203) Harn, N.; Allan, C.; Oliver, C.; Middaugh, C. R. *J Pharm Sci* **2007**, *96*, 532.

(204) Ionescu, R. M.; Vlasak, J.; Price, C.; Kirchmeier, M. *J Pharm Sci* **2008**, *97*, 1414.

(205) Garber, E.; Demarest, S. J. *Biochem Biophys Res Commun* **2007**, *355*, 751.

(206) Tischenko, V. M.; Abramov, V. M.; Zav'yalov, V. P. *Biochemistry* **1998**, *37*, 5576.

(207) Baynes, B. M.; Wang, D. I.; Trout, B. L. *Biochemistry* **2005**, *44*, 4919.

(208) Henzler-Wildman, K.; Kern, D. *Nature* **2007**, *450*, 964.

(209) Leopold, P. E.; Montal, M.; Onuchic, J. N. *Proc Natl Acad Sci U S A* **1992**, *89*, 8721.

(210) Brooks, C. L., 3rd; Gruebele, M.; Onuchic, J. N.; Wolynes, P. G. *Proc Natl Acad Sci U S A* **1998**, *95*, 11037.

(211) Keskin, O. *BMC Struct Biol* **2007**, *7*, 31.

(212) Singh, S. K. *J Pharm Sci* **2011**, *100*, 354.

(213) Yadav, S.; Shire, S. J.; Kalonia, D. S. *J Pharm Sci* **2010**, *99*, 4812.

(214) Gregory, R. B.; Knox, D. G.; Percy, A. J.; Rosenberg, A. *Biochemistry* **1982**, *21*, 6523.

(215) Gregory, R. B.; Lumry, R. *Biopolymers* **1985**, *24*, 301.

(216) Kuwajima, K.; Schmid, F. X. *Adv Biophys* **1984**, *18*, 43.

(217) Czapiewski, D.; Zielkiewicz, J. *J Phys Chem B* **2010**, *114*, 4536.

(218) Arakawa, T.; Timasheff, S. N. *Biophys J* **1985**, *47*, 411.

(219) Parsegian, V. A.; Rand, R. P.; Rau, D. C. *Proc Natl Acad Sci U S A* **2000**, *97*, 3987.

(220) Schellman, J. A. *Biophys J* **2003**, *85*, 108.

(221) Itoh, K.-i.; Azumi, T. *The Journal of Chemical Physics* **1975**, *62*, 3431.

(222) Bhattacharya, M.; Mukhopadhyay, S. *J Phys Chem B* **2012**, *116*, 520.

(223) Demchenko, A. P. *Eur Biophys J* **1988**, *16*, 121.

(224) Demchenko, A. P. *Trends Biochem Sci* **1988**, *13*, 374.

(225) Kelkar, D. A.; Chaudhuri, A.; Haldar, S.; Chattopadhyay, A. *Eur Biophys J* **2010**, *39*, 1453.

(226) Edelman, G. M. *Biochemistry* **1970**, *9*, 3197.

(227) Edmundson, A. B.; Ely, K. R.; Abola, E. E.; Schiffer, M.; Panagiotopoulos, N. *Biochemistry* **1975**, *14*, 3953.

(228) Epp, O.; Colman, P.; Fehlhammer, H.; Bode, W.; Schiffer, M.; Huber, R.; Palm, W. *Eur J Biochem* **1974**, *45*, 513.

(229) Huber, R.; Deisenhofer, J.; Colman, P. M.; Matsushima, M.; Palm, W. *Nature* **1976**, *264*, 415.

(230) Poljak, R. J.; Amzel, L. M.; Chen, B. L.; Phizackerley, R. P.; Saul, F. *Proc Natl Acad Sci U S A* **1974**, *71*, 3440.

(231) Segal, D. M.; Padlan, E. A.; Cohen, G. H.; Rudikoff, S.; Potter, M.; Davies, D. R. *Proc Natl Acad Sci U S A* **1974**, *71*, 4298.

(232) Deisenhofer, J.; Colman, P. M.; Epp, O.; Huber, R. *Hoppe Seylers Z Physiol Chem* **1976**, *357*, 1421.

(233) Litman, G. W.; Good, R. A.; Frommel, D.; Rosenberg, A. *Proc Natl Acad Sci U S A* **1970**, *67*, 1085.

(234) Middaugh, C. R.; Litman, G. W. *Biochim Biophys Acta* **1978**, *535*, 33.

(235) England, P.; Bregegere, F.; Bedouelle, H. *Biochemistry* **1997**, *36*, 164.

(236) Longworth, J. W.; McLaughlin, C. L.; Solomon, A. *Biochemistry* **1976**, *15*, 2953.

(237) Baldwin, R. L. *Biophys J* **1996**, *71*, 2056.

(238) Eftink, M. R.; Ghiron, C. A. *Proc Natl Acad Sci U S A* **1975**, *72*, 3290.

(239) Eftink, M. R.; Ghiron, C. A. *Biochemistry* **1976**, *15*, 672.

(240) Eftink, M. R.; Ghiron, C. A. *Biochemistry* **1977**, *16*, 5546.

(241) Lakowicz, J. R. *Principles of fluorescence spectroscopy*, 3rd ed.; Springer: New York, 2006.

(242) Ladokhin, A. S. *Journal of Fluorescence* **1999**, *9*, 1.

(243) Zhang, Y.; Cremer, P. S. *Annu Rev Phys Chem* **2010**, *61*, 63.

(244) Baldwin, R. L. *Proc Natl Acad Sci U S A* **1986**, *83*, 8069.

(245) Mancera, R. L.; Buckingham, A. D. *Chemical Physics Letters* **1995**, *234*, 296.

(246) Skipper, N. T. *Chemical Physics Letters* **1993**, *207*, 424.

(247) Tian, F.; Middaugh, C. R.; Offerdahl, T.; Munson, E.; Sane, S.; Rytting, J. H. *Int J Pharm* **2007**, *335*, 20.

(248) Wernersson, E.; Heyda, J.; Vazdar, M.; Lund, M.; Mason, P. E.; Jungwirth, P. *J Phys Chem B* **2011**, *115*, 12521.

(249) Alberts, B. *Cell* **1998**, *92*, 291.

(250) Canziani, G.; Zhang, W.; Cines, D.; Rux, A.; Willis, S.; Cohen, G.; Eisenberg, R.; Chaiken, I. *Methods* **1999**, *19*, 253.

(251) Chen, Y.; Müller, J. D.; Berland, K. M.; Gratton, E. *Methods* **1999**, *19*, 234.

(252) Appling, D. *Methods* **1999**, *19*, 338.

(253) Jameson, D. M.; Seifried, S. E. *Methods* **1999**, *19*, 222.

(254) McAlister-Henn, L.; Gibson, N.; Panisko, E. *Methods* **1999**, *19*, 330.

(255) Phizicky, E. M.; Fields, S. *Microbiol Rev* **1995**, *59*, 94.

(256) Pierce, M. M.; Raman, C. S.; Nall, B. T. *Methods* **1999**, *19*, 213.

(257) Rivas, G.; Stafford, W.; Minton, A. P. *Methods* **1999**, *19*, 194.

(258) Sonia, B. *Methods* **1999**, *19*, 278.

(259) Spivey, H. O.; Ovádi, J. *Methods* **1999**, *19*, 306.

(260) Vergnon, A. L.; Chu, Y.-H. *Methods* **1999**, *19*, 270.

(261) Yang, W.; Somerville, R. L. *Methods* **1999**, *19*, 322.

(262) Ellis, R. J.; Minton, A. P. *Nature* **2003**, *425*, 27.

(263) Haas, C.; Drenth, J.; Wilson, W. W. *The Journal of Physical Chemistry B* **1999**, *103*, 2808.

(264) Rosgen, J.; Pettitt, B. M.; Bolen, D. W. *Biochemistry* **2004**, *43*, 14472.

(265) George, A.; Chiang, Y.; Guo, B.; Arabshahi, A.; Cai, Z.; Wilson, W. W.; Charles W. Carter, Jr. [6] Second virial coefficient as predictor in protein crystal growth. In *Methods in Enzymology*; Academic Press, 1997; Vol. Volume 276; pp 100.

(266) George, A.; Wilson, W. W. *Acta Crystallogr D Biol Crystallogr* **1994**, *50*, 361.

(267) Tessier, P. M.; Lenhoff, A. M. *Curr Opin Biotechnol* **2003**, *14*, 512.

(268) Valente, J. J.; Payne, R. W.; Manning, M. C.; Wilson, W. W.; Henry, C. S. *Curr Pharm Biotechnol* **2005**, *6*, 427.

(269) Attri, A. K.; Minton, A. P. *Anal Biochem* **2005**, *337*, 103.

(270) Yadav, S.; Liu, J.; Shire, S. J.; Kalonia, D. S. *J Pharm Sci* **2010**, *99*, 1152.

(271) Yadav, S.; Shire, S. J.; Kalonia, D. S. *Pharm Res* **2011**, *28*, 1973.

(272) Le Brun, V.; Friess, W.; Schultz-Fademrecht, T.; Muehlau, S.; Garidel, P. *Biotechnol J* **2009**, *4*, 1305.

(273) Minton, A. P. *Biophys J* **2007**, *93*, 1321.

(274) Fernandez, C.; Minton, A. P. *Anal Biochem* **2008**, *381*, 254.

(275) Fernandez, C.; Minton, A. P. *Biophys J* **2009**, *96*, 1992.

(276) Scherer, T. M.; Liu, J.; Shire, S. J.; Minton, A. P. *J Phys Chem B* **2010**, *114*, 12948.

(277) Fernandez, C.; Minton, A. P. *J Phys Chem B* **2011**, *115*, 1289.

(278) Weidman, P. J.; Teller, D. C.; Shapiro, B. M. *J Biol Chem* **1987**, *262*, 15076.

(279) Gill, S. C.; von Hippel, P. H. *Anal Biochem* **1989**, *182*, 319.

(280) Permar, S. R.; Wilks, A. B.; Ehlinger, E. P.; Kang, H. H.; Mahlokozera, T.; Coffey, R. T.; Carville, A.; Letvin, N. L.; Seaman, M. S. *J Virol* **2010**, *84*, 8209.

(281) Nishi, H.; Miyajima, M.; Nakagami, H.; Noda, M.; Uchiyama, S.; Fukui, K. *Pharm Res* **2010**, *27*, 1348.

(282) Timasheff, S. N. *Journal of Colloid and Interface Science* **1966**, *21*, 489.

(283) Chari, R.; Jerath, K.; Badkar, A. V.; Kalonia, D. S. *Pharm Res* **2009**, *26*, 2607.

(284) Saluja, A.; Badkar, A. V.; Zeng, D. L.; Nema, S.; Kalonia, D. S. *Biophys J* **2007**, *92*, 234.

(285) Hall, D.; Minton, A. P. *Biochim Biophys Acta* **2003**, *1649*, 127.

(286) Moon, Y. U.; Curtis, R. A.; Anderson, C. O.; Blanch, H. W.; Prausnitz, J. M. *Journal of Solution Chemistry* **2000**, *29*, 699.

(287) Payne, R. W.; Nayar, R.; Tarantino, R.; Del Terzo, S.; Moschera, J.; Di, J.; Heilman, D.; Bray, B.; Manning, M. C.; Henry, C. S. *Biopolymers* **2006**, *84*, 527.

(288) Curtis, R. A.; Prausnitz, J. M.; Blanch, H. W. *Biotechnol Bioeng* **1998**, *57*, 11.

(289) Jimenez, M.; Rivas, G.; Minton, A. P. *Biochemistry* **2007**, *46*, 8373.

(290) Duysens, L. N. *Biochim Biophys Acta* **1956**, *19*, 1.

(291) Mason, B. D.; Zhang, L.; Remmele, R. L., Jr.; Zhang, J. *J Pharm Sci* **2011**, *100*, 4587.

(292) Salinas, B. A.; Sathish, H. A.; Bishop, S. M.; Harn, N.; Carpenter, J. F.; Randolph, T. W. *J Pharm Sci* **2010**, *99*, 82.

(293) Benedek, G. B. *Appl Opt* **1971**, *10*, 459.

(294) Bloemendal, H.; de Jong, W.; Jaenicke, R.; Lubsen, N. H.; Slingsby, C.; Tardieu, A. *Prog Biophys Mol Biol* **2004**, *86*, 407.

(295) Delaye, M.; Tardieu, A. *Nature* **1983**, *302*, 415.

(296) Liu, J.; Nguyen, M. D.; Andya, J. D.; Shire, S. J. *J Pharm Sci* **2005**, *94*, 1928.

(297) Buzzell, J. G.; Tanford, C. *The Journal of Physical Chemistry* **1956**, *60*, 1204.

(298) Kanai, S.; Liu, J.; Patapoff, T. W.; Shire, S. J. *J Pharm Sci* **2008**, *97*, 4219.

(299) Robinson, G. W.; Cho, C. H. *Biophys J* **1999**, *77*, 3311.

(300) Yadav, S.; Laue, T. M.; Kalonia, D. S.; Singh, S. N.; Shire, S. J. *Mol Pharm* **2012**, *9*, 791.

(301) Yadav, S.; Shire, S. J.; Kalonia, D. S. *J Pharm Sci* **2012**, *101*, 998.

(302) Finkelstein, I. J.; Massari, A. M.; Fayer, M. D. *Biophys J* **2007**, *92*, 3652.

(303) Kamerzell, T. J.; Kanai, S.; Liu, J.; Shire, S. J.; Wang, Y. J. *J Phys Chem B* **2009**, *113*, 6109.